UiO : Department of Mathematics
University of Oslo

Nonlinear interpolatory curve subdivision schemes

Espen Christian Lybekk

Master's Thesis, Spring 2017

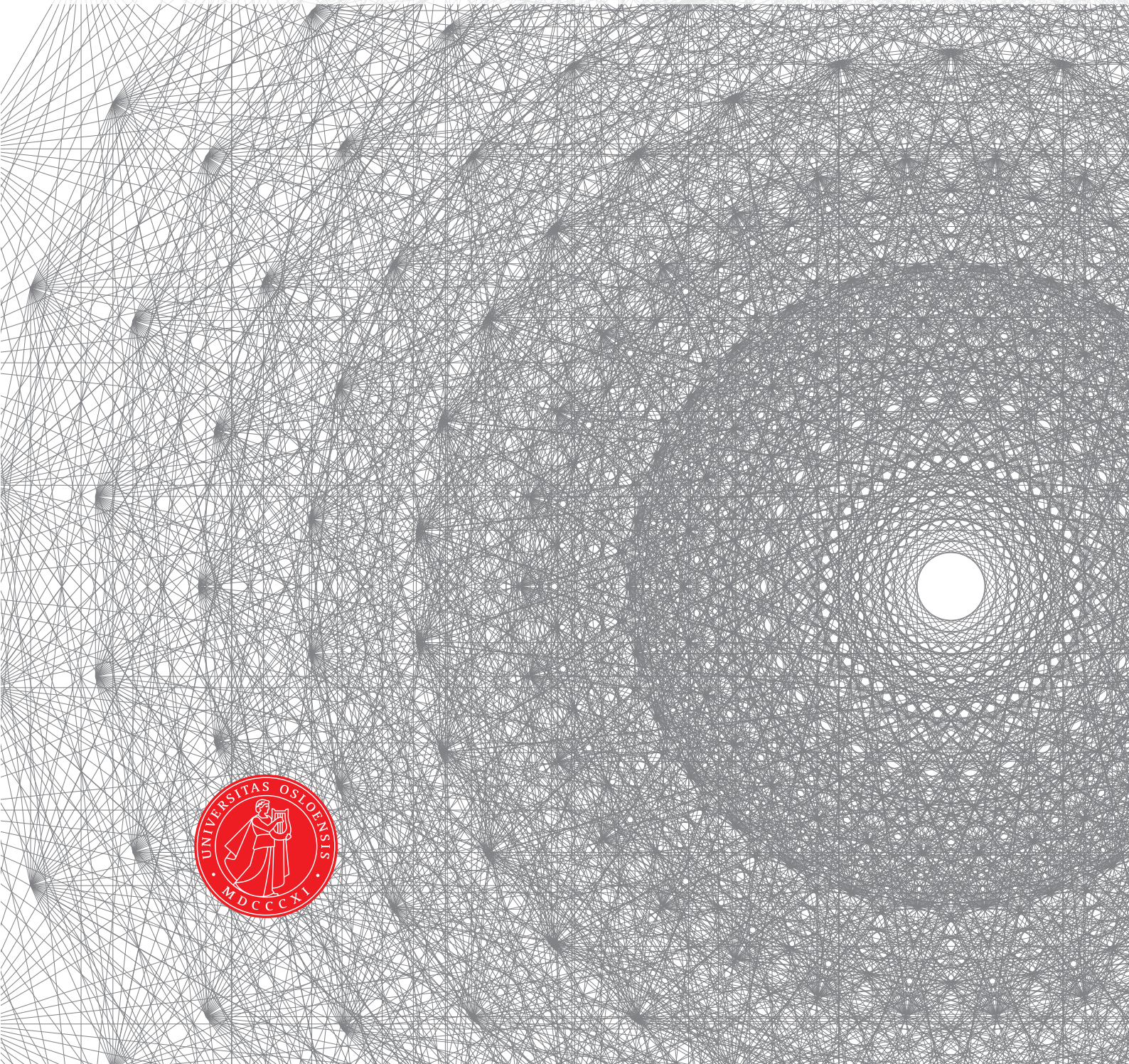

This master's thesis is submitted under the master's programme *Computational Science and Engineering*, with programme option *Computational Science*, at the Department of Mathematics, University of Oslo. The scope of the thesis is 60 credits.

The front page depicts a section of the root system of the exceptional Lie group E_8, projected into the plane. Lie groups were invented by the Norwegian mathematician Sophus Lie (1842–1899) to express symmetries in differential equations and today they play a central role in various parts of mathematics.

Contents

Abstract **3**

Acknowledgments **4**

Introduction **5**

1 Methods of interpolation **7**
1.1 Polynomial interpolation 7
1.2 Spline interpolation 9
1.3 Linear interpolatory subdivision schemes 10
1.4 Parameterization and multilevel grids 13
1.5 Convergence and smoothness of a subdivision scheme 15

2 Analysis of linear subdivision schemes **19**
2.1 Convergence analysis using divided differences 19
2.2 Convergence analysis using Laurent polynomials 24
2.3 Application to nonlinear subdivision 27

3 Nonlinear interpolatory subdivision schemes **28**
3.1 Fractal subdivision (Koch snowflake) 29
3.2 Adaptive tension parameter 31

4 Iterated geometric schemes **34**
4.1 The iterated geometric schemes 34
4.2 Convergence of the IG4-scheme 36
4.3 Validity of the iterated geometric schemes 42
4.4 Distance bounds for the IG4-scheme 52
4.5 Smoothness of the iterated geometric schemes 56
4.6 Convergence of the IG6-scheme 57
4.7 The iterated geometric blending schemes 64

5 Analysis of geometric subdivision **70**
5.1 Circle preserving subdivision 70
5.2 Convergence analysis of GLUE-schemes 71

6 Numerical results and conclusion **79**
6.1 Numerical results for the iterated geometric schemes 79
6.2 Conclusion 87
6.3 Future work 87

Bibliography **88**

Abstract

The aim of this thesis is to study the convergence and smoothness of certain nonlinear interpolatory curve subdivision schemes. The emphasis will be on the *iterated geometric schemes*, which are extensions of the nonlinear four-point scheme of [1] by Dyn, Floater and Hormann, based on iterated chordal and centripetal parameterizations. In [1] convergence of the scheme is shown for uniform, centripetal and chordal parameterizations, i.e. $\alpha = 0, 1/2, 1$, but we here consider the entire interval $\alpha \in [0, 1]$, and derive new results concerning convergence. In particular, we show that the scheme of [1] is C^0 for all $\alpha \in [1/2, 1]$, but that there always exist control points such that the limit curve is not well defined for all $\alpha \in (0, 1/2)$. We also show that a scheme based on the iterated geometric schemes and the six-point scheme with tension parameter, is C^0 for a range of parameters.

We show that the aforementioned schemes fit into a recent framework by Ewald et al. in [13], for studying smoothness criteria, and propose modified refinement rules based on [12] to better fit this framework. Lastly, numerical experiments are carried out to measure the smoothness of the schemes, and a new way to generate the multilevel grid based on the geometry of the points, is proposed.

Acknowledgments

I would like to thank my supervisor Michael Floater for all the helpful discussions and guidance throughout the completion of this thesis. My gratitude also goes to my friends and family for all the support along the way.

Espen Christian Lybekk
Oslo, May 2017.

Introduction

Subdivision is a powerful method to generate smooth curves and surfaces from initial points through iterated refinement. Historically, subdivision was first used in corner cutting algorithms and to generate splines and Bézier curves. Throughout the end of the 20th century and the last decades, subdivision has been one of the leading methods in computer graphics, and especially for generating smooth surfaces in Computer Aided Geometric Design (CAGD). The theory of subdivision curves is important as much of the analysis of subdivision surfaces builds upon the concepts in the analysis of subdivision curves. Subdivision has also proved to be useful in other mathematical fields such as wavelet and multi-resolution theory, and in the study of partial differential equations. Most of the subdivision schemes studied before year 2000 were of a linear nature, meaning that the subdivision refinement rules are based on linear combinations. In recent years however, there has been a shift in focus over to nonlinear schemes. The nonlinearity of a subdivision scheme can allow it to have different properties than what is possible with a linear scheme, but often leads to a more difficult analysis, and new ideas are needed in order to understand these schemes better.

Note on notation

We write sets of numbers with subscripts to impose restrictions on these sets, e.g. $\mathbb{Z}_{\geq 0} = \{0, 1, 2, \dots\}$, to avoid ambiguity when discussing sets of numbers. Whenever we talk about $\mathbb{R}^d$, we let d be a finite positive integer. For a vector $\boldsymbol{a} = [a_0, a_1, \dots, a_{d-1}] \in \mathbb{R}^d$, we let $(\boldsymbol{a})_i = a_i$ be the i-th coordinate component of that vector, with indexation starting at 0.

Structure of the thesis

The reader is strongly encouraged to follow the chapters in order as new concepts are introduced along the way. In chapter 1, we in particular discuss basic polynomial in-

terpolation theory, and introduce linear interpolatory subdivision schemes. Chapter 2 deals with fundamental analysis of these linear schemes. In chapter 3, we look at two nonlinear schemes as examples of how we in some cases can adapt the analysis of linear schemes to analyze nonlinear schemes. In chapter 4, which in many respects is the main chapter of this thesis, we deal with the iterated geometric schemes based on [1], which require further thought. Chapters 1 – 3 can therefore be regarded as being introductory, while the main focus of this thesis starts at chapter 4. In chapter 5, we discuss some aspects of the recent framework by Ewald et al., and look at how this may be used to analyze the smoothness of the iterated geometric schemes. In the last chapter, chapter 6, we discuss some ideas which may be useful for further studies of the smoothness of the iterated geometric schemes, and do numerical experiments.

Chapter One

Methods of interpolation

1.1 Polynomial interpolation

The perhaps most fundamental way to smoothly interpolate a sequence of points $\{\boldsymbol{y}_i\}_{i=0}^n$, where $\boldsymbol{y}_i \in \mathbb{R}^d$ for $i = 0, 1, \ldots, n$, and $d \in \mathbb{Z}_{\geq 1}$, is to fit a polynomial $\boldsymbol{p} : \mathbb{R} \to \mathbb{R}^d \in \Pi_n$, where Π_n is the space of all polynomials of degree $\leq n$ spanned by the monomial basis $\{1, x, x^2, \ldots, x^n\}$. Thus,

$$\boldsymbol{p}(x_i) = \boldsymbol{y}_i, \quad i = 0, 1, \ldots, n,$$

where $\{x_i\}_{i=0}^n$ are distinct parameter values, or nodes, which are either given or calculated. The polynomial interpolant $\boldsymbol{p}$ may therefore be expressed

$$\boldsymbol{p}(x) = \sum_{j=0}^{n} \boldsymbol{c}_j x^j,$$

where the $\{\boldsymbol{c}_j\}_{j=0}^n$ are coefficient vectors that need to be determined. This leads to d linear systems $\boldsymbol{V}\boldsymbol{c} = \boldsymbol{y}$ for each dimensional component, where the k-th system with $k \in \{0, 1, \ldots, d-1\}$, becomes

$$\boldsymbol{V} = \begin{bmatrix} 1 & x_0 & x_0^2 & \ldots & x_0^n \\ 1 & x_1 & x_1^2 & \ldots & x_1^n \\ \vdots & \vdots & \vdots & \ddots & \vdots \\ 1 & x_n & x_n^2 & \ldots & x_n^n \end{bmatrix}, \quad \boldsymbol{c} = \begin{bmatrix} (\boldsymbol{c}_0)_k \\ (\boldsymbol{c}_1)_k \\ \vdots \\ (\boldsymbol{c}_n)_k \end{bmatrix}, \quad \boldsymbol{y} = \begin{bmatrix} (\boldsymbol{y}_0)_k \\ (\boldsymbol{y}_1)_k \\ \vdots \\ (\boldsymbol{y}_n)_k \end{bmatrix}.$$

The collocation matrix $\boldsymbol{V}$ is known as a Vandermonde matrix, and it can be shown that the determinant for a square Vandermonde matrix is given by

$$\det(\boldsymbol{V}) = \prod_{0 \leq i < j \leq n} (x_j - x_i),$$

which is nonzero for distinct x_i, and thus the matrix is nonsingular and the system has a unique solution.

With respect to the analysis of the resulting interpolating polynomial, it is however often preferable to choose the Lagrangian basis to represent the polynomials of degree $\leq n$. In this setting, the basis functions $\{L_j\}_{j=0}^n$ are written

$$L_j(x) = \prod_{\substack{i=0 \\ i \neq j}}^{n} \frac{x - x_i}{x_j - x_i}, \quad j = 0, \ldots, n.$$

Consequently, the basis functions equal the Kronecker delta at the parameter values, i.e.

$$L_j(x_i) = \delta_{i,j} = \begin{cases} 1 & \text{if} \quad i = j, \\ 0 & \text{if} \quad i \neq j, \end{cases}$$

and hence the left hand matrix $\boldsymbol{V}$ in the matrix-vector form of the polynomial interpolation problem is the identity matrix in this case, so there is no linear system to solve. Therefore, $\boldsymbol{p}$ can simply be written as

$$\boldsymbol{p}(x) = \sum_{j=0}^{n} \boldsymbol{y}_j L_j(x).$$

An often used property of the Lagrange basis functions is that they form a partition of unity, meaning that $\sum_{i=0}^{n} L_i(x) = 1$ for all x.

Another important form of the interpolation problem often utilized in analysis and error bounds is Newton's interpolation formula, which is given by

$$\boldsymbol{p}(x) = \sum_{j=0}^{n} \boldsymbol{c}_j \Phi_{j-1}(x),$$

where $\boldsymbol{c}_j = [x_0, \ldots, x_j]\boldsymbol{f}$ with $\boldsymbol{f}(x_i) := \boldsymbol{y}_i$ is the divided difference, and the Φ_j are defined

$$\Phi_{-1}(x) = 1, \quad \Phi_j(x) = \prod_{k=0}^{j} (x - x_j), \quad j = 0, 1, \ldots, n-1.$$

An r-th divided difference $[x_i, \ldots, x_{i+r}]f$ on the parameters $x_0, \ldots, x_k$ is defined by the recurrence relation

$$[x_i, \ldots, x_{i+r}]f = \frac{[x_{i+1}, \ldots, x_{i+r}]f - [x_i, \ldots, x_{i+r-1}]}{x_{i+r} - x_i},$$
$$i \in \{0, \ldots, k-r\},\ r \in \{1, \ldots, k\},$$

where $[x_i]f := f(x_i)$ for $i = 0, \ldots, k$. An important property of Newton's interpolation formula, which we will use later, is that the ordering of the parameters does not matter since the divided differences are symmetric in their arguments.

For actual implementation, the Newton form or the iterative Neville-Aitken algorithm are often used. However, the Lagrange form can also be adapted to be more efficient with the barycentric Lagrange form. For more details about polynomial interpolation, see e.g. chapter 4 of [6].

An obvious drawback of polynomial interpolation is that the degree of the polynomial is directly tied to the number of points, which leads to instability when n grows. Furthermore, we have to be careful when choosing the nodes as oscillations in the interpolant between the data points, known as Runge's phenomenon, may occur for large n. While this effect is minimized by choosing Chebyshev nodes, using direct polynomial interpolation for a large amount of points is generally ill-advised.

By instead utilizing the theory of splines, which are a family of piecewise polynomials with multitudes of valuable properties such as controllable smoothness at the joints, we can obtain much better results. In fact, the common choice of cubic spline interpolation with natural boundary conditions yields the interpolant that minimizes bending energy[1].

1.2 Spline interpolation

Given a non-decreasing knot vector $\boldsymbol{\tau} = (\tau_j)_{j=1}^{p+n+1}$, a polynomial degree $p \in \mathbb{Z}_{\geq 0}$, and control points $\{\boldsymbol{c}_i\}_{i=1}^{n} \in \mathbb{R}^d$, then a spline curve $\boldsymbol{s}$ in the spline space $\mathbb{S}^d_{p,\boldsymbol{\tau}}$, is a linear combination of the B-spline basis functions $B_{j,p,\boldsymbol{\tau}}$ defined

$$B_{j,0,\boldsymbol{\tau}}(x) = \begin{cases} 1 & \text{if} \quad \tau_j \leq x < \tau_{j+1}, \\ 0 & \text{otherwise,} \end{cases} \qquad \text{for} \quad p = 0,$$

$$B_{j,p,\boldsymbol{\tau}}(x) = \frac{x - \tau_j}{\tau_{j+p} - \tau_j} B_{j,p-1,\boldsymbol{\tau}}(x) + \frac{\tau_{j+p+1} - x}{\tau_{j+p+1} - \tau_{j+1}} B_{j+1,p-1,\boldsymbol{\tau}}(x) \quad \forall \quad p \geq 1.$$

I.e.

$$\boldsymbol{s}(u) = \sum_{i=0}^{n} \boldsymbol{c}_i B_{i,p,\boldsymbol{\tau}}(u).$$

If $\boldsymbol{\tau}$ satisfies the Schoenberg-Whitney conditions, i.e. that the positivity of the main diagonal of the B-spline collocation matrix with elements $(B_{j,p}(x_i))_{i=1,j=1}^{n,n}$ is guaranteed, where x_i are the parameters or data abscissae, then there exists a unique spline curve

[1] See e.g chapter 5 of [22]

interpolant. This is only a very brief look at the theory of splines, and a much more comprehensive study may be found in e.g. [22].

While splines are a powerful tool for many purposes, both the simplicity of the construction and implementation, and intuition behind subdivision is appealing. In fact, it has been shown that certain types of approximating splines can be computed by choosing the subdivision masks carefully. In particular, Chaikin's algorithm can compute quadratic cardinal splines, i.e. quadratic splines with uniformly spaced knots, and the procedure can be generalized to any polynomial degree with the Lane-Riesenfeld algorithms, where the weights, or mask coefficients, are chosen from the rows of Pascal's triangle.

1.3 Linear interpolatory subdivision schemes

Let the initial control points $\{\boldsymbol{p}_{0,k}\}_{k\in\mathbb{Z}}$ where $\boldsymbol{p}_{0,k} \in \mathbb{R}^d$ be available, and where only a finite number of points $\{\boldsymbol{p}_{0,k}\}_{k=0}^{n}$ are the points we are typically interested in, and are the ones given in an actual implementation. The role of the points $\{\boldsymbol{p}_{0,k}\}_{k\in\mathbb{Z}\setminus\{0,n\}}$ will be discussed later, but may be thought of as boundary points. A linear subdivision scheme on the data is then defined by the refinement process

$$\boldsymbol{p}_{j+1,k} = \sum_i m_{j,k-ai}\,\boldsymbol{p}_{j,i}, \quad k \in \mathbb{Z}, \quad j = 0, 1, 2, \ldots, \tag{1.1}$$

where $\boldsymbol{m}_j = \{m_{j,k}\}_{k\in\mathbb{Z}}$ is called the subdivision mask of the scheme, and $\{\boldsymbol{p}_{j,k}\}_{k\in\mathbb{Z}}$ are the refined points generated by the subdivision scheme at level j. If the mask changes for each level j, then the scheme is called nonstationary, and otherwise the scheme is called stationary. Similarly, if the mask is dependent on the index k, then the scheme is called nonuniform, and thus called uniform if the mask does not depend on k. The number $a \in \mathbb{Z}_{\geq 1}$ is called the arity of the scheme and is related to the number of points at any given level $j+1$ compared to the number of points at level j. Likewise, the arity of the scheme may be viewed as the number of stencils in the mask, so that the computation of (1.1) may be split into a parts. A common choice of arity is $a = 2$, leading to a binary subdivision scheme, in which case (1.1) may be written

$$\begin{aligned}
\boldsymbol{p}_{j+1,2k} &= \sum_i m_{j,2k-2i}\,\boldsymbol{p}_{j,i}, \quad k \in \mathbb{Z}, \quad j = 0, 1, 2, \ldots, \\
\boldsymbol{p}_{j+1,2k+1} &= \sum_i m_{j,2k+1-2i}\,\boldsymbol{p}_{j,i}, \quad k \in \mathbb{Z}, \quad j = 0, 1, 2, \ldots,
\end{aligned}$$

for the even and odd refined points. The term linear subdivision refers to the fact that the generated points at each level $j+1$ are linear combinations of those at the previous level j. Moreover, if the subdivision mask is constructed such that $\boldsymbol{p}_{j+1,ak} = \boldsymbol{p}_{j,k}$ is

satisfied, then the scheme is called interpolatory, as both the original control points and the points generated at each level are kept, and otherwise the scheme is called approximating. Chaikin's algorithm is an example of an approximating subdivision scheme.

Binary interpolatory subdivision schemes will be the main type of schemes studied in this thesis and all results in this and the next chapter apply to these unless otherwise stated. By letting $\boldsymbol{P}_{j,i} = [(\boldsymbol{p}_{j,k})_i]_{k\in\mathbb{Z}}$ for each spatial component $i \in \{0, \ldots, d-1\}$, we can componentwise let a subdivision step be written as a matrix-vector product

$$\boldsymbol{P}_{j+1,i} = \boldsymbol{S}_j \boldsymbol{P}_{j,i},$$

where $\boldsymbol{S}_j$ is a bi-infinite matrix, with rows based on the stencils of the subdivision mask, and is called the subdivision matrix of the scheme at level j, and $\boldsymbol{P}_{j,i}$ is an infinite vector of the i-th coordinate component of the control points. The subdivision matrix is an important tool for studying linear subdivision schemes, but we will in this thesis instead consider alternative techniques, which in essence are based on many of the same principles as studying the subdivision matrix.

Since a linear subdivision scheme treats each coordinate component independently, it does not matter if we use vectors or scalars for the points when we define these schemes.

The two-point scheme

For completeness we will first discuss the two-point scheme, which essentially just connects the control points by straight lines, and thus is of little practical use. The scheme is defined as

$$p_{j+1,2k} = p_{j,k}, \tag{1.2}$$

$$p_{j+1,2k+1} = \frac{p_{j,k} + p_{j,k+1}}{2}, \tag{1.3}$$

such that $p_{j+1,2k+1}$ is the midpoint of the neighboring two points at the previous level, and its mask is thus given as $\boldsymbol{m} = \frac{1}{2}(1, 2, 1)$. It is trivial that this leads to a curve that cannot be smooth at the joints, as is apparent in Figure 1.1. The resulting limit curve[2] is in fact the linear spline interpolant with knots of multiplicity one.

The four-point scheme and the Dubuc-Deslauriers schemes

One of the earliest and most studied interpolatory subdivision schemes, first devised by Dubuc in 1986 [3], is called the four-point scheme. In its most basic form, the mask of

[2]Loosely defined as the limit of curves as the number of iterations of the subdivision scheme approaches infinity. We will define this in detail later.

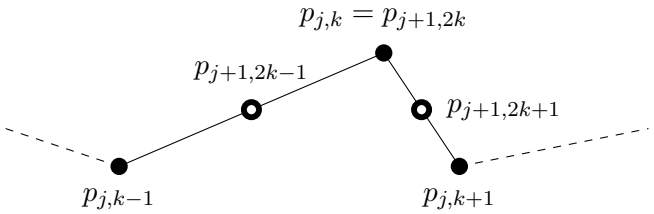

Figure 1.1: Two-point scheme construction after one subdivision step.

the four-point scheme is given as $\boldsymbol{m} = \frac{1}{16}(-1, 0, 9, 16, 9, 0, -1)$ such that the even stencil is $(0, 1, 0)$ and the odd stencil is $\frac{1}{16}(-1, 9, 9, -1)$. Therefore, the scheme may be written

$$p_{j+1,2k} = p_{j,k}, \tag{1.4}$$

$$p_{j+1,2k+1} = -\frac{1}{16}\left(p_{j,k-1} + p_{j,k+2}\right) + \frac{9}{16}\left(p_{j,k} + p_{j,k+1}\right). \tag{1.5}$$

It turns out that the scheme reproduces cubic polynomials. This follows from the fact that the elements of the odd stencil are chosen from the Lagrange basis functions with uniform parameters $\{x_i\}_{i=0}^{3} = \{-1, 0, 1, 2\}$, evaluated at $x = (x_1 + x_2)/2 = 1/2$. A slightly different and more general variation of the scheme, introduced by Dyn, Gregory and Levin in [5], independently and almost simultaneously as the work by Dubuc, can be written as follows

$$p_{j+1,2k} = p_{j,k}, \tag{1.6}$$

$$p_{j+1,2k+1} = -w\left(p_{j,k-1} + p_{j,k+2}\right) + \left(\frac{1}{2} + w\right)\left(p_{j,k} + p_{j,k+1}\right). \tag{1.7}$$

The parameter $w \in \mathbb{R}$ can be regarded as a tension parameter, where a lower absolute value reflects a limit curve closer to the control polygon[3]. Observe that the choice $w = \frac{1}{16}$ results in a scheme equivalent to the Dubuc four-point scheme (1.4)-(1.5), and thus for $w \neq \frac{1}{16}$, this scheme in fact only reproduces linear polynomials.

If we do not restrict Dubuc's four-point scheme to uniformly spaced parameters, we can write

$$p_{j+1,2k} = p_{j,k} \tag{1.8}$$

$$p_{j+1,2k+1} = \pi_{j,k}(x_{j+1,2k+1}), \tag{1.9}$$

where $\pi_{j,k}$ is the cubic Lagrange interpolant to the data $\{p_{j,i}\}_{i=k-1}^{k+2}$ at the parameters $\{x_{j,i}\}_{i=k-1}^{k+2}$, evaluated at $x = x_{j+1,2k+1}$. The role of these parameters will be discussed

[3]The piecewise linear interpolant to the control points.

in the next sections. This generalization of Dubuc's four-point scheme was studied by Daubechies, Guskov and Sweldens in [11].

An extension of the four-point scheme (1.4)–(1.5) to an even number m points was studied by Dubuc and Deslauriers in [4], where the odd stencil entries come from the Lagrange basis functions with parameters $\{x_i\}_{i=0}^{m-1} = \{-m/2+1, -m/2+2, \ldots, m/2\}$ evaluated at $x = 1/2$. By this fact it follows that an m-point Dubuc-Deslauriers scheme has polynomial precision $m-1$. Thus, the four-point Dubuc-Deslauriers scheme is the four-point scheme (1.4)–(1.5), and the six-point Dubuc-Deslauriers scheme is for example given by

$$p_{j+1,2k} = p_{j,k}, \tag{1.10}$$

$$p_{j+1,2k+1} = \frac{3}{256}\left(p_{j,k-2} + p_{j,k+3}\right) - \frac{25}{256}\left(p_{j,k-1} + p_{j,k+2}\right) + \frac{75}{128}\left(p_{j,k} + p_{j,k+1}\right). \tag{1.11}$$

Properties of the limit curve of a general subdivision scheme such as C^k continuity and shape preservation is of great interest as this guarantees certain behaviors of the limit curve when applied to a given sequence of control points. Thus, in the next chapter, we will review a few of the existing methods for analyzing linear subdivision schemes and discuss the difficulties in extending these to nonlinear schemes.

1.4 Parameterization and multilevel grids

We begin our analysis of limit curves by introducing a concept known as multilevel grids, which is in a sense the foundation or support on which the limit curve of a subdivision scheme is defined. Most of the principles discussed here are based on [11] and [8], in particular. Suppose we are given a sequence of control points, which are thought to be samples $\{f(x_k)\}_{k\in\mathbb{Z}}$, where f is some real valued function $f : \mathbb{R} \to \mathbb{R}$, and $X_0 := \{x_k\}_{k\in\mathbb{Z}}$ is the sequence of strictly increasing real valued parameter values, or grid points such that

$$\cdots < x_{-2} < x_{-1} < x_0 < x_1 < x_2 < \ldots, \quad \lim_{k\to-\infty} x_k = -\infty, \quad \lim_{k\to\infty} x_k = \infty.$$

By requiring that we are given only a finite sequence of control points, we can impose the restriction that f has compact support, i.e. that f is non-zero only at a finite number of the x_k. We concentrate here on the case for binary subdivision, but the case for higher arities follows similarly. With each new level of subdivision, new refined grid points $X_{j+1} = \{x_{j+1,k}\}_{k\in\mathbb{Z}}$ are generated from the previous level of coarse grid points $X_j = \{x_{j,k}\}$, using a rule satisfying

$$x_{j+1,2k} = x_{j,k},$$
$$x_{j+1,2k+1} \in (x_{j,k}, x_{j,k+1}),$$

where $x_{0,k} := x_k$ for all indices k. We denote the full multilevel grid, i.e. the grid that incorporates all levels, by $\boldsymbol{X}$. There are a few main types of grids on which subdivision schemes typically are defined

Definition 1.4.1. *Common types of multilevel grids*

1. *Regular grid:*
   A regular grid, or a uniform grid, is a multilevel grid where the grid points are equidistantly spaced at each level. This means that $X_0 = q\mathbb{Z}$ for some positive real number q, and the X_j for $j > 0$ are generated according to $x_{j+1,2k+1} = (x_{j,k} + x_{j,k+1})/2$, $j = 0, 1, \ldots$. A common choice for binary subdivision is to set $\{x_{j,k}\} := \{2^{-j}k\}$ for $j = 0, 1, 2, \ldots$, and $k \in \mathbb{Z}$. These are called the dyadic points.

2. *Semi-regular grid:*
   A semi-regular grid is a multilevel grid such that the initial $\{x_{0,k}\}$ may be irregularly or non-uniformly spaced, but then $x_{j+1,2k+1} = \frac{x_{j,k}+x_{j,k+1}}{2}$ for $j \geq 0$.

3. *Irregular grid:*
   An irregular grid is a multilevel grid where the grid points may be irregularly spaced at every level.

4. *Dyadically balanced grid:*
   A dyadically balanced grid is an irregular multilevel grid type with constraints on the generation of grid points at each level. Given

$$\lambda = \sup_{j,k} \max\left(\frac{h_{j+1,2k}}{h_{j,k}}, \frac{h_{j+1,2k+1}}{h_{j,k}}\right),$$
$$h_{j,k} := x_{j,k+1} - x_{j,k},$$

   then it follows that $1/2 \leq \lambda \leq 1$, and the grid is called dyadically balanced if $\lambda < 1$.

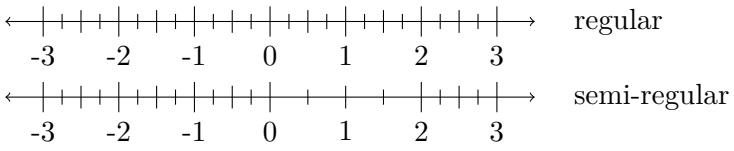

Figure 1.2: Examples of X_2 for different types of multilevel grids.

Note in particular that both a general regular grid and a semi-regular grid is dyadically balanced with $\lambda = 1/2$. To shorten notation we from now on let the four-point scheme with tension parameter on a regular grid be called the FPTS, and let the standard corresponding four-point scheme with $w = 1/16$ on a regular grid be called the FPS[4].

[4]I.e. Dubuc's four-point scheme on a regular grid.

Parametric subdivision schemes

The above definition of multilevel grids assumed that the data was given together with corresponding parameter values. However, if the data $\{\boldsymbol{p}_k\}_{k=0}^n$ is thought of as geometric points, and there are no given parameter values, which is often the case in CAGD, then it is possible to determine the initial parameters X_0 as functions of the control points. Typically, this is done as follows

$$\begin{aligned} x_0 &= 0, \\ x_{k+1} &= x_k + \|\boldsymbol{p}_{k+1} - \boldsymbol{p}_k\|^\alpha, \quad k = 0, 1, \ldots, n-1, \end{aligned}$$

where $\alpha \in [0, 1]$ is a constant parameter, and $\|\cdot\|$ commonly is chosen as the Euclidean l_2-norm. For $\alpha = 0, 1/2, 1$, this is known as uniform, centripetal, and chordal parameterizations, respectively. Observe that $\alpha = 0$ implies that the grid is independent of the geometry of the points, while for $\alpha = 1$, we get an initial grid spacing that approximates the chord length, and hence the name. The centripetal parameterization, introduced by Lee, has been shown to yield cubic spline interpolants close to the control polygon, and will turn out to be important in the later chapters of this thesis. It has been shown for Dubuc's four-point scheme that the chord length parameterization yields degree four approximation order, while the uniform- and centripetal parameterizations only yield degree two approximation order.

Subsequent levels of the multilevel grid can then be chosen from these values in a way such that the satisfactory type of grid is achieved. When plotting the output of a subdivision scheme applied to vector valued control points, we only consider the vector values, while the parameters are used solely in the computation of each new level of subdivision. All the examples in this thesis will be of a parametric nature.

1.5 Convergence and smoothness of a subdivision scheme

In order to precisely define what we mean by the convergence of a subdivision scheme, we first define the ∞-norm, or sup-norm, $\|\cdot\|_\infty$ of a function $\boldsymbol{f}(x) : I \to \mathbb{R}^d$, where I is a closed interval in $\mathbb{R}$, as

$$\|\boldsymbol{f}\|_\infty := \sup_{x \in I} \|\boldsymbol{f}(x)\|_\infty, \tag{1.12}$$

where $\|\boldsymbol{v}\|_\infty := \max_i |(\boldsymbol{v})_i|$, $\boldsymbol{v} \in \mathbb{R}^d$ is the vector ∞-norm. We usually set $I = [x_0, x_n]$. In the analysis, we use the property that a linear subdivision scheme treats each coordinate component independently, and thus only need to look at the one dimensional case $f(x)$:

$I \to \mathbb{R}$, and hence simply consider

$$\|f\|_\infty := \sup_{x \in I} |f(x)|.$$

Definition 1.5.1. *We say that a subdivision scheme has a continuous limit function (or curve) $\boldsymbol{g}(x) \in C(I, \mathbb{R}^d)$, if for any bounded initial data $\{\boldsymbol{p}_{0,k}\}_{k \in \mathbb{Z}}$ and constant $\epsilon \in \mathbb{R}_{>0}$, there exists an index $N \in \mathbb{Z}_{\geq 0}$ such that*

$$\|\boldsymbol{g}_i - \boldsymbol{g}_j\|_\infty < \epsilon \quad \forall \quad i, j \geq N,$$

where $\boldsymbol{g}_j(x)$ is the piecewise linear interpolant interpolating the data $(x_{j,k}, \boldsymbol{p}_{j,k})_{k \in \mathbb{Z}}$ in sequence, such that $\boldsymbol{g}_j(x_{j,k}) = \boldsymbol{p}_{j,k}$ and $\boldsymbol{g}_j$ is affine on $[x_{j,k}, x_{j,k+1}]$. $\boldsymbol{g}_j$ is sometimes referred to as the polygon at level j. For $j = 0$ this polygon is called the control polygon. If such a function $\boldsymbol{g}(x) = \lim_{j \to \infty} \boldsymbol{g}_j(x)$ exists, we say that the corresponding subdivision scheme converges (converges uniformly) with respect to the multilevel grid $\boldsymbol{X}$, or that the subdivision scheme is $C^0(I, \mathbb{R}^d)$ with respect to $\boldsymbol{X}$. We say that a subdivision scheme is C^k if its limit curve $\boldsymbol{g}$ has continuous derivatives $\boldsymbol{g}^{(q)}(x)$ for $q = 0, 1, \ldots, k$, and $x \in I$. We remark that if a specific multi level grid is not specified in a convergence context, it is understood that a regular grid is used.

In this thesis, we use the convention that the control polygon is marked by dots connected by dashed lines, in the plots[5]. For a linear subdivision scheme it is more convenient to analyze each coordinate component independently with respect to (1.12), and thus using absolute values. We remark that in Definition 1.5.1 we implicitly demand uniform convergence, and although weaker conditions are available, uniform convergence shall be the focus in this thesis. This condition comes from the uniform convergence theorem. A convenient way to show that a sequence of polygons is a Cauchy sequence is presented in the following lemma.

Lemma 1.5.1. *[7] Given constants $C, \lambda \in \mathbb{R}_{>0}$ where $\lambda < 1$. If*

$$\|\boldsymbol{g}_{j+1} - \boldsymbol{g}_j\| \leq C\lambda^j, \quad j = 0, 1, 2, \ldots, \tag{1.13}$$

is satisfied, then the sequence $\{\boldsymbol{g}_j\}_{j=0,1,2,\ldots}$ is a Cauchy sequence.

Proof. Using the condition (1.13), we get that for $i > j \geq N$,

$$\begin{aligned}
\|\boldsymbol{g}_i - \boldsymbol{g}_j\| &\leq \|\boldsymbol{g}_{j+1} - \boldsymbol{g}_j\| + \|\boldsymbol{g}_{j+2} - \boldsymbol{g}_{j+1}\| + \cdots + \|\boldsymbol{g}_i - \boldsymbol{g}_{i-1}\| \\
&\leq C\lambda^j \sum_{k=0}^{i-j-1} \lambda^k = C\lambda^j \frac{1 - \lambda^{i-j}}{1 - \lambda} = C\frac{\lambda^j - \lambda^i}{1 - \lambda} \\
&\leq C\frac{\lambda^j}{1 - \lambda} \leq C\frac{\lambda^N}{1 - \lambda} \xrightarrow[N \to \infty]{} 0.
\end{aligned}$$

[5] Not necessarily always in the illustrations of various subdivision refinement rules.

Thus the result follows by choosing N large enough so that $C\lambda^N/(1-\lambda) \leq \epsilon$. □

Although some subdivision schemes are limited to a set degree of smoothness, they can sometimes be shown to be close to being the next degree of smoothness. I.e. there are cases where a subdivision scheme that is e.g. C^1 can be shown to be *almost* C^2, or somewhere between being C^1 and C^2. This concept can be studied using the notion of Hölder continuity.

Definition 1.5.2. *A function $f : [a,b] \to \mathbb{R}$ is called Hölder continuous with Hölder exponent $\beta \in (0,1)$, if there exists a real constant $C > 0$ such that*

$$|f(y) - f(x)| \leq C|y-x|^\beta \quad \forall \quad a \leq x < y \leq b,$$

for some parameter interval $[a,b]$, in which case say that $f \in C^\beta([a,b])$, or $f \in C^\beta$. If $f^{(q)} \in C^\beta$ for $q = 1,2,\ldots,k$, we write $f \in C^{k+\beta}$ or $f \in C^{k,\beta}$. In cases where β is allowed to be arbitrarily close but not equal to 1, we sometimes write $f \in C^{k+1-\epsilon}$, to indicate that f is almost C^{k+1}. Alternatively we can write $f \in C^{k,1}$. This notion of Hölder continuity extends naturally to subdivision schemes by applying it componentwise to the limit curve of a subdivision scheme.

Boundary conditions for subdivision schemes

If we start with a finite sequence of control points $\{\boldsymbol{p}_{0,k}\}_{k=0}^n$ and an m-point subdivision scheme, where $m \geq 4$ is an even number, we need in total $m/2$ extra points at the indices $-m/2,\ldots,-1$ and $n+1,\ldots,n+m/2$ in order for the limit curve to be defined for the whole of $x \in I$. Two-point schemes do by nature not require boundary conditions. The way the boundary problem is handled influences the geometry of the final limit curve. For closed control polygons, where the first and last control points are equal, then the natural choice of boundary conditions is to use a cyclical boundary. As this choice does not require any additional data points to be extrapolated in a not necessarily intuitive way at each end, we use closed control polygons and cyclical boundaries in almost every example in this thesis, and use simple linear extrapolation otherwise.

Some established results

It was shown in [10] that the FPTS is $C^{2-\epsilon}$ for $w \in \left(0, \frac{1+\sqrt{5}}{8}\right)$. Moreover, it was proven in [9] that the limit curve is C^1 if and only if $w \in (0, w^\star)$, $w^\star \approx 0.19278$. In [11] it was proven that the four-point scheme is C^1 for a dyadically balanced grid, as well as being $C^{2-\epsilon}$ Hölder continuous for $\lambda \leq 2/3$. Floater later improved this bound in [8], using an approach based on piecewise polynomials, and showed that the Hölder continuity holds

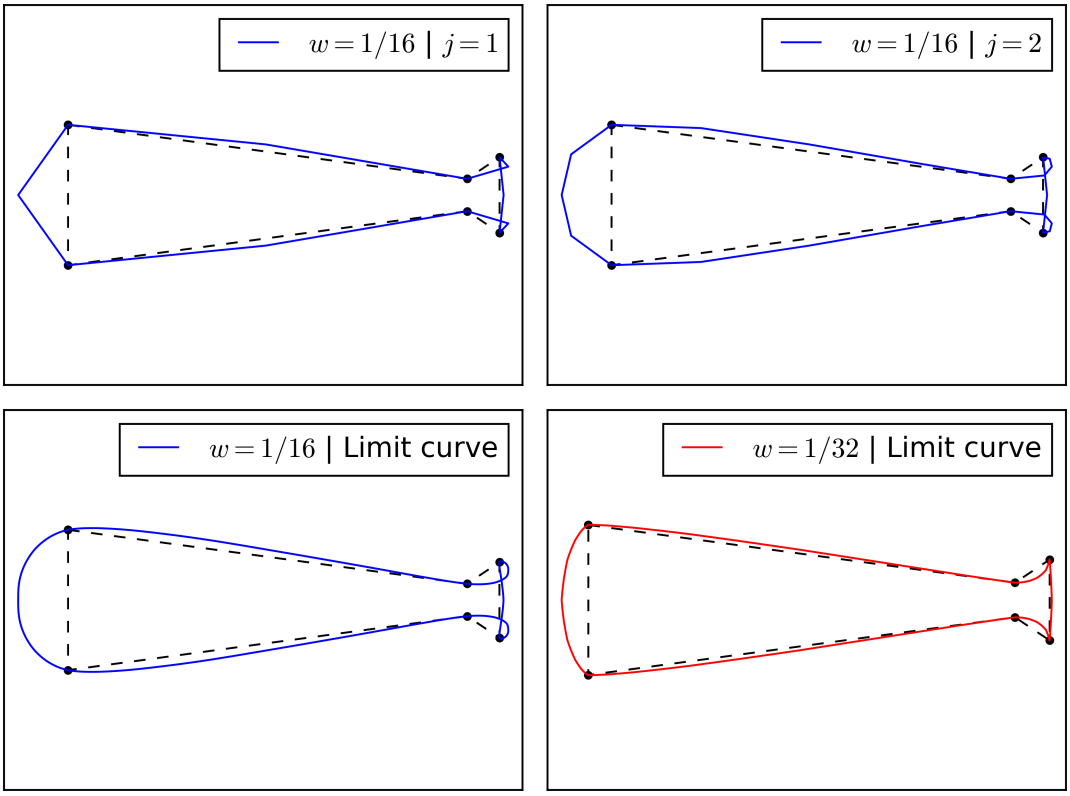

Figure 1.3: Different values of w for the FPTS with tension parameter w applied to a closed control polygon with control points in $\mathbb{R}^2$. The control points are based on one of the figures in [1].

for $\lambda \leq \lambda_0 \approx 0.7142$. In fact, the converse has also been shown, i.e. that loss of regularity may follow as a result of choosing too large of a deviation between new points and the midpoints of the previous level. Thus the four point scheme is implicitly also shown to be $C^{2-\epsilon}$ for the regular and semi-regular case. Below we will review some of the existing techniques for establishing some of the results stated above for the four-point scheme, but we will restrict the analysis to regular grids.

Chapter Two

Analysis of linear subdivision schemes

There have been developed many techniques for studying linear subdivision schemes. We shall in this chapter review the method of using divided differences for convergence analysis, but also a method based on Laurent polynomials. The analysis is here restricted to regular grids, but techniques also exist for generalizing these methods to other types of multilevel grids.

2.1 Convergence analysis using divided differences

We shall first investigate the smoothness of the four-point scheme defined on a regular grid, i.e. the FPS, using the formalism of divided differences as our approach. Let g_j be the linear interpolant at level j that interpolates all points in sequence, using the dyadic points as parameters. As these functions live on the prescribed grids X_j, and $[x_{j,i}, x_{j,i+1}]g_j$ resembles their discrete first derivatives at a point $x_{j,i}$, it is perhaps not too surprising that our first method of analysis will be based on this concept. We begin by proving that the four-point scheme converges to a continuous function, i.e. a function in C^0, and then establish using divided differences that this function is also in C^1.

In preparation of the theorem showing C^1 of the FPS, we will prove the following auxiliary lemma, which will be useful in our analysis.

Lemma 2.1.1. *Given a Bernstein basis function*

$$B_i^N(t) = \binom{N}{i} \left(\frac{t-a}{b-a}\right)^i \left(\frac{b-t}{b-a}\right)^{N-i}, \quad 0 \le i \le N, \tag{2.1}$$

on a real interval $[a, b]$*, and defining* $n := b - a$*, we have that*

$$\frac{d}{dt}B_i^N(t) = \frac{N}{n}\left(B_{i-1}^{N-1}(t) - B_i^{N-1}(t)\right). \tag{2.2}$$

Proof.

$$\begin{aligned}
\frac{d}{dt}B_i^N(t) &= \binom{N}{i}\left\{\frac{i}{n}\left(\frac{t}{n}\right)^{i-1}\left(1-\frac{t}{n}\right)^{N-i} - \left(\frac{t}{n}\right)^{i}\frac{N-i}{n}\left(1-\frac{t}{n}\right)^{N-i-1}\right\} \\
&= \frac{1}{n}\left\{\frac{N!i}{i!(N-i)!}\left(\frac{t}{n}\right)^{i-1}\left(1-\frac{t}{n}\right)^{N-i} - \right. \\
&\qquad \left.\frac{N!(N-i)}{i!(N-i)!}\left(\frac{t}{n}\right)^{i}\left(1-\frac{t}{n}\right)^{N-i-1}\right\} \\
&= \frac{1}{n}\left\{\frac{N(N-1)!}{(i-1)!(N-1)!}\left(\frac{t}{n}\right)^{i-1}\left(1-\frac{t}{n}\right)^{N-i} - \right. \\
&\qquad \left.\frac{N(N-1)!}{i!(N-i-1)!}\left(\frac{t}{n}\right)^{i}\left(1-\frac{t}{n}\right)^{N-i-1}\right\} \\
&= \frac{N}{n}\left(B_{i-1}^{N-1}(t) - B_i^{N-1}(t)\right).
\end{aligned}$$

□

The proof of the following theorem is based on [7] and [5]. This proof concentrates on a finite number of initial control points $\{p_{0,i}\}_{i=0}^{n}$, where it is assumed that the required boundary points also are assigned, and we here use the convention that $x_{0,0} = 0$ and $x_{0,n} = n$, such that $I = [0, n]$. This means that we use a regular grid with dyadic grid points.

Theorem 2.1.1. *The FPS is* $C^1([0, n], \mathbb{R}^d)$.

Proof. As discussed, we can work componentwise and thus analyze the one dimensional case. Let $g(x) := \lim_{j\to\infty} g_j(x)$ be the limit function of the FPS, where the g_j are the piecewise linear interpolants described above [1]. We observe that the difference $g_{j+1} - g_j$ is also a polygon, and that it must attain its maximum at an odd grid point $x_{j+1,2k+1}$, since the scheme is binary and interpolatory. Hence,

$$\|g_{j+1} - g_j\| = \max_k \left| p_{j+1,2k+1} - \frac{p_{j,k} + p_{j,k+1}}{2} \right|$$

[1] g_j is the piecewise linear interpolant to the data $(x_{j,k}, p_{j,k}) = (2^{-j}k, p_{j,k})$.

However, by defining the forward difference $\Delta p_{j,q} := p_{j,q+1} - p_{j,q} \,\forall\, q$, then we obtain from the subdivision scheme (1.4)–(1.5) that

$$\begin{aligned} p_{j+1,2k+1} - \frac{p_{j,k} + p_{j,k+1}}{2} &= \frac{1}{16}\Delta p_{j,k-1} - \frac{1}{16}\Delta p_{j,k+1} \\ \implies \|g_{j+1} - g_j\| &\leq \frac{1}{8}\max_k |\Delta p_{j,k}| \end{aligned}$$

Moreover, by taking differences in the subdivision scheme, we can obtain the forward difference variant of the scheme

$$\begin{aligned} \Delta p_{j+1,2k} &= p_{j+1,2k+1} - p_{j+1,2k} \\ &= \left\{ \frac{1}{16}\left(-p_{j,k-1} + 9p_{j,k} + 9p_{j,k+1} - p_{j,k+2}\right) \right\} - p_{j,k} \\ &= \frac{1}{16}\Delta p_{j,k-1} + \frac{1}{2}\Delta p_{j,k} - \frac{1}{16}\Delta p_{j,k+1}, \\ \Delta p_{j+1,2k+1} &= p_{j+1,2(k+1)} - p_{j+1,2k+1} \\ &= p_{j,k+1} - \left\{ \frac{1}{16}\left(-p_{j,k-1} + 9p_{j,k} + 9p_{j,k+1} - p_{j,k+2}\right) \right\} \\ &= -\frac{1}{16}\Delta p_{j,k-1} + \frac{1}{2}\Delta p_{j,k} + \frac{1}{16}\Delta p_{j,k+1}. \end{aligned}$$

Thus,

$$\max_k |\Delta p_{j+1,k}| \leq \frac{5}{8}\max_k |\Delta p_{j,k}|,$$

and consequently Lemma 1.5.1 is satisfied with $\lambda = 5/8$ and $C = \max_k |\Delta p_{0,k}|/8$. Therefore, we have established that the limit curve is C^0, and our next goal will be to investigate whether the C^1 criteria is fulfilled. To this end we will utilize the divided differences on the form

$$p^{[1]}_{j,k} := \frac{\Delta p_{j,k}}{x_{j,k+1} - x_{j,k}} = \frac{\Delta p_{j,k}}{2^{-j}} = 2^j \Delta p_{j,k},$$

and we introduce $g^{[1]}_j$ as the piecewise linear interpolant to the data $(x_{j,k}, p^{[1]}_{j,k})$. In order to guarantee that $g \in C^1$, we must ensure that the following two requirements are met:

(i) The sequence of polygons $\{g^{[1]}_j\}$ has a continuous limit $g^{[1]}(x) := \lim_{j\to\infty} g^{[1]}_j(x)$, $x \in [0, n]$.

(ii) $g'(x) = g^{[1]}(x) \quad \forall \quad x \in [0, n]$,

where $n := \max x_{0,k}$ is the grid point of the rightmost control point. To prove (i), we need in a similar fashion to the C^0 case, to establish that $\{g^{[1]}_j\}$ is a Cauchy sequence in

the max norm. From the forward difference scheme established above, we may as a result of the dyadic parameter values, easily extract a scheme for the first divided differences, namely

$$p^{[1]}_{j+1,2k} = \frac{1}{8}p^{[1]}_{j,k-1} + p^{[1]}_{j,k} - \frac{1}{8}p^{[1]}_{j,k+1}, \tag{2.3}$$

$$p^{[1]}_{j+1,2k+1} = -\frac{1}{8}p^{[1]}_{j,k-1} + p^{[1]}_{j,k} + \frac{1}{8}p^{[1]}_{j,k+1} \tag{2.4}$$

Moreover, since $g^{[1]}_{j+1} - g^{[1]}_j$ is also a polygon, then clearly it must take on its maximum value at one of the parameter values $x_{j+1,2k}$ or $x_{j+1,2k+1}$, so we have that

$$\begin{aligned}
\|g^{[1]}_{j+1} - g^{[1]}_j\| &\leq \max(\beta_{2k}, \beta_{2k+1}),\\
\beta_{2k} &:= \max_k \left|p^{[1]}_{j+1,2k} - p^{[1]}_{j,k}\right|,\\
\beta_{2k+1} &:= \max_k \left|p^{[1]}_{j+1,2k+1} - \frac{1}{2}\left(p^{[1]}_{j,k} + p^{[1]}_{j,k+1}\right)\right|.
\end{aligned}$$

Now, by using (2.3)–(2.4), it follows that

$$\begin{aligned}
\beta_{2k} &= \max_k \left|\frac{1}{8}p^{[1]}_{j,k-1} + \left(\frac{1}{8}p^{[1]}_{j,k} - \frac{1}{8}p^{[1]}_{j,k}\right) - \frac{1}{8}p^{[1]}_{j,k+1}\right|\\
&= \max_k \left|-\frac{1}{8}\Delta p^{[1]}_{j,k} - \frac{1}{8}\Delta p^{[1]}_{j,k-1}\right|,\\
\beta_{2k+1} &= \max_k \left|\frac{1}{8}p^{[1]}_{j,k} + \frac{3}{8}p^{[1]}_{j,k} - \frac{3}{8}p^{[1]}_{j,k+1} - \frac{1}{8}p^{[1]}_{j,k-1}\right|\\
&= \max_k \left|\frac{1}{8}\Delta p^{[1]}_{j,k-1} - \frac{3}{8}\Delta p^{[1]}_{j,k}\right|.
\end{aligned}$$

Furthermore, this implies that

$$\|g^{[1]}_{j+1} - g^{[1]}_j\| \leq \frac{1}{2}\max_k \left|\Delta p^{[1]}_{j,k}\right|.$$

Thus in order to use Lemma 1.5.1 on the sequence $\{g^{[1]}_j\}$, we now need to show that there exist new constants C and $\lambda < 1$ such that

$$\max_k \left|\Delta p^{[1]}_{j,k}\right| \leq C\lambda^j \quad \forall \quad j \in \mathbb{Z}_{\geq 0}.$$

From (2.3)–(2.4), we get the following difference scheme

$$\begin{aligned}
\Delta p^{[1]}_{j+1,2k} &= \frac{1}{4}\Delta p^{[1]}_{j,k-1} + \frac{1}{4}\Delta p^{[1]}_{j,k},\\
\Delta p^{[1]}_{j+1,2k+1} &= -\frac{1}{8}\Delta p^{[1]}_{j,k-1} + \frac{3}{4}\Delta p^{[1]}_{j,k} - \frac{1}{8}\Delta p^{[1]}_{j,k+1}.
\end{aligned}$$

However, this leads to an upper bound with $\lambda = 1$, which does not imply Cauchy. One way to remedy this is to take a second subdivision step. After some calculations, involving the techniques employed above, we find that

$$\begin{bmatrix} \Delta p^{[1]}_{j+2,4k} \\ \Delta p^{[1]}_{j+2,4k+1} \\ \Delta p^{[1]}_{j+2,4k+2} \\ \Delta p^{[1]}_{j+2,4k+3} \end{bmatrix} = \frac{1}{64} \begin{bmatrix} -2 & 16 & 2 & 0 \\ 1 & 7 & 7 & 1 \\ 0 & 2 & 16 & -2 \\ 0 & -8 & 32 & -8 \end{bmatrix} \begin{bmatrix} \Delta p^{[1]}_{j,k-2} \\ \Delta p^{[1]}_{j,k-1} \\ \Delta p^{[1]}_{j,k} \\ \Delta p^{[1]}_{j,k+1} \end{bmatrix},$$

which implies that

$$\max_k \left|\Delta p^{[1]}_{j+2,k}\right| \leq \frac{3}{4} \max_k \left|\Delta p^{[1]}_{j,k}\right|,$$

and thus

$$\max_k \left|\Delta p^{[1]}_{j+1,k}\right| \leq \frac{\sqrt{3}}{2} \max_k \left|\Delta p^{[1]}_{j,k}\right|.$$

Therefore, (i) is satisfied as Lemma 1.5.1 holds for the sequence $\{g^{[1]}_j\}$ with $C = \max_k |\Delta p^{[1]}_{0,k}|/2$ and $\lambda = \sqrt{3}/2$. Now, let $\phi_j(x)$ be the Bernstein polynomial to the $\{p_{j,k}\}$ on the interval $[0, n]$. We can then write

$$\phi_j(x) = \sum_{i=0}^{N} B_i^N(x) p_{j,i}, \quad N := 2^j n.$$

Note that the ϕ_j are in fact the functions used in the famous constructive proof of the Weierstrass approximation theorem based on Bernstein polynomials. By Lemma 2.1.1, we have that

$$\begin{aligned} \phi_j'(x) &= \frac{N}{n} \sum_{i=0}^{N-1} B_i^{N-1}(x) \{p_{j,i+1} - p_{j,i}\} = \frac{N}{n} \sum_{i=0}^{N-1} B_i^{N-1}(x) \Delta p_{j,i} \\ &= \sum_{i=0}^{N-1} B_i^{N-1}(x) 2^j \Delta p_{j,i} = \sum_{i=0}^{N-1} B_i^{N-1}(x) p^{[1]}_{j,i}, \end{aligned}$$

which is exactly the Bernstein polynomial to the $\{p^{[1]}_{j,k}\}$. We have that as $g_j \to g$ uniformly and $g^{[1]}_j \to f$ uniformly for some function $f \in C([0, n])$, then by the uniform convergence of the Bernstein polynomials, it follows that $f = g'$, and we conclude that $g'(x) = g^{[1]}(x)$ for all $x \in [0, n]$. Thus (ii) holds and the result follows. □

Alternatively, it is possible to show that $g(x) - g(0) = \int_0^x g^{[1]}(u)\, du$ for $x \in [0, n]$ by constructing a Riemann type sum based on the $(x_{j,k}, g^{[1]}_{j,k})$ that converges to the given integral, which is equivalent to (ii) by the fundamental theorem of calculus. Similar conditions are required for higher order continuity.

2.2 Convergence analysis using Laurent polynomials

An alternative while related method of analysis is the method of analyzing the Laurent polynomials generated from the masks of subdivision schemes. The results in this section are mainly based on [14].

For a stationary subdivision scheme with mask $\boldsymbol{m} = (m_k)_{k\in\mathbb{Z}}$, we define the z-transform m of the mask, or the symbol of the scheme, as the series

$$m(z) = \sum_{k\in\mathbb{Z}} m_k z^k.$$

We also define the z-transform F_j of the data $\{p_{j,k}\}$ at level j as

$$F_j(z) = \sum_{i\in\mathbb{Z}} p_{j,i} z^i.$$

This allows us to write the subdivision process as

$$F_{j+1}(z) = m(z)F_j(z^2).$$

Since the insertion rule of most subdivision schemes is connected to the points on either side of the insertion point, then the above series expansions involve polynomial powers of positive and negative degrees, and thus can be viewed as Laurent polynomials. In light of the four-point scheme with tension parameter w (FPTS) and mask

$$\boldsymbol{m} = \left(-w,\, 0\,,\, w+\frac{1}{2},\, 1,\, w+\frac{1}{2},\, 0,\, -w\right),$$

we find that its symbol can be written

$$\begin{aligned} m(z) &= -wz^{-3} + \left(w+\frac{1}{2}\right)z^{-1} + 1 + \left(w+\frac{1}{2}\right)z - wz^3 \\ &= \frac{(z+1)^2}{2z}\left\{1 - 2wz^{-2}(1-z)^2(z^2+1)\right\}. \end{aligned} \tag{2.5}$$

For some subdivision mask $\boldsymbol{m}$, we denote its corresponding subdivision scheme as $S_{\boldsymbol{m}}$.

Definition 2.2.1. *[14] A subdivision scheme $S_{\boldsymbol{b}}$, with mask $\boldsymbol{b}$ and symbol $b(z)$, is called contractive if there exists an $\ell \in \mathbb{Z}_{\geq 1}$ such that*

$$\|S_{\boldsymbol{b}}^{\ell}\|_\infty := \max\left\{\sum_{j\in\mathbb{Z}} \left|b^{[\ell]}_{i-2^\ell j}\right| \,:\, 0 \leq i < 2^\ell\right\} < 1,$$

where the $b_k^{[\ell]}$ are the coefficients of the Laurent polynomial

$$b^{[\ell]}(z) := \prod_{j=1}^{\ell} b(z^{2^{j-1}}).$$

Theorem 2.2.1. *[14] Let* $m(z) = \frac{(z+1)^{n+1}}{2^n} b(z)$ *with* $S_{\boldsymbol{b}}$ *contractive. Then the limit curve of* $S_{\boldsymbol{m}}$ *is* C^n*.*

Although the above theorem may seem somewhat complicated to use, it is in fact fairly easy to apply to a general uniform binary subdivision scheme. Increasing ℓ typically produces better contractive bounds when applied to a scheme with some parameter, e.g. the tension parameter w of FPTS. However, this may lead to more complicated Laurent polynomials, which makes analysis harder. It is also worth noting that for high ℓ, then a high number of subdivision steps is required for the corresponding smoothness to be visible, which means that one should consider a maximum ℓ.

Theorem 2.2.2. *The FPTS is*

$$C^0 \quad \textit{for} \quad w \in \left(-\frac{3}{8}, \frac{\sqrt{13}-1}{8}\right) \approx (-0.375,\, 0.325),$$
$$C^1 \quad \textit{for} \quad w \in \left(0, \frac{\sqrt{5}-1}{8}\right) \approx (0,\, 0.154).$$

Proof. Using Theorem 2.2.1 and (2.5), and looking at the $n = 0$ case for C^0 analysis, we find that for FPTS we clearly have

$$b^{[1]}(z) = b(z) = \frac{(z+1)}{2z}\left\{1 - 2wz^{-2}(1-z)^2(z^2+1)\right\},$$
$$b^{[2]}(z) = b(z)b(z^2) = \frac{(z+1)}{2z}\left\{1 - 2wz^{-2}(1-z)^2(z^2+1)\right\} \times \frac{(z^2+1)}{2z^2}\left\{1 - 2wz^{-4}(1-z^2)^2(z^4+1)\right\}$$

Thus,

$$\|S^1_{\boldsymbol{b}}\|_\infty = 2|w| + 1/2 < 1$$

which holds for $w \in (-1/4, 1/4)$. Increasing ℓ to $\ell = 2$ yields

$$\|S^2_{\boldsymbol{b}}\|_\infty = \max\Big(\Big|w^2 - w/2\Big| + \Big|-w^2 + w/2 + 1/4\Big| + 2w^2, \Big|w^2 + w\Big| + \Big|w^2 + w/2\Big| + \Big|w^2 - w/2 + 1/4\Big| + w^2\Big).$$

We find that $\|S^2_{\boldsymbol{b}}\|_\infty < 1$ holds for $w \in (-3/8,\, (\sqrt{13}-1)/8)$, in which case we have thus shown that the scheme has a C^0 limit.
Likewise, for $n = 1$, i.e. C^1 analysis,

$$b^{[1]}(z) = b(z) = z^{-1} - 2wz^{-3}(1-z)^2(z^2+1),$$
$$b^{[2]}(z) = (z^{-1} - 2wz^{-3}(1-z)^2(z^2+1))(z^{-2} - 2wz^{-6}(1-z^2)^2(z^4+1)).$$

The case $\ell = 1$ is inconclusive, but for $\ell = 2$ we get

$$\|S_{\boldsymbol{b}}^2\|_\infty = \max\left(2\left|4w^2 - 2w\right| + 8w^2,\, 4|w| + 16w^2,\, |8w-1| + 4|w|\right) < 1$$
$$\implies w \in \left(0,\, \frac{\sqrt{5}-1}{8}\right).$$

And hence, the limit curve is C^1 for $w \in (0,\, (\sqrt{5}-1)/8)$. Note that duplicate inequalities, due to symmetries in the Laurent polynomial coefficients, have been intentionally omitted as they do not influence the results. Note also that the approximations in the approximate intervals are chosen such that the numbers are not rounded outside the permissible values. □

Programmatic Laurent analysis

It is actually possible, and not overly difficult using symbolic computing, to write a program that takes the symbol $m(z)$, or mask $\boldsymbol{m}$, of a general stationary and uniform linear subdivision scheme $S_{\boldsymbol{m}}$ with some parameter w and outputs the bounds on w for $S_{\boldsymbol{m}}$ to be C^n, for some chosen n and ℓ. Using this program, it is then easy to analyze convergence of linear schemes, needing only to find their mask, and avoiding all the tedious details of the previous divided difference proof method. Take for example the approximating four-point scheme [24], by the same authors as [1], given as

$$p_{j+1,2k} = -7wp_{j,k-1} + \left(\frac{3}{4} + 9w\right)p_{j,k} + \left(\frac{1}{4} + 3w\right)p_{j,k+1} - 5wp_{j,k+2},$$
$$p_{j+1,2k+1} = -5wp_{j,k-1} + \left(\frac{1}{4} + 3w\right)p_{j,k} + \left(\frac{3}{4} + 9w\right)p_{j,k+1} - 7wp_{j,k+2}.$$

We find that its symbol is

$$m(z) = -5w(z^{-3} + z^4) - 7w(z^{-2} + z^3) + \left(\frac{1}{4} + 3w\right)(z^{-1} + z^2) + \left(\frac{3}{4} + 9w\right)(z+1)$$

Using the symbol $\boldsymbol{m}$ directly as input into a program `laur`, which just implements the symbolic details of the Laurent analysis and solves the resulting inequalities, we get

```
>>laur(m, ell=2, n=2)

0 < w < 6^(1/2)/80 - 1/80
```

This is exactly the interval $w \in (0, (\sqrt{6}-1)/80)$ for C^2 found by the authors in [24], and demonstrates just how simple the Laurent polynomial analysis of linear stationary subdivision schemes on regular grids really can be. In chapter 4 we will use this method on a linear subfamily of a family of nonlinear schemes to prove smoothness bounds.

2.3 Application to nonlinear subdivision

We finally note that the entire linear subdivision analysis machinery relies on the simplicity of the concept of subdivision masks, and if we cannot access such a mask nor a subdivision matrix that holds in general, then little of the analysis of this chapter is applicable. This is also true for the other main methods of linear subdivision such as eigenanalysis and Fourier analysis.

Some techniques exist for studying the proximity of a nonlinear subdivision scheme to a linear subdivision scheme. If the nonlinear scheme is in a sense sufficiently close to the linear scheme then properties such as smoothness can be inherited by the nonlinear scheme. See e.g. the paper [26] by Wallner and Dyn for more information about this. The main nonlinear schemes we will discuss in this thesis are however not compliant with these proximity conditions.

We remark that it is possible to construct basis functions from linear subdivision schemes and write the limit function as a linear combination of these and the control points, which also means that proving convergence and smoothness for tensor product linear subdivision schemes becomes trivial. As such basis functions do not necessarily exist for nonlinear subdivision, we shall not review it here.

Chapter Three

Nonlinear interpolatory subdivision schemes

A nonlinear subdivision scheme is characterized by the fact that the linear combination in the rule (1.1) is replaced by nonlinear operations on the data, and does not necessarily abide by the concept of subdivision masks, which the divided difference and Laurent polynomial analysis, among others, strongly rely on. As several of the nonlinear schemes we consider in this thesis are defined such that the coordinate component of a new point is dependent on not just the same coordinate at the previous level, it makes more sense to use an alternative to (1.12) to study these schemes. We in some instances instead define

$$\|\boldsymbol{f}\|_\infty := \sup_{x\in\mathbb{R}} \|\boldsymbol{f}(x)\|_2, \tag{3.1}$$

where $\|\cdot\|_2$ is the Euclidean norm, and we use vectors in our arguments. By the equivalence of norms in finite dimensional vector spaces, and in particular that $\|\boldsymbol{v}\|_\infty \leq \|\boldsymbol{v}\|_2$ for $\boldsymbol{v} \in \mathbb{R}^d$, this is well founded. Note that we here have omitted I and just write $x \in \mathbb{R}$ as this interval is in many respects arbitrary, and we can select it as large as we want when given an infinite sequence of control points.

As we saw in the previous chapters, linear interpolatory subdivision schemes pose a powerful method for generating smooth interpolants to data. In this chapter, we show two nonlinear schemes as examples of how the analysis of nonlinear schemes may differ from that of linear schemes.

3.1 Fractal subdivision (Koch snowflake)

The purpose of subdivision schemes is not always to generate limit curves of high smoothness. In fact, it is possible to construct schemes that yield fractal limit curves, i.e. curves of a self-similar nature that are nowhere smooth. One such scheme, which in fact also is interpolatory, for the Koch snowflake fractal, discovered in 1904 by Helge von Koch [16] and regarded as one of the earliest discovered fractals, can be written as follows for planar control points,

$$\boldsymbol{p}_{j+1,4k} = \boldsymbol{p}_{j,k}, \tag{3.2}$$

$$\boldsymbol{p}_{j+1,4k+1} = \boldsymbol{p}_{j,k} + \frac{1}{3}(\boldsymbol{p}_{j,k+1} - \boldsymbol{p}_{j,k}) =: \boldsymbol{b}, \tag{3.3}$$

$$\boldsymbol{p}_{j+1,4k+2} = \boldsymbol{b} + \boldsymbol{R}_{\frac{\pi}{3}}(\boldsymbol{b} - \boldsymbol{p}_{j,k}), \tag{3.4}$$

$$\boldsymbol{p}_{j+1,4k+3} = \boldsymbol{p}_{j,k} + \frac{2}{3}(\boldsymbol{p}_{j,k+1} - \boldsymbol{p}_{j,k}), \tag{3.5}$$

$$\text{where } \boldsymbol{R}_{\frac{\pi}{3}} := \begin{bmatrix} \cos(\frac{\pi}{3}) & -\sin(\frac{\pi}{3}) \\ \sin(\frac{\pi}{3}) & \cos(\frac{\pi}{3}) \end{bmatrix} = \frac{1}{2}\begin{bmatrix} 1 & -\sqrt{3} \\ \sqrt{3} & 1 \end{bmatrix}. \tag{3.6}$$

We note that the scheme has arity 4[1], and that it is a type of two-point scheme as only $\boldsymbol{p}_{j,k}$ and $\boldsymbol{p}_{j,k+1}$ are used for computing the points $\{\boldsymbol{p}_{j+1,4k+i}\}_{i=0}^{3}$. However, as the points $\boldsymbol{p}_{j+1,4k+2}$ are formed by a matrix-vector product using the rotation matrix $\boldsymbol{R}_{\frac{\pi}{3}}$, which is not a linear combination in each of the coordinates, then the scheme is nonlinear. In Figure 3.1, the process at each level of subdivision is evident, and the self-similarity aspects of the fractal limit curve are clearly visible in the zoomed region. Interestingly and somewhat counterintuitively, the shape of the limit curve of the scheme applied to initial data amounting to the corners of an equilateral triangle, as in Figure 3.1, can be shown to have an infinite perimeter while having finite area. Furthermore, this last observation is in fact related to many features in nature, such as the measurement of geographical coastlines, where the accuracy of physical measurements always can be increased, leading to a fractal-like scenario.

Theorem 3.1.1. *The Koch scheme is C^0.*

Proof. Note that as the scheme is nonlinear in the sense that the rule (3.4) makes the spatial coordinates not independent at each subdivision step, then it is necessary to work with the vectors $\boldsymbol{p}_{j,k} \in \mathbb{R}^2$ in our arguments. Let $\boldsymbol{g}_j$ be the piecewise linear interpolant to the data $(x_{j,k}, \boldsymbol{p}_{j,k})_{k\in\mathbb{Z}}$, where $x_{j,k} := 4^{-j}k$. Note that these $\{x_{j,k}\}$ constitute a regular grid for a subdivision scheme of arity $a = 4$. The maximum difference between $\boldsymbol{g}_{j+1}$ and $\boldsymbol{g}_j$ is determined by the rule (3.4) with the difference being largest at

[1]Which means that the scheme is *quaternary*.

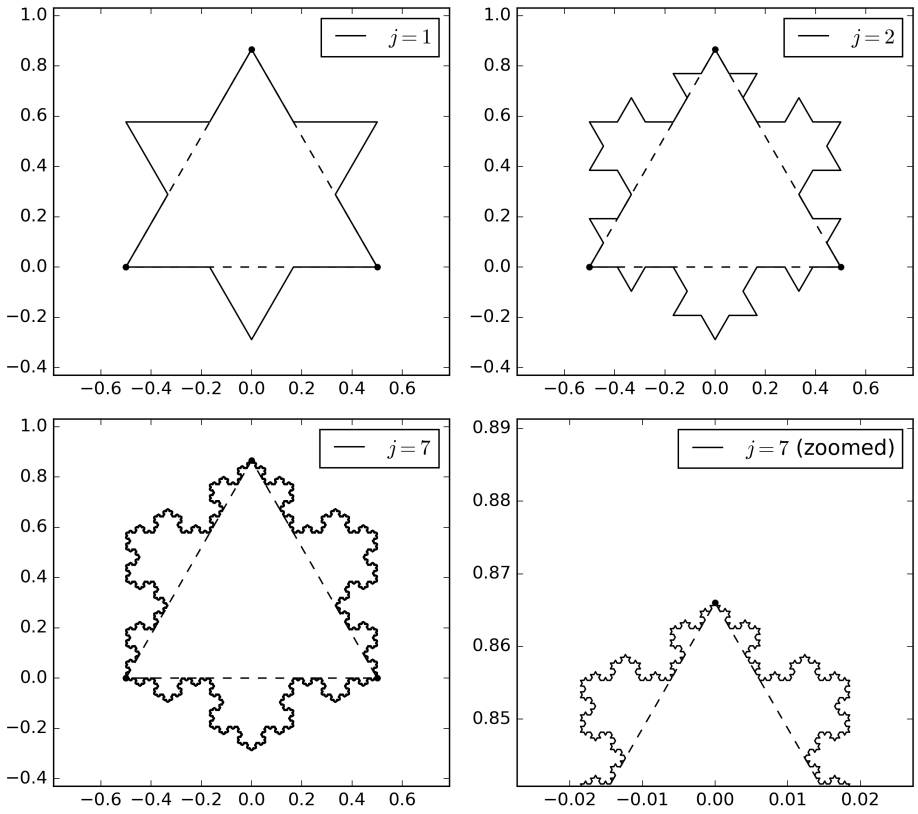

Figure 3.1: Koch snowflake curve at various stages of subdivision. The bottom right plot is a zoomed in view of the curve near the uppermost control polygon at level $j = 7$.

the maximum of the distances between the apex $\boldsymbol{p}_{j+1,4k+2}$ of the equilateral triangle $\boldsymbol{p}_{j+1,4k+1}$, $\boldsymbol{p}_{j+1,4k+2}$, $\boldsymbol{p}_{j+1,4k+3}$, and its orthogonal projection onto the line between $\boldsymbol{p}_{j,k}$ and $\boldsymbol{p}_{j,k+1}$, i.e. simply the point $(\boldsymbol{p}_{j,k} + \boldsymbol{p}_{j,k+1})/2$. It thus follows that

$$\|\boldsymbol{g}_{j+1} - \boldsymbol{g}_j\|_\infty = \frac{\sqrt{3}}{6} \sup_{k\in\mathbb{Z}} \|\Delta \boldsymbol{p}_{j,k}\|_2,$$

where $\Delta \boldsymbol{p}_{j,k} = \boldsymbol{p}_{j,k+1} - \boldsymbol{p}_{j,k}$ and we used Pythagoras' theorem to find the relative height of the triangle. Moreover, we have that

$$\sup_{k\in\mathbb{Z}} \|\Delta \boldsymbol{p}_{j,k}\|_2 \leq \frac{1}{3} \sup_{k\in\mathbb{Z}} \|\Delta \boldsymbol{p}_{j-1,k}\|_2 \leq \cdots \leq \left(\frac{1}{3}\right)^j \sup_{k\in\mathbb{Z}} \|\Delta \boldsymbol{p}_{0,k}\|_2.$$

Therefore,

$$\|\boldsymbol{g}_{j+1} - \boldsymbol{g}_j\|_\infty \leq \frac{\sqrt{3}}{6} \left(\frac{1}{3}\right)^j \sup_{k\in\mathbb{Z}} \|\Delta \boldsymbol{p}_{0,k}\|_2,$$

which implies C^0 as the sequence $\{\boldsymbol{g}_j : j \in \mathbb{Z}_{\geq 0}\}$ is a Cauchy sequence in the ∞-norm by Lemma 1.5.1. □

We note that the ordering of the control points influences which way the rotation matrix $\boldsymbol{R}_{\frac{\pi}{3}}$ places the new insertion point about the previous edge. However, we could just as easily have used $\boldsymbol{R}_{\frac{-\pi}{3}}$, as no assumption about this was used the proof of Theorem 3.1.1. In Figure 3.2, the points control points are sampled outward, and we observe that the fractals segments are oriented inwards. We remark that even though the proof would be analogous for an $\mathbb{R}^3$ extension of the scheme, the two-point nature of the scheme does not allow for an unique axis of rotation to be determined at each insertion, without further modifications. Although the Koch scheme is inherently nonlinear, we have seen that the proof for its C^0 convergence if fairly similar in principle to that of the regular four-point scheme, even though the subdivision mask is not obtainable. This is due to the very simple nature of the nonlinearity in the insertion rules, but we shall see in the following chapters that this very mild case is not characteristic for all nonlinear schemes.

In [19] a more general class of p-ary subdivision schemes based on normal vectors is presented, where a vast family of known and new fractals, including the Koch curve and the Sierpiński gasket, are possible limit curves. However, the proofs for C^0 of many of these schemes will be similar to the one above, as simple geometrical constructs are used to insert every new point.

3.2 Adaptive tension parameter

Before moving on to the highly nonlinear schemes of the next chapter, we shall here briefly look at a nonlinear scheme that is based on the FPTS. Although the tension parameter w of the FPTS may be lowered from $w = 1/16$ to mitigate the visual artifacts of the limit curve, especially when used on control points of significantly uneven spacing, this causes the limit curve to appear less smooth with a finite number of subdivision steps. This apparent loss of smoothness is particularly visible at the original control points, even though the limit curve is shown to be C^1 in Theorem 2.2.2. This can be seen in Figure 1.3 and Figure 3.3. Furthermore, there is no clear strategy for choosing a global tension parameter w that works well in general for some given sequence of control points. A way around this problem, introduced in [17] by Marinov et al., is to use geometrically controlled tension parameters $w_{j,k}$, dependent on j and k, which means that the scheme is both nonstationary and nonuniform. The standard nonuniform and nonstationary four-point scheme with variable tension parameters $\{w_{j,k}\}$ can be written

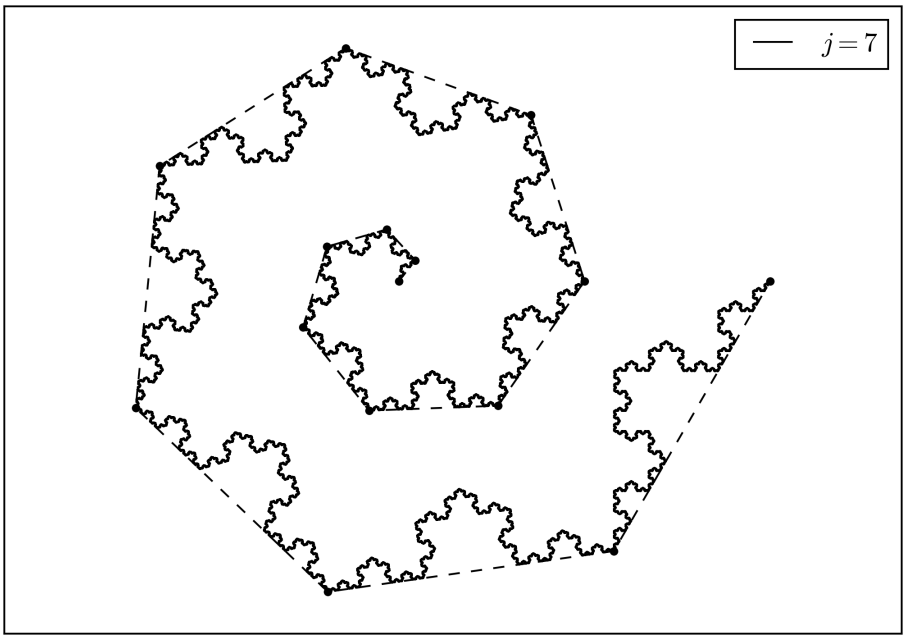

Figure 3.2: Koch scheme applied to control points sampled from a spiral.

as follows,

$$p_{j+1,2k} = p_{j,k}, \tag{3.7}$$

$$p_{j+1,2k+1} = -w_{j,k}\left(p_{j,k-1} + p_{j,k+2}\right) + \left(\frac{1}{2} + w_{j,k}\right)\left(p_{j,k} + p_{j,k+1}\right). \tag{3.8}$$

It turns out that one can adapt the Laurent analysis of the previous chapter to work with schemes of this type, as done in [18] by Levin. We paraphrase the following useful theorem from that paper.

Theorem 3.2.1. *[18] If $\{w_{j,k}\}$ are the tension parameters of the scheme* (3.7)–(3.8)*, and $w_{j,k} \in (0, 1/8)\,\forall\, k \in \mathbb{Z}$, $j \in \mathbb{Z}_{\geq 0}$, then the scheme is C^1.*

We define $\boldsymbol{e}_{j,k} := \boldsymbol{p}_{j,k+1} - \boldsymbol{p}_{j,k}$, and let the $w_{j,k}$ be defined as the composition $f \circ g$ of two specialized functions f and g. The function $g(j,k)$ is called a *characterizing* function, which measures the regularity of the edge $\boldsymbol{e}_{j,k}$, and the function $f(x)$, which is called a *selecting* function, maps the range of g into the range of possible tension parameters. In [17], the following rule for generating the $\{w_{j,k}\}$ is proposed,

$$g(j,k) = \frac{3\|\boldsymbol{e}_{j,k}\|}{\|\boldsymbol{e}_{j,k-1}\| + \|\boldsymbol{e}_{j,k}\| + \|\boldsymbol{e}_{j,k}\|}, \quad f(x) = \begin{cases} Wx, & 0 \leq x \leq 1, \\ W, & 1 < x \leq 3, \end{cases} \tag{3.9}$$

where $W \in \mathbb{R}$ is a constant, and $g(j,k) := 0$ if $\|\boldsymbol{e}_{j,k-1}\| + \|\boldsymbol{e}_{j,k}\| + \|\boldsymbol{e}_{j,k}\| = 0$. This means that $w_{j,k} = f(g(j,k))$. Typically $W := 1/16$ is chosen such that for an edge of high regularity, the canonical four-point scheme is used for that insertion. Since the tension parameters depend nonlinearly on the points, then the scheme is therefore also nonlinear. Clearly, using $W = 1/16$, then $w_{j,k} < 1/8$ is satisfied. To guarantee that the limit curve using this rule will be C^1, we have to ensure that the $\{w_{j,k}\}$ are bounded away from zero. A strategy from [17] to achieve this, is to first complete a set amount of subdivision steps with the adaptive rule above, and then for each subsequent step let

$$w_{j+1,2k} = \max(\tilde{w}_{j+1,2k}, w_{j,k}), \quad w_{j+1,2k+1} = \max(\tilde{w}_{j+1,2k+1}, w_{j,k}), \tag{3.10}$$

where the $\tilde{w}_{j+1,2k+1}$ and $\tilde{w}_{j+1,2k}$ are computed without this modification, i.e. using the adaptive rules. By Theorem 3.2.1, the scheme (3.7) – (3.10) is C^1. In Figure 3.3, the advantage of the adaptive scheme for a control polygon of highly varying edge lengths, versus the standard FPS and the FPTS with lowered tension parameter, is apparent.

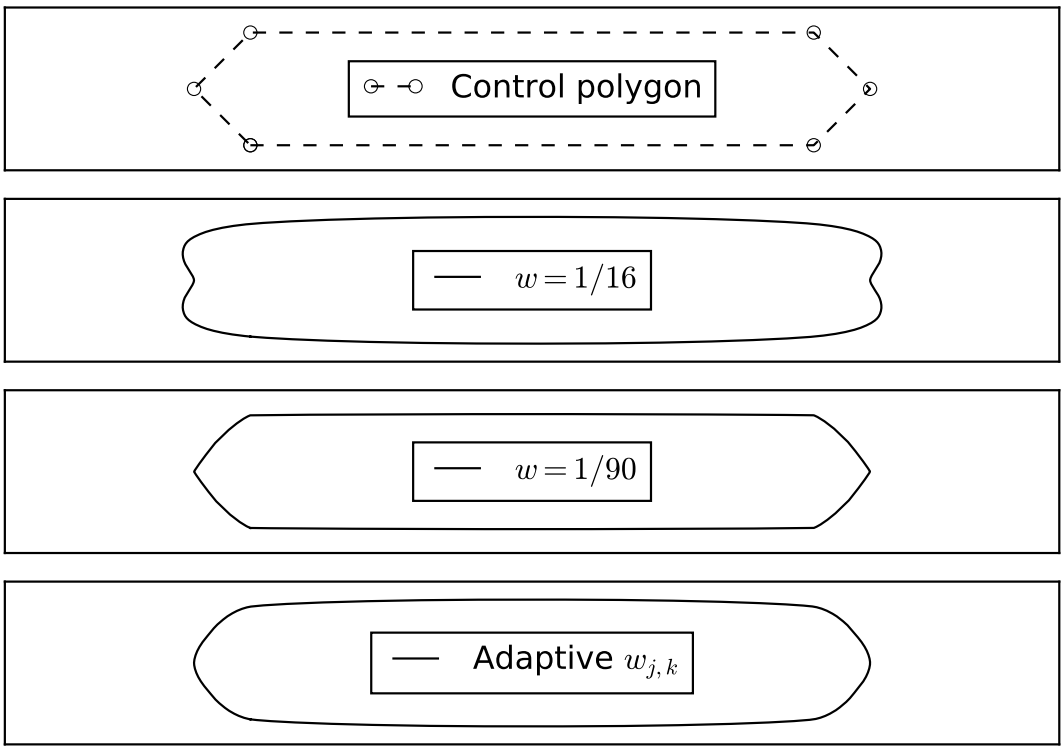

Figure 3.3: Effect of the adaptive tension parameter scheme using (3.9) compared to the FPTS with different w.

Chapter Four

Iterated geometric schemes

The nonlinear schemes we saw in chapter 3 had properties outside what is possible with linear schemes. They were however analyzable with techniques adapted from the analysis of linear subdivision schemes. The schemes we now present, based on the paper [1] by Dyn, Floater and Hormann, are in a sense more nonlinear and thus outside the scope of most types of analysis.

4.1 The iterated geometric schemes

Let $P_0 = \{\boldsymbol{p}_{0,k} : k \in \mathbb{Z}\}$ such that $\boldsymbol{p}_{0,k} \neq \boldsymbol{p}_{0,k+1}$, be the set of initial control points with $\boldsymbol{p}_{0,k} \in \mathbb{R}^d$, $d \in \mathbb{Z}_{\geq 1}$. As usual, we are only interested in a finite number of P_0 for actual applications. Let then $P_j = \{\boldsymbol{p}_{j,k} : k \in \mathbb{Z}\}$, with $\boldsymbol{p}_{j,k} \in \mathbb{R}^d$, be the set of refined points at level j. Generally, we can define the class of binary iterated geometric schemes in the following manner. At each level $j \in \mathbb{Z}_{\geq 0}$, we define the parameterization

$$t_{j,k+1} - t_{j,k} = \|\boldsymbol{p}_{j,k+1} - \boldsymbol{p}_{j,k}\|_2^{\alpha}, \quad t_{j,0} = 0, \quad k \in \mathbb{Z}, \tag{4.1}$$

where the parameterization process at each level j will from now on be referred to as an α-*parameterization*. Likewise, we define an $\alpha-$*interpolant* as the polynomial interpolant to data using an α-parameterization. Importantly, the α-parameterization is recomputed at each level, and is not the same as the grid points $\{x_{j,k}\}$ we assign to $\boldsymbol{g}_j$. Given an even integer $m \geq 2$, the subdivision refinement rules for the iterated geometric m-point schemes (IGm-schemes), are defined as

$$\boldsymbol{p}_{j+1,2k} = \boldsymbol{p}_{j,k}, \tag{4.2}$$

$$\boldsymbol{p}_{j+1,2k+1} = \boldsymbol{\pi}_{j,k}^{m}(t_\star), \tag{4.3}$$

$$t_\star := \frac{t_{j,k} + t_{j,k+1}}{2}, \tag{4.4}$$

where $\boldsymbol{\pi}_{j,k}^m$ is the odd degree $m-1$ Lagrange interpolant to the data $\{\boldsymbol{p}_{j,i}\}_{i=k-m/2+1}^{k+m/2}$ at the parameter values $\{t_{j,i}\}_{i=k-m/2+1}^{k+m/2}$, and $t_\star := (t_{j,k} + t_{j,k+1})/2$ is the evaluation point. For $m = 4$, we get the scheme in the original article [1], and for $m = 6$ we get the corresponding six-point scheme, both of which shall be discussed in particular in this thesis. For convenience, we will from now on refer to the iterated geometric scheme for $m = 4$ as the IG4-scheme, the scheme for $m = 6$ as the IG6-scheme, and in general the m-point scheme as the IGm-scheme. Observe that for $\alpha = 0$, the IGm-schemes coincide with the linear m-point Dubuc-Deslauriers schemes, but for $\alpha \neq 0$, the IGm-schemes are inherently nonlinear.

As in chapter 3, we let $\boldsymbol{e}_{j,k} := \boldsymbol{p}_{j,k+1} - \boldsymbol{p}_{j,k}$. It is often enough to look at a local insertion when considering subdivision schemes of this type, where the cumbersome indexation $i = k - m/2 + 1, \dots, k + m/2$ is replaced with $i = 0, \dots, m-1$, and the level j may be left out as the same process happens at each level. To this end, we introduce a list of definitions to simplify notation in these cases,

$$\begin{aligned} \boldsymbol{e}_i &:= \Delta_+ \boldsymbol{p}_i = \boldsymbol{p}_{i+1} - \boldsymbol{p}_i, \quad l_i := \|\boldsymbol{e}_i\|_2, \quad u_i := l_i^\alpha, \\ u_{[a,b]} &:= (u_a + \cdots + u_b), \quad L_i^\star := L_i(t_\star), \end{aligned} \tag{4.5}$$

where the L_i are the Lagrangian basis functions, and it is understood that the above notation also applies analogously to cases where we use the standard indexation $k - m/2 + 1, \dots, k + m/2$. The $\boldsymbol{e}_i$ can be thought of as edge vectors, and are not to be confused with the Cartesian unit vectors. Sometimes we also write $\boldsymbol{p}_m^\star := \boldsymbol{p}_{j+1,2k+1}$ to denote the new point at each insertion where the m-point scheme was used. If the degree is obvious we may also simply write $\boldsymbol{p}^\star$. Using (4.5), we in particular have from the α-parameterization that $t_{i+1} - t_i = \|\boldsymbol{e}_i\|^\alpha = l_i^\alpha = u_i$, so that we may use telescoping sums and $u_{[a,b]}$ to greatly simplify notation in cases such as for example

$$t_3 - t_0 = (t_3 - t_2) + (t_2 - t_1) + (t_1 - t_0) = u_0 + u_1 + u_2 = u_{[0,2]}.$$

This means that we can write the Lagrange basis functions, evaluated at $t_\star$, only based on the u_i. For example the first cubic Lagrange basis function evaluated at $t_\star$, in the context of the IG4-scheme, can be written as

$$\begin{aligned} L_0^\star = L_0(t_\star) = L_0\left(\frac{t_1+t_2}{2}\right) &= \prod_{\substack{r=0 \\ r\neq 0}}^{3} \frac{t_\star - t_r}{t_0 - t_r} = \frac{(t_\star - t_1)(t_\star - t_2)(t_\star - t_3)}{(t_0 - t_1)(t_0 - t_2)(t_0 - t_3)} \\ &= \frac{(\{t_1+t_2\} - 2t_1)(\{t_1+t_2\} - 2t_2)(\{t_1+t_2\} - 2t_3)}{(2\{t_0 - t_1\})(2\{t_0 - t_2\})(2\{t_0 - t_3\})} \\ &= \frac{(t_2 - t_1)(t_1 - t_2)(t_1 + t_2 - 2t_3)}{8(t_0 - t_1)(t_0 - t_2)(t_0 - t_3)} = \frac{(u_1)(-u_1)(-\{u_1 + 2u_2\})}{8(-u_0)(-\{u_0 + u_1\})(-\{u_0 + u_1 + u_2\})} \\ &= -\frac{u_1^2(u_1 + 2u_2)}{8u_0(u_0 + u_1)(u_0 + u_1 + u_2)} = -\frac{u_1^2(u_1 + 2u_2)}{8u_0 u_{[0,1]} u_{[0,2]}}. \end{aligned} \tag{4.6}$$

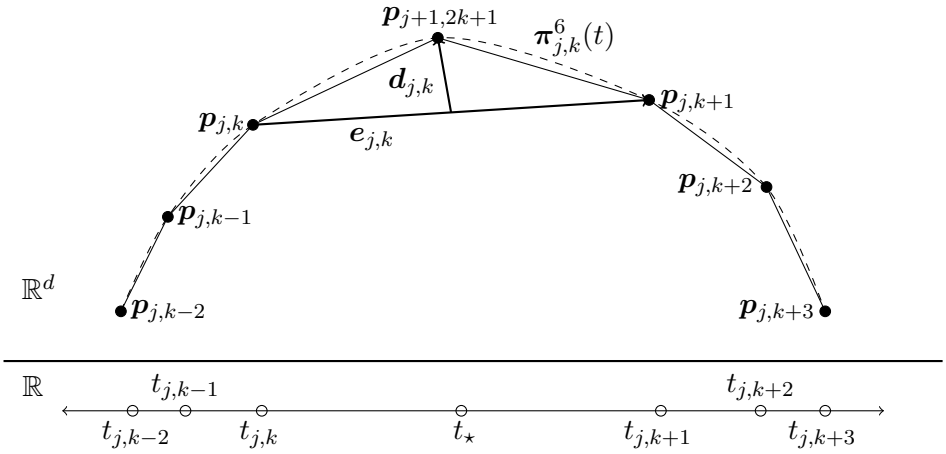

Figure 4.1: Illustration of the six-point iterated geometric subdivision refinement rule.

A key ingredient in many of the following proofs will be studying the vector

$$\boldsymbol{d}_{j,k} = \boldsymbol{p}_{j+1,2k+1} - \frac{\boldsymbol{p}_{j,k} + \boldsymbol{p}_{j,k+1}}{2}, \tag{4.7}$$

which may be viewed as a displacement vector between the new point $\boldsymbol{p}_{j+1,2k+1}$ and the center of the middle edge $\boldsymbol{e}_{j,k}$. Note that this vector is different for each IGm-scheme, since $\boldsymbol{p}_{j+1,2k+1}$ is not defined equally for all IGm-schemes. See Figure 4.1 for an illustration of this vector for the IG6-scheme, based on Figure 1 of [1].

4.2 Convergence of the IG4-scheme

It is readily apparent that the method of analysis used on the standard four-point scheme will not work for this family of nonlinear schemes, as the insertion rule is data-dependent and the parameterization itself is recomputed at each level based on the previous geometry. In [1], a more geometric approach is utilized to prove C^0 convergence of the IG4-scheme for certain values of α, which we shall review here. Many of the proofs of this section will therefore be based on [1]. Furthermore, we will later investigate the IG4- and IG6-schemes for values of α in the entire interval $\alpha \in [0, 1]$. In preparation of the convergence proof, the following lemma on polynomial interpolation is proved.

Lemma 4.2.1. *[1] Consider cubic polynomial interpolation, with data points $y_i = f(t_i)$, and parameter values t_i, $i = 0, 1, 2, 3$. Let g be the cubic polynomial that satisfies $g(t_i) = y_i$, $i = 0, 1, 2, 3$, and let h be the linear polynomial that satisfies $h(t_i) = y_i$, $i = 1, 2$.*

Then,

$$g(t) - h(t) = \frac{(t-t_1)(t-t_2)}{t_3-t_0}\left((t_3-t)[t_0,t_1,t_2]f + (t-t_0)[t_1,t_2,t_3]f\right) \;\forall\, t \in \mathbb{R}.$$

Proof. Let $\{\tilde{t_0},\tilde{t_1},\tilde{t_2},\tilde{t_3}\}$ be an ordering of the parameters $\{t_0,t_1,t_2,t_3\}$. Then by writing out the Newton forms of g and h, we get

$$\begin{aligned} g(t) &= f(\tilde{t_0}) + (t-\tilde{t_0})[\tilde{t_0},\tilde{t_1}]f + (t-\tilde{t_0})(t-\tilde{t_1})[\tilde{t_0},\tilde{t_1},\tilde{t_2}]f \\ &\quad + (t-\tilde{t_0})(t-\tilde{t_1})(t-\tilde{t_2})[\tilde{t_0},\tilde{t_1},\tilde{t_2},\tilde{t_3}]f, \\ h(t) &= f(\tilde{t_0}) + (t-\tilde{t_0})[\tilde{t_0},\tilde{t_1}]f. \\ \implies d(t) := g(t) - h(t) &= (t-\tilde{t_0})(t-\tilde{t_1})[\tilde{t_0},\tilde{t_1},\tilde{t_2}]f \\ &\quad + (t-\tilde{t_0})(t-\tilde{t_1})(t-\tilde{t_2})[\tilde{t_0},\tilde{t_1},\tilde{t_2},\tilde{t_3}]f. \end{aligned}$$

So fixing $\{\tilde{t_0},\tilde{t_1},\tilde{t_2},\tilde{t_3}\} \to \{t_1,t_2,t_0,t_3\}$ yields

$$\begin{aligned} d(t) &= (t-t_1)(t-t_2)[t_0,t_1,t_2]f + (t-t_0)(t-t_1)(t-t_2)[t_0,t_1,t_2,t_3]f \\ &= (t-t_1)(t-t_2)[t_0,t_1,t_2]f + (t-t_0)(t-t_1)(t-t_2)\frac{[t_1,t_2,t_3]f - [t_0,t_1,t_2]f}{t_3-t_0} \\ &= \frac{(t-t_1)(t-t_2)}{t_3-t_0}\left((t_3-t)[t_0,t_1,t_2]f + (t-t_0)[t_1,t_2,t_3]f\right). \end{aligned}$$

□

At the evaluation point $t_\star = (t_1+t_2)/2$ for the IG4-scheme, Lemma 4.2.1 reads

$$\begin{aligned} d(t_\star) &= \frac{(t_\star-t_1)(t_\star-t_2)}{t_3-t_0}\left((t_3-t_\star)[t_0,t_1,t_2]f + (t_\star-t_0)[t_1,t_2,t_3]f\right) \\ &= -\frac{1}{4}\frac{(t_2-t_1)^2}{t_3-t_0}\left((t_3-t_\star)[t_0,t_1,t_2]f + (t_\star-t_0)[t_1,t_2,t_3]f\right) \end{aligned} \tag{4.8}$$

It is now convenient to introduce the following definition of divided differences of the vector data and the corresponding parameters.

Definition 4.2.1. *Let*

$$\boldsymbol{p}_{j,k}^{[r]} := \frac{\boldsymbol{p}_{j,k+1}^{[r-1]} - \boldsymbol{p}_{j,k}^{[r-1]}}{t_{j,k+r} - t_{j,k}} \quad \forall r \geq 1, \quad \boldsymbol{p}_{j,k}^{[0]} := \boldsymbol{p}_{j,k},$$

denote the r-th divided difference at the vector points P_j with respect to the parameters $\{t_{j,k}\}_{k\in\mathbb{Z}}$.

Combined with the subdivision rule for the IG4-scheme, this allows us to write the following lemma, containing two convenient forms of the vector $\boldsymbol{d}_{j,k}$ in (4.7).

Lemma 4.2.2. *[1] For the IG4-scheme,*

$$\boldsymbol{d}_{j,k} = -\frac{1}{4}\frac{(t_{j,k+1}-t_{j,k})^2}{a+b+1}\left((a+1/2)\boldsymbol{p}^{[2]}_{j,k} + (b+1/2)\boldsymbol{p}^{[2]}_{j,k-1}\right), \tag{4.9}$$

$$\boldsymbol{d}_{j,k} = -\frac{1}{4}\frac{t_{j,k+1}-t_{j,k}}{a+b+1}\left(A(\boldsymbol{p}^{[1]}_{j,k+1} - \boldsymbol{p}^{[1]}_{j,k}) + B(\boldsymbol{p}^{[1]}_{j,k} - \boldsymbol{p}^{[1]}_{j,k-1})\right), \tag{4.10}$$

where

$$a := \frac{t_{j,k}-t_{j,k-1}}{t_{j,k+1}-t_{j,k}}, \quad b := \frac{t_{j,k+2}-t_{j,k+1}}{t_{j,k+1}-t_{j,k}}, \quad A := \frac{a+1/2}{b+1}, \quad B := \frac{b+1/2}{a+1}.$$

Proof. This follows easily by using the definition of $\boldsymbol{d}_{j,k}$ for the IG4-scheme, and using (4.8) in vector form. □

It shall now be our aim to prove the following lemma, showing that the norm of the $\boldsymbol{d}_{j,k}$ vector is bounded by a constant less than one times the max of a selection of the norms of the surrounding edge lengths $\{\|\boldsymbol{e}_{j,i}\|\}_{i=k-1}^{k+1}$.

Lemma 4.2.3. *[1] For the IG4-scheme,*

$$\|\boldsymbol{d}_{j,k}\| \le \frac{1}{8}\max\left(\|\boldsymbol{e}_{j,k-1}\|, \|\boldsymbol{e}_{j,k+1}\|\right) \quad \textit{for} \quad \alpha = 0, \tag{4.11}$$

$$\|\boldsymbol{d}_{j,k}\| \le \frac{1}{4}\|\boldsymbol{e}_{j,k}\| \quad \textit{for} \quad \alpha = \frac{1}{2}, \tag{4.12}$$

$$\|\boldsymbol{d}_{j,k}\| \le \frac{3}{8}\max\left(\|\boldsymbol{e}_{j,k-1}\|, \|\boldsymbol{e}_{j,k}\|, \|\boldsymbol{e}_{j,k+1}\|\right) \quad \forall\, \alpha \in [0,1], \tag{4.13}$$

$$\|\boldsymbol{d}_{j,k}\| < \frac{1}{2}\|\boldsymbol{e}_{j,k}\| \quad \textit{for} \quad \alpha = 1. \tag{4.14}$$

The estimate (4.13) *only holds if the points P_j and P_{j+1} are well defined.*

Proof. For $\alpha = 0$ (uniform parameterization),
$\boldsymbol{p}^{[1]}_{j,k} = \boldsymbol{e}_{j,k}/(\|\boldsymbol{e}_{j,k}\|^0) = \boldsymbol{e}_{j,k}$. Therefore,

$$\boldsymbol{p}^{[2]}_{j,k} = \frac{\boldsymbol{p}^{[1]}_{j,k+1} - \boldsymbol{p}^{[1]}_{j,k}}{t_{j,k+2}-t_{j,k}} = \frac{\boldsymbol{p}^{[1]}_{j,k+1} - \boldsymbol{p}^{[1]}_{j,k}}{2} = \frac{\boldsymbol{e}_{j,k+1} - \boldsymbol{e}_{j,k}}{2}.$$

We have that $a = b = 1$ in (4.9), so (4.9) reduces to

$$\boldsymbol{d}_{j,k} = -\frac{1}{16}\left(\boldsymbol{e}_{j,k+1} - \boldsymbol{e}_{j,k-1}\right),$$

which implies that

$$\|\boldsymbol{d}_{j,k}\| \leq \frac{1}{8}\max\left(\|\boldsymbol{e}_{j,k-1}\|, \|\boldsymbol{e}_{j,k+1}\|\right).$$

For $\alpha = 1/2$ (centripetal parameterization),

$$\|\boldsymbol{p}^{[2]}_{j,k}\| \leq \frac{\|\boldsymbol{p}^{[1]}_{j,k+1}\| + \|\boldsymbol{p}^{[1]}_{j,k}\|}{t_{j,k+2} - t_{j,k}} = \frac{\|\boldsymbol{p}^{[1]}_{j,k+1}\| + \|\boldsymbol{p}^{[1]}_{j,k}\|}{\|\boldsymbol{e}_{j,k+1}\|^{1/2} + \|\boldsymbol{e}_{j,k}\|^{1/2}} = \frac{\|\boldsymbol{e}_{j,k+1}\|^{1/2} + \|\boldsymbol{e}_{j,k}\|^{1/2}}{\|\boldsymbol{e}_{j,k+1}\|^{1/2} + \|\boldsymbol{e}_{j,k}\|^{1/2}} = 1.$$

By using (4.9), the required result (4.12) follows immediately, i.e.

$$\|\boldsymbol{d}_{j,k}\| \leq \frac{1}{4}\|\boldsymbol{e}_{j,k}\|,$$

since $(t_{j,k+1} - t_{j,k})^2 = (\|\boldsymbol{e}_{j,k}\|^{\frac{1}{2}})^2 = \|\boldsymbol{e}_{j,k}\|$.
For $\alpha \in [0, 1]$ (general α-parameterization),

$$\|\boldsymbol{p}^{[1]}_{j,k}\| = \frac{\|\boldsymbol{p}_{j,k+1} - \boldsymbol{p}_{j,k}\|}{t_{j,k+1} - t_{j,k}} = \frac{\|\boldsymbol{e}_{j,k}\|}{\|\boldsymbol{e}_{j,k}\|^{\alpha}} = \|\boldsymbol{e}_{j,k}\|^{1-\alpha}.$$

Thus, using (4.10),

$$\|\boldsymbol{d}_{j,k}\| \leq \frac{1}{4}\frac{\|\boldsymbol{e}_{j,k}\|^{\alpha}}{a+b+1}\left\{A\|\boldsymbol{e}_{j,k+1}\|^{1-\alpha} + |A-B|\|\boldsymbol{e}_{j,k}\|^{1-\alpha} + B\|\boldsymbol{e}_{j,k-1}\|^{1-\alpha}\right\}.$$

We now first look at the case $a \geq b$, which implies $A \geq B$ and $|A - B| = A - B$. Therefore,

$$\|\boldsymbol{d}_{j,k}\| \leq \frac{1}{2}\frac{\|\boldsymbol{e}_{j,k}\|^{\alpha}\Gamma_{j,k}^{1-\alpha}A}{a+b+1}, \quad \Gamma_{j,k} := \max_{i=k-1,k,k+1}\left(\|\boldsymbol{e}_{j,i}\|\right).$$

Furthermore, by using the definition of A, and that $a, b > 0$,

$$\begin{aligned}\|\boldsymbol{d}_{j,k}\| &\leq \frac{2a+1}{4(a+b+1)(b+1)}\|\boldsymbol{e}_{j,k}\|^{\alpha}\Gamma_{j,k}^{1-\alpha} \leq \frac{2a+1}{4(a+1)}\|\boldsymbol{e}_{j,k}\|^{\alpha}\Gamma_{j,k}^{1-\alpha} \\ &= C(a)\|\boldsymbol{e}_{j,k}\|^{\alpha}\Gamma_{j,k}^{1-\alpha}, \quad C(a) := \frac{2a+1}{4(a+1)}.\end{aligned} \tag{4.15}$$

Letting $a \leq 1$ implies

$$\|\boldsymbol{d}_{j,k}\| \leq \frac{3}{8}\|\boldsymbol{e}_{j,k}\|^{\alpha}\Gamma_{j,k}^{1-\alpha} \leq \frac{3}{8}\Gamma_{j,k}^{\alpha}\Gamma_{j,k}^{1-\alpha} = \frac{3}{8}\Gamma_{j,k},$$

where we have used that $C(a)$ has a positive derivative for $a \in (0, 1]$, and therefore attains its maximum $3/8$ at $a = 1$. By instead looking at $a \geq 1$, and using the fact that $a = (\|\boldsymbol{e}_{j,k-1}\|^{\alpha})/(\|\boldsymbol{e}_{j,k}\|^{\alpha})$, then

$$\|\boldsymbol{d}_{j,k}\| \leq \frac{2a+1}{4a(a+1)}\|\boldsymbol{e}_{j,k-1}\|^{\alpha}\Gamma_{j,k}^{1-\alpha} \leq \frac{3}{8}\Gamma_{j,k},$$

where we used that the function $D(a) := (2a+1)/(4a[a+1])$ has a negative derivative for $a \geq 1$, and therefore attains its maximum $3/8$ at $a = 1$.
We now look at the opposite case $b \geq a$, which implies that $B \geq A$ and that $|A - B| = B - A$. It then follows that

$$\begin{aligned} \|\boldsymbol{d}_{j,k}\| &\leq \frac{1}{2}\frac{\|\boldsymbol{e}_{j,k}\|^{\alpha}\Gamma_{j,k}^{1-\alpha}B}{a+b+1} = \frac{2b+1}{4(a+b+1)(a+1)}\|\boldsymbol{e}_{j,k}\|^{\alpha}\Gamma_{j,k}^{1-\alpha} \\ &\leq \frac{2b+1}{4(b+1)}\|\boldsymbol{e}_{j,k}\|^{\alpha}\Gamma_{j,k}^{1-\alpha}. \end{aligned} \tag{4.16}$$

It is now evident that the bound $\|\boldsymbol{d}_{j,k}\| \leq (3/8)\Gamma_{j,k}$ also holds for the case $b \geq a$, as we can simply apply analogous arguments as above for $b \leq 1$ and $b \geq 1$ where we use $\|\boldsymbol{e}_{j,k+1}\|$ instead of $\|\boldsymbol{e}_{j,k-1}\|$, since $b = (\|\boldsymbol{e}_{j,k+1}\|^{\alpha})/(\|\boldsymbol{e}_{j,k}\|^{\alpha})$. Thus (4.13) holds in general for all $\alpha \in [0,1]$, assuming that the points P_j and P_{j+1} are well defined.
For $\alpha = 1$ (chordal parameterization),
$\|\boldsymbol{e}_{j,k}\|^{\alpha}\Gamma_{j,k}^{1-\alpha} = \|\boldsymbol{e}_{j,k}\|\Gamma_{j,k}^{0} = \|\boldsymbol{e}_{j,k}\|$, so the bound (4.14) follows from (4.15) for $a \geq b$, since $(2a+1)/(4(a+1)) < 1/2$ for $a > 0$, and similarly from (4.16) for $b \geq a$, since $(2b+1)/(4(b+1)) < 1/2$ for $b > 0$. This completes the proof. □

We will now use Lemma 4.2.3 to prove the following result, stating that the edge lengths $\|\boldsymbol{e}_{j+1,2k}\|$ and $\|\boldsymbol{e}_{j+1,2k+1}\|$ on each side of the inserted point $\boldsymbol{p}_{j+1,2k+1}$ indeed get shorter as the subdivision level j increases.

Lemma 4.2.4. *[1] For the IG4-scheme, the following bounds hold.*
For $\alpha = 0$,

$$\max\left(\|\boldsymbol{e}_{j+1,2k}\|,\, \|\boldsymbol{e}_{j+1,2k+1}\|\right) \leq \frac{5}{8}\max\left(\|\boldsymbol{e}_{j,k-1}\|,\, \|\boldsymbol{e}_{j,k}\|,\, \|\boldsymbol{e}_{j,k+1}\|\right).$$

For $\alpha = 1/2$,

$$\max\left(\|\boldsymbol{e}_{j+1,2k}\|,\, \|\boldsymbol{e}_{j+1,2k+1}\|\right) \leq \frac{3}{4}\|\boldsymbol{e}_{j,k}\|.$$

For $\alpha \in [0,1]$,

$$\max\left(\|\boldsymbol{e}_{j+1,2k}\|,\, \|\boldsymbol{e}_{j+1,2k+1}\|\right) \leq \frac{7}{8}\max\left(\|\boldsymbol{e}_{j,k-1}\|,\, \|\boldsymbol{e}_{j,k}\|,\, \|\boldsymbol{e}_{j,k+1}\|\right). \tag{4.17}$$

For $\alpha = 1$,

$$\max\left(\|\boldsymbol{e}_{j+1,2k}\|,\, \|\boldsymbol{e}_{j+1,2k+1}\|\right) < \|\boldsymbol{e}_{j,k}\|.$$

Similarly to Lemma 4.2.3, (4.17) *only holds if the points* P_j *and* P_{j+1} *are well defined.*

Proof. The results easily follow by the definitions of $\boldsymbol{e}_{j,k}$ and $\boldsymbol{d}_{j,k}$ and using Lemma 4.2.3, so we here only show the case (4.17). Assuming that the points P_j and P_{j+1} are well defined, we have that

$$\begin{aligned}
\boldsymbol{e}_{j+1,2k} &= \boldsymbol{p}_{j+1,2k+1} - \boldsymbol{p}_{j+1,2k} = \boldsymbol{p}_{j+1,2k+1} - \boldsymbol{p}_{j,k} \\
&= \boldsymbol{p}_{j+1,2k+1} - \frac{\boldsymbol{p}_{j,k} + \boldsymbol{p}_{j,k+1}}{2} + \frac{\boldsymbol{p}_{j,k+1} - \boldsymbol{p}_{j,k}}{2} = \frac{\boldsymbol{e}_{j,k}}{2} + \boldsymbol{d}_{j,k}, \\
\boldsymbol{e}_{j+1,2k+1} &= \boldsymbol{p}_{j+1,2(k+1)} - \boldsymbol{p}_{j+1,k+1} = \boldsymbol{p}_{j,k+1} - \boldsymbol{p}_{j+1,2k+1} \\
&= \frac{\boldsymbol{p}_{j,k+1} - \boldsymbol{p}_{j,k}}{2} - \left(\boldsymbol{p}_{j+1,2k+1} - \frac{\boldsymbol{p}_{j,k+1} + \boldsymbol{p}_{j,k}}{2} \right) = \frac{\boldsymbol{e}_{j,k}}{2} - \boldsymbol{d}_{j,k}.
\end{aligned}$$

Therefore, by Lemma 4.2.3 with $\alpha \in [0, 1]$,

$$\begin{aligned}
\|\boldsymbol{e}_{j+1,2k}\| &\leq \frac{1}{2}\|\boldsymbol{e}_{j,k}\| + \|\boldsymbol{d}_{j,k}\| \leq \frac{1}{2}\|\boldsymbol{e}_{j,k}\| + \frac{3}{8} \max_{i=k-1,k,k+1} (\|\boldsymbol{e}_{j,i}\|) \\
&\leq \frac{7}{8} \max_{i=k-1,k,k+1} (\|\boldsymbol{e}_{j,i}\|), \\
\|\boldsymbol{e}_{j+1,2k+1}\| &\leq \frac{1}{2}\|\boldsymbol{e}_{j,k}\| + \|\boldsymbol{d}_{j,k}\| \leq \frac{7}{8} \max_{i=k-1,k,k+1} (\|\boldsymbol{e}_{j,i}\|).
\end{aligned}$$

Thus the result follows by taking the maximum of $\|\boldsymbol{e}_{j+1,2k}\|$ and $\|\boldsymbol{e}_{j+1,2k+1}\|$. □

Lemma 4.2.5. *For the IG4-scheme, the points P_j at any level j are well defined for $\alpha = 1/2$ and $\alpha = 1$. Thus,* (4.13) *and* (4.17) *hold unconditionally for $\alpha = 1/2$ and $\alpha = 1$.*

Proof. This follows from Lemma 4.2.3 as $\|\boldsymbol{d}_{j,k}\| < (1/2)\|\boldsymbol{e}_{j,k}\|$ for both $\alpha = 1/2$ and $\alpha = 1$, which means that $\boldsymbol{p}_{j,k} \neq \boldsymbol{p}_{j,k+1}$ always holds and $\boldsymbol{p}_{j+1,2k+1}$ is well defined. □

We have now developed the tools needed to prove the C^0 convergence of the IG4-scheme for certain values of α, namely the centripetal and chordal choices.

Theorem 4.2.1. *[1] The IG4-scheme is C^0 for $\alpha = 1/2$ and for $\alpha = 1$.*

Proof. By Lemma 4.2.5, the points P_j at every level of subdivision are well defined for both $\alpha = 1/2$ and $\alpha = 1$. Let $\boldsymbol{g}_j$ be the piecewise linear interpolant to the data $(2^{-j}k, \boldsymbol{p}_{j,k})$. We have that

$$\|\boldsymbol{g}_{j+1} - \boldsymbol{g}_j\|_\infty = \sup_{x \in \mathbb{R}} \|\boldsymbol{g}_{j+1}(x) - \boldsymbol{g}_j(x)\| = \sup_{k \in \mathbb{Z}} \|\boldsymbol{d}_{j,k}\|.$$

For both cases of $\alpha \in \{1/2, 1\}$, it follows from Lemma 4.2.3 that

$$\|\boldsymbol{g}_{j+1} - \boldsymbol{g}_j\|_\infty \leq \frac{3}{8} \sup_{k \in \mathbb{Z}} \|\boldsymbol{e}_{j,k}\|.$$

Therefore, by Lemma 4.2.4 lemma, we get

$$\sup_{k\in\mathbb{Z}} \|\boldsymbol{e}_{j,k}\| \leq \eta \sup_{k\in\mathbb{Z}} \|\boldsymbol{e}_{j-1,k}\| \leq \cdots \leq \eta^j \sup_{k\in\mathbb{Z}} \|\boldsymbol{e}_{0,k}\|, \tag{4.18}$$

where $\eta < 1$ is a positive constant. Thus the sequence $\{\boldsymbol{g}_j\}_{j\in\mathbb{Z}_{\geq 0}}$ is a Cauchy sequence in the sup norm, which implies that the scheme is C^0 in both cases, and the proof is complete. □

As mentioned by the authors in [1], the estimates (4.13) and (4.17) hold for all $\alpha \in [0, 1]$, assuming that the points P_j and P_{j+1} are well defined, and one would thus expect the scheme to produce a C^0 limit curve for the entire range $[0, 1]$ of α. However, there may be cases where the points after subdivision are not consecutively distinct, which implies that points on the subsequent level are not well defined. This is not further investigated in [1], but will be a fairly large topic in this thesis.

4.3 Validity of the iterated geometric schemes

The only scenario where P_{j+1} for an iterated geometric scheme is not defined for a new level $j + 1$ of subdivision, is if the points at the previous level j are not consecutively distinct, such that two parameters $t_{j,k}, t_{j,k+1}$ become equal, and a division by zero appears in the evaluation of the Lagrangian basis functions. It was stated in [1] that the authors had found examples for $\alpha = [0, 1/2)$ where this occurred, but no proof that such examples exist for every $\alpha \in [0, 1/2)$ is given in [1]. The aim in this section is to formally prove that consecutive distinctness is not guaranteed for any $\alpha \in [0, 1/2)$, for both the IG4- and IG6-schemes. Contrarily, we show that consecutive distinctness is guaranteed for all $\alpha \in [1/2, 1]$ for the IG4-scheme, which will also lead to a more general C^0 result. To this end we introduce the following definition.

Definition 4.3.1. *Let the control point data $\{\boldsymbol{p}_{0,k}\}_{k\in\mathbb{Z}}$, $d \in \mathbb{Z}_{\geq 1}$, satisfy*

$$\boldsymbol{p}_{0,k} \neq \boldsymbol{p}_{0,k+1} \quad \forall \quad k \in \mathbb{Z},$$

then this data is called consecutively distinct. If

$$\boldsymbol{p}_{j,k} \neq \boldsymbol{p}_{j,k+1} \quad \forall \quad k \in \mathbb{Z}, \quad j \in \mathbb{Z}_{\geq 1}, \tag{4.19}$$

where $\{\boldsymbol{p}_{j,i}\}_{i\in\mathbb{Z}}$ are the points generated by a subdivision scheme applied to consecutively distinct initial data, i.e. that consecutive distinctness of the data is guaranteed at all levels j of subdivision, then the scheme is called safe. On the other hand, if it can be shown that (4.19) *does not hold, then the scheme is called unsafe.*

To prove that a binary interpolatory subdivision scheme is unsafe, it it suffices to show that there exists a solution to the invalidity problem for the scheme, given by

$$\boldsymbol{p}_{j+1,2k+1} = \boldsymbol{p}_{j,k} \quad \text{or} \quad \boldsymbol{p}_{j+1,2k+1} = \boldsymbol{p}_{j,k+1}, \tag{4.20}$$

for some level $j \geq 0$ and index $k \in \mathbb{Z}$, where the initial points are assumed to be consecutively distinct. Remark that not being able to prove that a scheme is safe is not the same as the scheme being unsafe, because it is required that the invalidity problem for the scheme is shown to have a solution. For some schemes, such as the iterated geometric m-point schemes, the two cases of (4.20) become equivalent by symmetry, so we only need to show that $\boldsymbol{p}_{j+1,2k+1} = \boldsymbol{p}_{j,k}$, and it also suffices to look at the first subdivision step. In the proof of the following theorem, we show the existence of solutions to the invalidity problem for the IG4- and IG6-schemes by analyzing the algebraic expressions arising from choosing variable control points.

Theorem 4.3.1. *The IG4- and IG6-schemes are unsafe for all $\alpha \in [0, 1/2)$.*

Proof. Our general strategy for this proof, for both the IG4- and IG6-schemes, will be to write the problem as a nonlinear equation in one variable x, where α is a parameter that controls the behavior of the equation, and show that this equation must have a solution for all $\alpha \in [0, 1/2)$. We start with the IG4-scheme, and construct dynamic control points as follows,

$$p_1 = 0, \quad p_2 = 1, \quad p_0 = x, \quad p_3 = x + 1, \tag{4.21}$$

where we without loss of dimensional generality choose control points in $\mathbb{R}$, and moreover we assume that $x > 0$ and $x \in \mathbb{R}$. Note in particular that the control points $\{p_i\}_{i=0}^3$ are not in order by index on the line, and note also that x is just a variable here and is not related to the x of $\boldsymbol{g}$ and $\boldsymbol{g}_j$. In the general $\mathbb{R}^d$ case, we can simply let e.g. $\boldsymbol{p}_i = p_i \boldsymbol{i}_v$, $\boldsymbol{i}_v \in \mathbb{R}^d$, $d \in \mathbb{Z}_{\geq 1}$, for some fixed $v \in \{0, 1, \ldots, d-1\}$, where $\boldsymbol{i}_v$ is the v-th Cartesian unit vector, such that the points are located on a straight line along one of the coordinate axes[1] in $\mathbb{R}^d$. See Figure 4.3 for a basic illustration. In general we have that the IG4 invalidity problem is

$$\sum_{i=0}^{3} \boldsymbol{p}_i L_i^\star = \boldsymbol{p}_1 \implies (\boldsymbol{p}_0 - \boldsymbol{p}_1)L_0^\star + (\boldsymbol{p}_2 - \boldsymbol{p}_1)L_2^\star + (\boldsymbol{p}_3 - \boldsymbol{p}_1)L_3^\star = 0,$$

where we used the Lagrange form of the α-interpolant, and the partition of unity property of the Lagrange basis functions. Rewriting this in terms of differences of control points, $\boldsymbol{e}_i = \boldsymbol{p}_{i+1} - \boldsymbol{p}_i$, yields

$$-\boldsymbol{e}_0 L_0^\star + \boldsymbol{e}_1 L_2^\star + (\boldsymbol{e}_1 + \boldsymbol{e}_2)L_3^\star = 0, \tag{4.22}$$

[1] For example the y-axis.

where

$$L_0^\star = -\frac{u_1^2(u_1+2u_2)}{8u_0u_{[0,1]}u_{[0,2]}}, \quad L_2^\star = \frac{(2u_0+u_1)(u_1+2u_2)}{8u_{[0,1]}u_2}, \quad L_3^\star = -\frac{u_1^2(2u_0+u_1)}{8u_2u_{[1,2]}u_{[0,2]}}, \tag{4.23}$$

and we used the local notation (4.5) and the strategy from (4.6). By using the control point construction (4.21), and observing that only the v-th equation of the nonlinear system (4.22) is nontrivial, i.e. all the other equations in the system hold for all x, we get

$$\begin{bmatrix} e_0 \\ l_0 \\ u_0 \end{bmatrix} = \begin{bmatrix} -x \\ x \\ x^\alpha \end{bmatrix}, \quad \begin{bmatrix} e_1 \\ l_1 \\ u_1 \end{bmatrix} = \begin{bmatrix} 1 \\ 1 \\ 1 \end{bmatrix}, \quad \begin{bmatrix} e_2 \\ l_2 \\ u_2 \end{bmatrix} = \begin{bmatrix} x \\ x \\ x^\alpha \end{bmatrix},$$
$$L_0^\star = L_3^\star = -\frac{1}{8x^\alpha(x^\alpha+1)}, \quad L_2^\star = \frac{(2x^\alpha+1)^2}{8x^\alpha(x^\alpha+1)},$$

where we let e_i be the nonzero v-th element of $\boldsymbol{e}_i$ for all indices i. Thus, the one dimensional case[2] of (4.22) becomes

$$-e_0L_0^\star + e_1L_2^\star + (e_1+e_2)L_3^\star =$$
$$(2x+1)L_0^\star + L_2^\star = \frac{(2x^\alpha+1)^2}{8x^\alpha(x^\alpha+1)} - \frac{(2x+1)}{8x^\alpha(x^\alpha+1)} = 0.$$

By factoring out the common denominator $D = 8x^\alpha(x^\alpha+1)$, we get

$$\frac{1}{D}\left\{(2x^\alpha+1)^2 - (2x+1)\right\} = \frac{1}{D}\left\{a(x) - b(x)\right\} = 0, \tag{4.24}$$

where

$$a(x) := (2x^\alpha+1)^2 = 4x^{2\alpha} + 4x^\alpha + 1,$$
$$b(x) := 2x+1.$$

By looking at the interior equation $a(x) = b(x)$ of (4.24), we observe that since $a(x) = O(x^{2\alpha})$, $b(x) = 2x + o(x)$, for $\alpha \geq 0$ as $x \to \infty$, then we get the exponent inequality $2\alpha < 1 \implies \alpha < 1/2$. Here, O and o denote the Big-O and little-o notations, respectively[3]. Thus, for $\alpha \in [0, 1/2)$, $b(x)$ is a linear polynomial function that will dominate the strictly sublinear function $a(x) = o(x)$ as x grows. It is now sufficient to show that there exists an $\tilde{x} \in (0, \infty)$ such that $a(\tilde{x}) \geq b(\tilde{x})$. For simplicity, we choose $\tilde{x} = 1$. So the inequality $a(\tilde{x}) \geq b(\tilde{x})$ becomes

$$(2+1)^2 \geq 2+1 \implies 9 \geq 3,$$

[2]Meaning that we only consider the control points (4.21) in $\mathbb{R}$, and do not need to consider the general $\mathbb{R}^d$ case.

[3]We use the little-o notation here to more precisely write "+ lower order terms".

which clearly holds, and the result follows as there then exists a solution $x \in (1,\infty)$ to $a(x) = b(x)$ for all $\alpha \in [0,1/2)$, since a, b are continuous in the interval in question. Hence a solution exists to the invalidity problem (4.22). This proves that the IG4-scheme is unsafe for all $\alpha \in [0,1/2)$, as claimed.
Consider next the invalidity problem for the IG6-scheme,

$$\sum_{i=0}^{5} \boldsymbol{p}_i L_i^\star = \boldsymbol{p}_2.$$

This can be written as

$$-(\boldsymbol{e}_0+\boldsymbol{e}_1)L_0^\star - \boldsymbol{e}_1 L_1^\star + \boldsymbol{e}_2 L_3^\star + (\boldsymbol{e}_2+\boldsymbol{e}_3)L_4^\star + (\boldsymbol{e}_2+\boldsymbol{e}_3+\boldsymbol{e}_4)L_5^\star = 0, \tag{4.25}$$

where

$$\begin{aligned}
L_0^\star &= \frac{(2u_1+u_2)u_2^2(u_2+2u_3)(u_2+2u_{[3,4]})}{32u_0u_{[0,1]}u_{[0,2]}u_{[0,3]}u_{[0,4]}},\\
L_1^\star &= -\frac{(2u_{[0,1]}+u_2)u_2^2(u_2+2u_3)(u_2+2u_{[3,4]})}{32u_0u_1u_{[0,1]}u_{[1,3]}u_{[1,4]}},\\
L_3^\star &= \frac{(2u_{[0,1]}+u_2)(2u_1+u_2)(u_2+2u_3)(u_2+2u_{[3,4]})}{32u_3u_{[0,2]}u_{[1,2]}u_{[3,4]}},\\
L_4^\star &= -\frac{(2u_{[0,1]}+u_2)(2u_1+u_2)u_2^2(u_2+2u_{[3,4]})}{32u_3u_4u_{[0,3]}u_{[1,3]}u_{[2,3]}},\\
L_5^\star &= \frac{(2u_{[0,1]}+u_2)(2u_1+u_2)u_2^2(u_2+2u_3)}{32u_4u_{[0,4]}u_{[1,4]}u_{[2,4]}u_{[3,4]}}.
\end{aligned}$$

We now construct control points as follows,

$$p_2 = 0, \quad p_3 = 1, \quad p_1 = x, \quad p_4 = p_0 = x+1, \quad p_5 = x+2, \tag{4.26}$$

where similar dimensional simplifications are applied as for the IG4-scheme, and we assume that $x > 0$. It follows that

$$\begin{bmatrix} e_0 \\ l_0 \\ u_0 \end{bmatrix} = \begin{bmatrix} -1 \\ 1 \\ 1 \end{bmatrix}, \quad \begin{bmatrix} e_1 \\ l_1 \\ u_1 \end{bmatrix} = \begin{bmatrix} -x \\ x \\ x^\alpha \end{bmatrix}, \quad \begin{bmatrix} e_2 \\ l_2 \\ u_2 \end{bmatrix} = \begin{bmatrix} 1 \\ 1 \\ 1 \end{bmatrix}, \quad \begin{bmatrix} e_3 \\ l_3 \\ u_3 \end{bmatrix} = \begin{bmatrix} x \\ x \\ x^\alpha \end{bmatrix}, \quad \begin{bmatrix} e_4 \\ l_4 \\ u_4 \end{bmatrix} = \begin{bmatrix} 1 \\ 1 \\ 1 \end{bmatrix},$$

$$L_0^\star = L_5^\star = \frac{(2x^\alpha+1)^2}{64(x^\alpha+1)^2(x^\alpha+2)}, \quad L_1^\star = L_4^\star = -\frac{(2x^\alpha+3)^2}{64x^\alpha(x^\alpha+1)^2},$$

$$L_3^\star = \frac{(2x^\alpha+3)^2(2x^\alpha+1)^2}{32(x^\alpha+2)(x^\alpha+1)^2x^\alpha}.$$

Thus (4.25) becomes

$$\begin{aligned}
&(2x+3)L_0^\star + (2x+1)L_1^\star + L_3^\star = \\
&\frac{(2x+3)(2x^\alpha+1)^2}{64(x^\alpha+1)^2(x^\alpha+2)} + \frac{(2x^\alpha+3)^2(2x^\alpha+1)^2}{32(x^\alpha+2)(x^\alpha+1)^2x^\alpha} - \frac{(2x+1)(2x^\alpha+3)^2}{64x^\alpha(x^\alpha+1)^2} = 0.
\end{aligned}$$

Factoring out the common denominator $D = 64x^{\alpha}(x^{\alpha}+1)^2(x^{\alpha}+2)$ yields

$$\begin{aligned}&\frac{1}{D}\Big\{(2x+3)(2x^{\alpha}+1)^2x^{\alpha}+2(2x^{\alpha}+3)^2(2x^{\alpha}+1)^2-(2x+1)(2x^{\alpha}+3)^2(x^{\alpha}+2)\Big\}\\ =&\frac{1}{D}\Big\{a(x)+b(x)-c(x)\Big\}=0,\end{aligned}$$

where

$$\begin{aligned}a(x)&:=(2x+3)(2x^{\alpha}+1)^2x^{\alpha},\\ b(x)&:=2(2x^{\alpha}+3)^2(2x^{\alpha}+1)^2,\\ c(x)&:=(2x+1)(2x^{\alpha}+3)^2(x^{\alpha}+2).\end{aligned}$$

We further observe that

$$\begin{aligned}a(x)&=8x^{3\alpha+1}+8x^{2\alpha+1}+o(x^{2\alpha+1}),\\ b(x)&=O(x^{4\alpha}),\\ c(x)&=8x^{3\alpha+1}+40x^{2\alpha+1}+o(x^{2\alpha+1}),\end{aligned}$$

with $\alpha \geq 0$ as $x \to \infty$. Thus we get the exponent inequality $4\alpha < 2\alpha+1 \implies \alpha < 1/2$, since the coefficients of $x^{3\alpha+1}$ are the same for a and c, but the coefficient of $x^{2\alpha+1}$ is higher in c than a. Therefore, $c(x)$ is a generalized polynomial function that will dominate $a(x)+b(x)$ as x increases for all $\alpha \in [0,1/2)$, and it remains to show that there exists an $\tilde{x} \in (0,\infty)$ such that $a(\tilde{x})+b(\tilde{x}) \geq c(\tilde{x})$. We again select $\tilde{x}=1$, and get the inequality

$$(2+3)(2+1)^2+2(2+3)^2(2+1)^2 \geq (2+1)(2+3)^2(1+2) \implies 495 \geq 225,$$

which clearly holds. This implies that there exists a solution to the IG6 invalidity problem for all $\alpha \in [0,1/2)$ and thus the IG6-scheme is unsafe for all $\alpha \in [0,1/2)$, which completes the proof. □

In Figure 4.4 and Figure 4.5, numerical solutions x to the IG4- and IG6-scheme invalidity problems are plotted in a semi-log plot against α. Observe that the solutions increase exponentially as α approaches $1/2$. Due to numerical limitations, it is difficult to produce numerical solutions closer to $\alpha = 1/2$ than shown, but we have proved that it is possible mathematically. In Figure 4.2, it is verified numerically that the auxiliary nonlinear equations used in the proof of Theorem 4.3.1 are indeed correct within machine precision.

	$m = 4$ (IG4)		$m = 6$ (IG6)	
α	x	$\|\boldsymbol{p}_4^\star - \boldsymbol{p}_1\|_2$	x	$\|\boldsymbol{p}_6^\star - \boldsymbol{p}_2\|_2$
0	4	0	67/22	0
0.1	5.128743597847651	$7.63 \cdot 10^{-17}$	3.637865697752739	$3.47 \cdot 10^{-17}$
0.2	7.456301281688527	$2.78 \cdot 10^{-17}$	4.685167284088005	$1.39 \cdot 10^{-16}$
0.3	14.321485381618711	$6.94 \cdot 10^{-17}$	6.981503534063591	$7.63 \cdot 10^{-17}$
0.4	73.100374044718293	$3.47 \cdot 10^{-17}$	15.217902823720854	$2.78 \cdot 10^{-16}$
0.45	1479.076451257438748	$1.67 \cdot 10^{-16}$	36.512587690056584	$1.53 \cdot 10^{-16}$

Figure 4.2: Numerical solutions x for different values of α to the nonlinear equations $(2x^\alpha+1)^2 = (2x+1)$ and $(2x+3)(2x^\alpha+1)^2x^\alpha + 2(2x^\alpha+3)^2(2x^\alpha+1)^2 = (2x+1)(2x^\alpha+3)^2(x^\alpha+2)$ for the IG4- and IG6- invalidity problems, respectively. The errors are also measured for the differences $\boldsymbol{p}_{j+1,2k+1} - \boldsymbol{p}_{j,k}$ after subdivision, using the dynamic control points and the numerical solutions x.

Remarks on the constructions (4.21) and (4.26)

These control point constructions may seem somewhat arbitrary, but there is an underlying structure that makes the analysis much more approachable. Primarily, the points are chosen such that all the points $\{\boldsymbol{p}_{0,i}\}_{i\neq k}$ are located on one side of $\boldsymbol{p}_{0,k}$, which makes the α-interpolant resemble a cusp near $\boldsymbol{p}_{0,k}$ as $x \to \infty$. Experiments indicate that this is necessary for a solution to the invalidity problem for $\alpha \in [1/3, 1/2)$. Thus it is conceivable that it might be possible to define restrictions on the control polygon for the limit curve to be well defined for $\alpha \in [1/3, 1/2)$ in general, but we will not pursue this further here. Furthermore, the exact differences between the control points are chosen such that we get a symmetry in the u_i, which make pairs of the $L_i^\star$ become equal, and algebraically simple. The differences are also chosen such that the x does not breach the requirement that the points at the previous level need to be consecutively distinct.

Thoughts on the general case $m \geq 4$

Although the above technique of analyzing the algebraic equations directly proved to be fruitful for $m = 4$ and $m = 6$, and may even be possible for slightly higher degrees m, the expressions rapidly grow out of hand with m. Therefore, it would be beneficial if we could use the already established basis case for $m = 4$ to extrapolate higher degree results by induction. Luckily, the concept of building higher degree polynomial interpolants from lower degree polynomial interpolants is exactly what the Newton polynomials are about. Assume for induction that the invalidity problem has a solution for even $m \in \mathbb{Z}_{\geq 4}$, and we want to show that it holds for the next case $m + 2$. We have already shown that the

basis case $m = 4$ holds. By using the fact that we can reorder the points and parameters as we want for the Newton interpolant, we get

$$\begin{aligned}\boldsymbol{p}^{\star}_{m+2} =&(t_\star - t_1)\boldsymbol{p}_1^{[1]} + (t_\star - t_1)(t_\star - t_2)\boldsymbol{p}_1^{[2]} + \cdots + (t_\star - t_1)\cdots(t_\star - t_{m-1})\boldsymbol{p}_1^{[m-1]} \\ &+ (t_\star - t_1)\cdots(t_\star - t_m)\boldsymbol{p}_1^{[m]} + (t_\star - t_1)\cdots(t_\star - t_{m+1})\boldsymbol{p}_0^{[m+1]} \\ &= \overline{\boldsymbol{p}^{\star}_m} + \boldsymbol{\chi}(\boldsymbol{p}_0, \ldots, \boldsymbol{p}_{m+1}) = \boldsymbol{p}_{m/2} + \boldsymbol{\chi}(\boldsymbol{p}_0, \ldots, \boldsymbol{p}_{m+1}), \\ \boldsymbol{\chi}(\boldsymbol{p}_0, \ldots, \boldsymbol{p}_{m+1}) &:= (t_\star - t_1)\cdots(t_\star - t_m)\boldsymbol{p}_1^{[m]} + (t_\star - t_1)\cdots(t_\star - t_{m+1})\boldsymbol{p}_0^{[m+1]},\end{aligned}$$

where we used the shift commutativity of the IGm-schemes, and the induction hypothesis to obtain $\overline{\boldsymbol{p}^{\star}_m} = \boldsymbol{p}_{m/2}$. We have not actually shown that the IGm-schemes commute with linear shifts yet, although this is evident from the fact that we can build the Lagrange basis function solely from the u_i, but we will prove this formally in Lemma 5.2.1. If we can show that $\boldsymbol{\chi} = \mathbf{0}$ in general for some choice of control points $\boldsymbol{p}_0, \ldots, \boldsymbol{p}_{m+1}$, where $\boldsymbol{p}_1, \ldots, \boldsymbol{p}_m$ need to be fixed, and we can alter $\boldsymbol{p}_0, \boldsymbol{p}_{m+1}$ in accordance to the other control points, then the general proof follows. However, the exact analytical procedure is not obvious, so we here simply conjecture the statement.

Conjecture 4.3.1. *The IGm-schemes are unsafe for $\alpha \in [0, 1/2)$ for all even $m \geq 4$.*

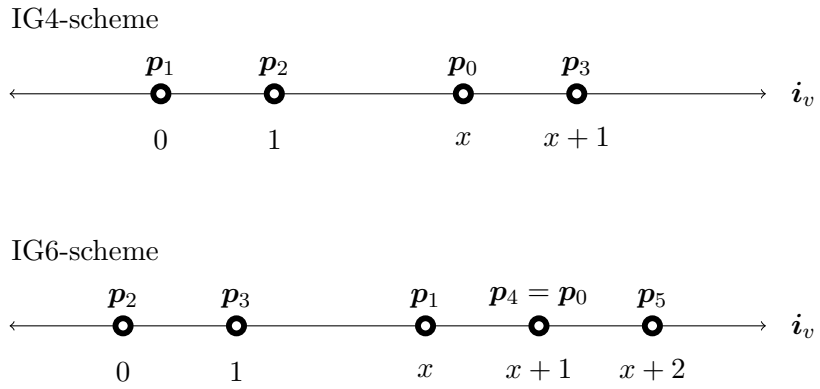

Figure 4.3: Dynamic control point constructions used in the proof of Theorem 4.3.1.

The special case $\alpha = 0$

Even though the IGm-schemes are unsafe for $m = 4$ and $m = 6$ with $\alpha = 0$, this will not necessarily lead to the subdivision algorithm stopping. If two consecutive points are equal, then $\boldsymbol{e}_i = \mathbf{0}$ for the corresponding index i, but since $t_{i+1} - t_i = \|\boldsymbol{e}_i\|^\alpha = 0^\alpha = 0^0$ for

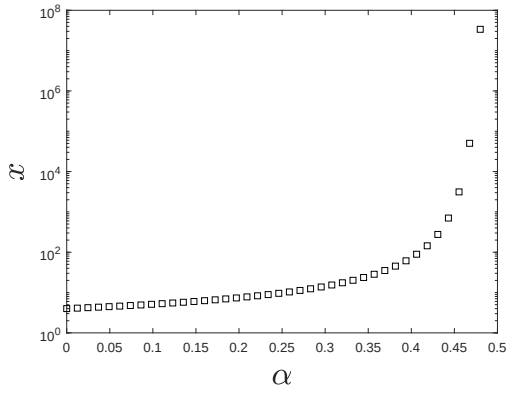

Figure 4.4: Numerical solutions to (4.22).

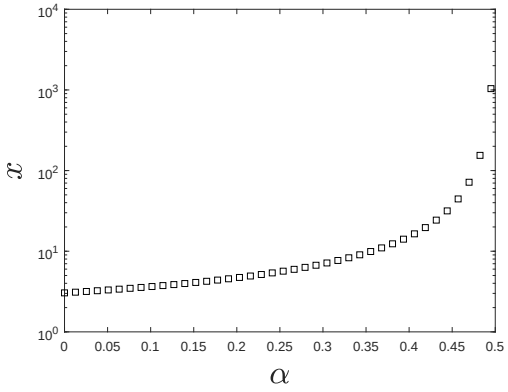

Figure 4.5: Numerical solutions to (4.25).

$\alpha = 0$, and $0^0 := 1$ in many implementations of basic arithmetic operations in computer systems, then the program will continue without crashing. It is especially therefore for the interval $\alpha \in (0, 1/2)$ where one should be careful.

Safety of the IG4-scheme

From experiments, it seems that for $\alpha \in [1/2, 1]$, and consecutively distinct control points, the IG4-scheme always generates consecutively distinct points. In order to show this, we first describe a condition, adapted from [17], that implies the safety of a binary interpolatory subdivision scheme.

Definition 4.3.2. *If*

$$\|\boldsymbol{d}_{j,k}\| < \frac{1}{2}\|\boldsymbol{e}_{j,k}\| \quad \forall \quad k \in \mathbb{Z},\, j \geq 0,$$

where $\{\boldsymbol{d}_{j,k}\}_{k\in\mathbb{Z}}$ *and* $\{\boldsymbol{e}_{j,k}\}_{k\in\mathbb{Z}}$ *are the displacement vectors and edge vectors of a subdivision scheme at level* j*, respectively, then the subdivision scheme is called displacement-safe. It is assumed that the control points are consecutively distinct.*

Clearly, a displacement-safe subdivision scheme is safe as the displacement vector $\boldsymbol{d}_{j,k}$ cannot stretch all the way to any of its neighboring points $\boldsymbol{p}_{j,k}$ or $\boldsymbol{p}_{j,k+1}$. This is what we used to prove that the limit curve of the IG4-scheme is well defined and C^0 for $\alpha = 1/2, 1$. We now turn to the more general case $\alpha \in [1/2, 1]$.

Theorem 4.3.2. *The IG4-scheme is displacement-safe for all* $\alpha \in [1/2, 1]$.

Proof. [4] Working with simplified notation and letting $\boldsymbol{d} = \boldsymbol{p}^\star - (\boldsymbol{p}_1 + \boldsymbol{p}_2)/2$ be the displacement vector for some insertion point $\boldsymbol{p}^\star$ based on $\boldsymbol{p}_0, \boldsymbol{p}_1, \boldsymbol{p}_2, \boldsymbol{p}_3$, we find that

$$\boldsymbol{d} = \sum_{i=0}^{3} L_i^\star \boldsymbol{p}_i - \frac{\boldsymbol{p}_1 + \boldsymbol{p}_2}{2} = -L_0^\star \boldsymbol{e}_0 - \left(L_0^\star + L_1^\star - \frac{1}{2} \right) \boldsymbol{e}_1 + L_3^\star \boldsymbol{e}_2,$$

where the $\{\boldsymbol{e}_i\}_{i=0}^3$ are the local edge vectors satisfying $\boldsymbol{e}_i = \boldsymbol{p}_{i+1} - \boldsymbol{p}_i$. Thus,

$$\|\boldsymbol{d}\| \leq |L_0^\star| l_0 + \left| L_0^\star + L_1^\star - \frac{1}{2} \right| l_1 + |L_3^\star| l_2,$$

where we again used the partition of unity property of the Lagrange basis functions. We already found $L_0^\star, L_3^\star$ in (4.23), and in addition we find by symmetry in the indices that

$$\begin{aligned} L_1^\star &= \frac{(2u_0 + u_1)(u_1 + 2u_2)}{8u_0 u_{[1,2]}}, \\ L_0^\star + L_1^\star - \frac{1}{2} &= -\frac{u_1^2(u_1 + 2u_2)}{8u_0 u_{[0,1]} u_{[0,2]}} + \frac{(2u_0 + u_1)(u_1 + 2u_2)}{8u_0 u_{[1,2]}} - \frac{1}{2} \\ &= \frac{u_1(u_2 - u_0)(2u_0 + 3u_1 + 2u_2)}{8u_{[0,1]} u_{[1,2]} u_{[0,2]}}. \end{aligned}$$

Therefore,

$$\|\boldsymbol{d}\| \leq \frac{u_1^2(u_1 + 2u_2)}{8u_0 u_{[0,1]} u_{[0,2]}} l_0 + \frac{u_1(u_0 + u_2)(2u_0 + 3u_1 + 2u_2)}{8u_{[0,1]} u_{[1,2]} u_{[0,2]}} l_1 + \frac{u_1^2(2u_0 + u_1)}{8u_{[0,2]} u_{[1,2]} u_2} l_2.$$

Thus by using $u_i = l_i^\alpha$, we get

$$\frac{\|\boldsymbol{d}\|}{l_1} \leq \frac{l_0^{1-\alpha} l_1^{2\alpha-1}(u_1 + 2u_2)}{8u_{[0,1]} u_{[0,2]}} + \frac{u_1(u_0 + u_2)(2u_0 + 3u_1 + 2u_2)}{8u_{[0,1]} u_{[1,2]} u_{[0,2]}} + \frac{l_1^{2\alpha-1} l_2^{1-\alpha}(2u_0 + u_1)}{8u_{[1,2]} u_{[0,2]}}.$$

By symmetry we can without loss of generality assume that $l_2 \geq l_0$. We now first consider the case $l_1 \leq l_0$. Then $l_1 \leq l_2$, so the inequalities

$$\begin{aligned} l_0^{1-\alpha} l_1^{2\alpha-1} &= l_0^\alpha \left(\frac{l_1}{l_0} \right)^{2\alpha-1} \leq l_0^\alpha = u_0, \\ l_1^{2\alpha-1} l_2^{1-\alpha} &= l_2^\alpha \left(\frac{l_1}{l_2} \right)^{2\alpha-1} \leq l_2^\alpha = u_2. \end{aligned}$$

[4] This proof builds upon unpublished notes by Chongyang Deng of Hangzhou Dianzi University from 2016, with permission.

hold for $\alpha \geq 1/2$. Thus, in this case,

$$\begin{aligned}\frac{\|\boldsymbol{d}\|}{l_1} &\leq \frac{u_0(u_1+2u_2)}{8u_{[0,1]}u_{[0,2]}} + \frac{u_1(u_0+u_2)(2u_0+3u_1+2u_2)}{8u_{[0,1]}u_{[1,2]}u_{[0,2]}} + \frac{u_2(2u_0+u_1)}{8u_{[1,2]}u_{[0,2]}} \\ &= \frac{u_0(u_1+2u_2)u_{[1,2]} + u_1(u_0+u_2)(2u_0+3u_1+2u_2) + u_2(2u_0+u_1)u_{[0,1]}}{8u_{[0,1]}u_{[1,2]}u_{[0,2]}} \\ &= \frac{4u_0u_1^2 + 2u_0^2u_1 + 2u_0u_2^2 + 2u_0^2u_2 + 2u_1u_2^2 + 4u_1^2u_2 + 10u_0u_1u_2}{2(8u_0u_1^2 + 4u_0^2u_1 + 4u_0u_2^2 + 4u_0^2u_2 + 4u_1u_2^2 + 8u_1^2u_2 + 12u_0u_1u_2) + 8u_1^3} < \frac{1}{2},\end{aligned} \tag{4.27}$$

where we compared the coefficients of terms in the numerator and denominator to obtain the bound, since only greater coefficients appear in the denominator. We then turn to the outstanding case $l_1 \geq l_0$, and discover that

$$l_0^{1-\alpha} l_1^{2\alpha-1} = l_1^\alpha \left(\frac{l_0}{l_1}\right)^{1-\alpha} \leq l_1^\alpha = u_1 \quad \forall \alpha \leq 1.$$

Since $l_1 \geq l_0$, $l_2 \geq l_0$ does not directly create a bound between l_1 and l_2, we consider each of the subcases $l_1 \geq l_2$ and $l_1 \leq l_2$. Let first $l_1 \geq l_2$, which implies that

$$l_1^{2\alpha-1} l_2^{1-\alpha} = l_1^\alpha \left(\frac{l_2}{l_1}\right)^{1-\alpha} \leq l_1^\alpha = u_1 \quad \forall \alpha \leq 1.$$

Then,

$$\begin{aligned}\frac{\|\boldsymbol{d}\|}{l_1} &\leq \frac{u_1(u_1+2u_2)}{8u_{[0,1]}u_{[0,2]}} + \frac{u_1(u_0+u_2)(2u_0+3u_1+2u_2)}{8u_{[0,1]}u_{[1,2]}u_{[0,2]}} + \frac{u_1(2u_0+u_1)}{8u_{[1,2]}u_{[0,2]}} \\ &= \frac{u_1(u_1+2u_2)u_{[1,2]} + u_1(u_2+u_0)(2u_0+3u_1+2u_2) + u_1(2u_0+u_1)u_{[0,1]}}{8u_{[0,1]}u_{[1,2]}u_{[0,2]}} \\ &= \frac{2u_1^3 + 6u_1^2u_2 + 4u_1u_2^2 + 4u_0u_1u_2 + 4u_0^2u_1 + 6u_0u_1^2}{2(4u_1^3 + 8u_1^2u_2 + 4u_1u_2^2 + 12u_0u_1u_2 + 4u_0^2u_1 + 8u_0u_1^2) + z} < \frac{1}{2},\end{aligned}$$

where $z > 0$ are the remaining terms of the denominator, and we used the triangle inequality and the same coefficient comparison process as in (4.27). On the other hand, for the last possible case $l_1 \leq l_2$, we have

$$l_1^{2\alpha-1} l_2^{1-\alpha} = l_2^\alpha \left(\frac{l_1}{l_2}\right)^{2\alpha-1} \leq l_2^\alpha = u_2 \quad \forall \alpha \geq 1/2.$$

Then,

$$\begin{aligned}\frac{\|\boldsymbol{d}\|}{l_1} &\leq \frac{u_1(u_1+2u_2)}{8u_{[0,1]}u_{[0,2]}} + \frac{u_1(u_0+u_2)(2u_0+3u_1+2u_2)}{8u_{[0,1]}u_{[1,2]}u_{[0,2]}} + \frac{u_2(2u_0+u_1)}{8u_{[1,2]}u_{[0,2]}} \\ &= \frac{u_1(u_1+2u_2)u_{[1,2]} + u_1(u_0+u_2)(2u_0+3u_1+2u_2) + u_2(2u_0+u_1)u_{[0,1]}}{8u_{[0,1]}u_{[1,2]}u_{[0,2]}} \\ &= \frac{3u_0u_1^2 + 2u_0^2u_1 + 2u_0^2u_2 + 4u_1u_2^2 + 7u_1^2u_2 + u_1^3 + 7u_0u_1u_2}{2(8u_0u_1^2 + 4u_0^2u_1 + 4u_0^2u_2 + 4u_1u_2^2 + 8u_1^2u_2 + 4u_1^3 + 12u_0u_1u_2) + \hat{z}} < \frac{1}{2},\end{aligned}$$

where $\hat{z} > 0$ are the remaining terms of the denominator, and we use the same argument as before. As the only assumption is that $\alpha \in [1/2, 1]$, and we considered an arbitrary insertion point, then $\|\boldsymbol{d}_{j,k}\| < (1/2)\|\boldsymbol{e}_{j,k}\|$ in general for all $\alpha \in [1/2, 1]$, and the proof is complete. □

Corollary 4.3.1. *The IG4-scheme is safe and C^0 for all $\alpha \in [1/2, 1]$.*

Proof. The safety of IG4-scheme for $\alpha \in [1/2, 1]$ follows directly from the displacement-safe property Theorem 4.3.2. This means that (4.13) and (4.17) hold unconditionally for all $\alpha \in [1/2, 1]$. The proof of Theorem 4.2.1 thus also applies to all cases $\alpha \in [1/2, 1]$, and the result follows. □

The definitions of a safe and displacement-safe subdivision scheme are adapted from the article [17].

4.4 Distance bounds for the IG4-scheme

In order to measure the distance between the control polygon and the limit curve, we use what is known as the Hausdorff distance d_H to bound the difference between the part of the limit curve $\{\boldsymbol{g}(x) : x \in [k, k+1]\}$ and the line segment $[\boldsymbol{p}_{0,k}, \boldsymbol{p}_{0,k+1}]$. This was also done in [1], but with the aid of (4.3.1), we will here be able to bound the Hausdorff distance not only for $\alpha = 0, 1/2, 1$, but also for all $\alpha \in (1/2, 1)$. We closely follow the discussion of [1], and first introduce the following local variants of (4.18).

Lemma 4.4.1. *[1] For $\alpha = 0$,*

$$\max_{2^j k - 2 \le i \le 2^j(k+1)+1} \|\boldsymbol{e}_{j,i}\| \le \left(\frac{5}{8}\right)^j \max_{k-2 \le \ell \le k+2} \|\boldsymbol{e}_{0,\ell}\|, \tag{4.28}$$

for $\alpha = 1/2$,

$$\max_{2^j k \le i \le 2^j(k+1)-1} \|\boldsymbol{e}_{j,i}\| \le \left(\frac{3}{4}\right)^j \|\boldsymbol{e}_{0,k}\|, \tag{4.29}$$

for $\alpha \in [1/2, 1]$,

$$\max_{2^j k - 2 \le i \le 2^j(k+1)+1} \|\boldsymbol{e}_{j,i}\| \le \left(\frac{7}{8}\right)^j \max_{k-2 \le \ell \le k+2} \|\boldsymbol{e}_{0,\ell}\|, \tag{4.30}$$

Proof. By the fact that all points at level j between $\boldsymbol{p}_{0,k} = \boldsymbol{p}_{j,2^j k}$ and $\boldsymbol{p}_{0,k+1} = \boldsymbol{p}_{j,2^j(k+1)}$ depend only on the six control point $\{\boldsymbol{p}_{0,i}\}_{i=k-2}^{k+3}$, then (4.28) and (4.30) follow by Lemma 4.2.4 and induction on j. We also used that the IG4-scheme is displacement-safe for $\alpha \in [1/2, 1]$, which means that the points at level j are well defined for these α. (4.29) also follows by induction on j and Lemma 4.2.4. □

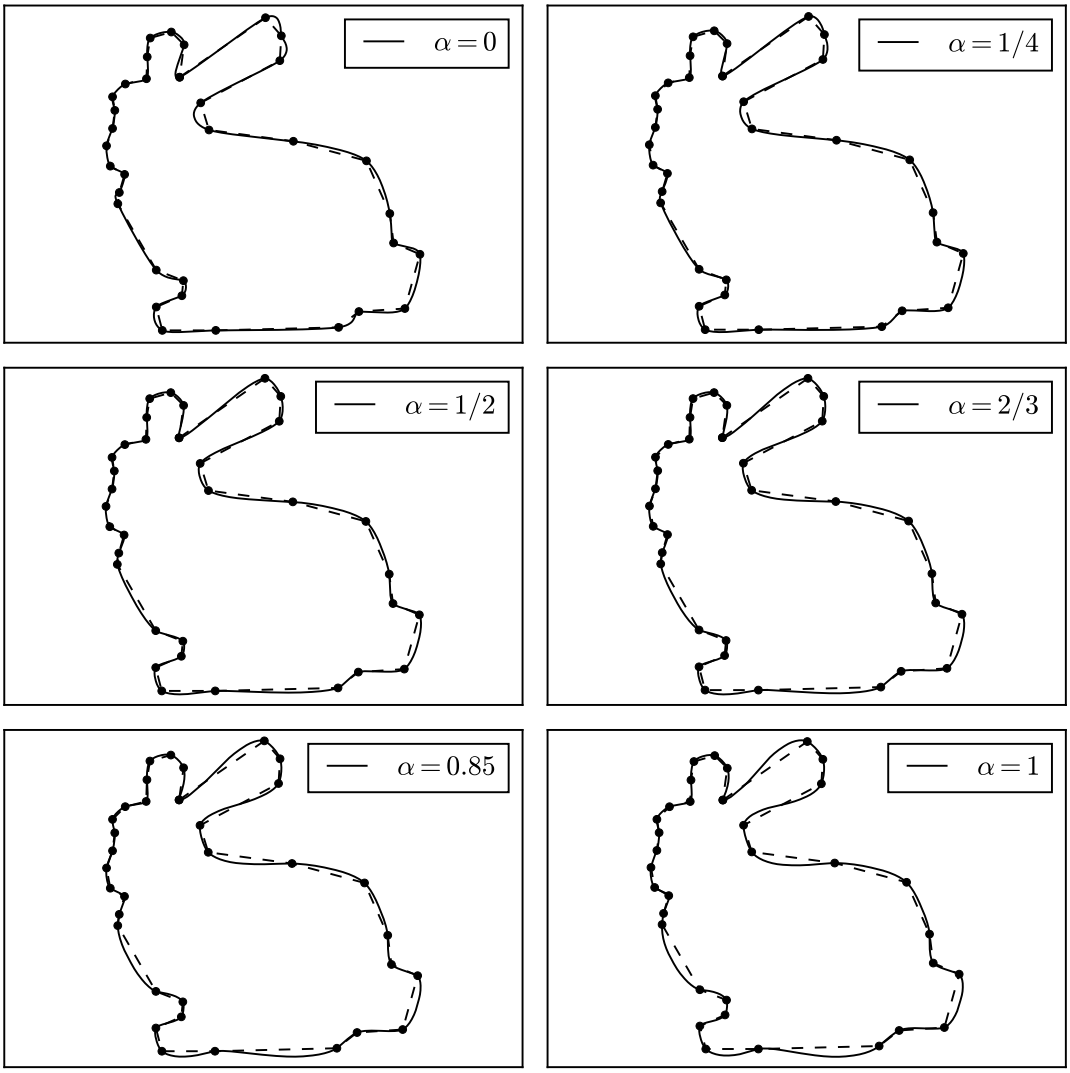

Figure 4.6: IG4 limit curves for various choices of α. The control points are based on the perimeter of a 2D projection of the famous Stanford Bunny by Stanford University Computer Graphics Laboratory, modified to contain regions of highly varying edge lengths. The limit curves of the lower four plots have now been shown be be C^0.

We note that here (4.30) holds for $\alpha \in [1/2, 1]$, and not just $\alpha = 1$ as in [1]. This allows us to prove Hausdorff bounds for all the α for which we have shown the IG4-scheme to be C^0. The Hausdorff distance between two sets is informally defined as the largest of all distances from a point in one set to the closest point in the other set. Below is a more formal definition usable in this setting.

Definition 4.4.1. *Given two functions $\boldsymbol{a} : X \to \mathbb{R}^d$, $\boldsymbol{b} : Y \to \mathbb{R}^d$, where $X, Y \subseteq \mathbb{R}$, we define the Hausdorff distance $d_H(\boldsymbol{a}(X), \boldsymbol{b}(Y))$ between $\boldsymbol{a}(X)$ and $\boldsymbol{b}(Y)$ as*

$$d_H(\boldsymbol{a}(X), \boldsymbol{b}(Y)) = \max\left(\sup_{x\in X}\inf_{y\in Y} d(\boldsymbol{a}(x),\, \boldsymbol{b}(y)),\, \sup_{y\in Y}\inf_{x\in X} d(\boldsymbol{a}(x),\, \boldsymbol{b}(y))\right),$$

where

$$d(\boldsymbol{a}(x), \boldsymbol{b}(y)) := \|\boldsymbol{a}(x) - \boldsymbol{b}(y)\|_2, \quad x \in X,\, y \in Y.$$

In the current context, we are looking at functions with domain $[k, k+1]$, as we are only interested at a section of the limit curve and the corresponding segment of the control polygon.

Theorem 4.4.1. *[1] For $\alpha = 0$,*

$$d_H\left(\boldsymbol{g}([k, k+1]), [\boldsymbol{p}_{0,k}, \boldsymbol{p}_{0,k+1}]\right) \le \frac{3}{13} \max_{k-2\le\ell\le k+2} \|\boldsymbol{e}_{0,\ell}\|, \tag{4.31}$$

for $\alpha = 1/2$,

$$d_H\left(\boldsymbol{g}([k, k+1]), [\boldsymbol{p}_{0,k}, \boldsymbol{p}_{0,k+1}]\right) \le \frac{5}{7} \|\boldsymbol{e}_{0,k}\|, \tag{4.32}$$

for $\alpha \in [1/2, 1]$,

$$d_H\left(\boldsymbol{g}([k, k+1]), [\boldsymbol{p}_{0,k}, \boldsymbol{p}_{0,k+1}]\right) \le \frac{11}{5} \max_{k-2\le\ell\le k+2} \|\boldsymbol{e}_{0,\ell}\|. \tag{4.33}$$

Proof. Let $x_{j,i} = 2^{-j} i$ be the dyadic grid points. Consider first the difference between $\boldsymbol{g}_{j+2}$ and $\boldsymbol{g}_j$. Let $\boldsymbol{h}_j(x) := \boldsymbol{g}_{j+2}(x) - \boldsymbol{g}_j(x)$, $x \in [k, k+1]$. We need to investigate $\boldsymbol{h}_j$ at the grid points $\{x_{j+2,w}\}_{w=4i}^{4i+3}$. The only nontrivial values of $\boldsymbol{h}_j$ to find are $\boldsymbol{h}_j(x_{j+2,4i+1})$ and $\boldsymbol{h}_j(x_{j+2,4i+3})$. We find that

$$\boldsymbol{h}_j(x_{j+2,4i}) = \boldsymbol{0}, \tag{4.34}$$

$$\boldsymbol{h}_j(x_{j+2,4i+1}) = \boldsymbol{p}_{j+2,4i+1} - \left(\boldsymbol{p}_{j,i} + \frac{\boldsymbol{p}_{j,i+1} - \boldsymbol{p}_{j,i}}{4}\right) = \boldsymbol{d}_{j,i}/2 + \boldsymbol{d}_{j+1,2i}, \tag{4.35}$$

$$\boldsymbol{h}_j(x_{j+2,4i+2}) = \boldsymbol{d}_{j,i}, \tag{4.36}$$

$$\boldsymbol{h}_j(x_{j+2,4i+3}) = \boldsymbol{p}_{j+2,4i+3} - \left(\boldsymbol{p}_{j,i+1} - \frac{\boldsymbol{p}_{j,i+1} - \boldsymbol{p}_{j,i}}{4}\right) = \boldsymbol{d}_{j,i}/2 + \boldsymbol{d}_{j+1,2i+1}. \tag{4.37}$$

Thus,

$$\sup_{x_{j,i}\le x\le x_{j,i+1}} \|\boldsymbol{h}_j(x)\| \le \max\left(\|\boldsymbol{d}_{j,i}\|/2 + \|\boldsymbol{d}_{j+1,2i}\|,\, \|\boldsymbol{d}_{j,i}\|,\, \|\boldsymbol{d}_{j,i}\|/2 + \|\boldsymbol{d}_{j+1,2i+1}\|\right).$$

Using Lemma 4.2.3 and Lemma 4.2.4, we get

$$\max\left(\|\boldsymbol{d}_{j+1,2i}\|,\, \|\boldsymbol{d}_{j+1,2i+1}\|\right) \leq \begin{cases} \frac{5}{64}\max_{i-2\leq\ell\leq i+2}\|\boldsymbol{e}_{j,\ell}\|, & \alpha = 0, \\ \frac{3}{16}\|\boldsymbol{e}_{j,i}\|, & \alpha = 1/2, \\ \frac{21}{64}\max_{i-2\leq\ell\leq i+2}\|\boldsymbol{e}_{j,\ell}\|, & \alpha \in [1/2, 1]. \end{cases}$$

Therefore, by (4.34)–(4.37) and Lemma 4.2.3, it follows that

$$\sup_{x_{j,i}\leq x\leq x_{j,i+1}} \|\boldsymbol{h}_j(x)\| \leq \begin{cases} \frac{9}{64}\max_{i-2\leq\ell\leq i+2}\|\boldsymbol{e}_{j,\ell}\|, & \alpha = 0, \\ \frac{5}{16}\|\boldsymbol{e}_{j,i}\|, & \alpha = 1/2, \\ \frac{33}{64}\max_{i-2\leq\ell\leq i+2}\|\boldsymbol{e}_{j,\ell}\|, & \alpha \in [1/2, 1]. \end{cases}$$

Consequently, by considering all intervals $[x_{j,i}, x_{j,i+1}]$ between k and $k+1$, which is $2^j k \leq i \leq 2^j(k+1) - 1$, and using Lemma 4.4.1, we get

$$\sup_{k\leq x\leq k+1} \|\boldsymbol{h}_j(x)\| \leq \begin{cases} \frac{9}{64}\left(\frac{5}{8}\right)^j \max_{k-2\leq\ell\leq k+2}\|\boldsymbol{e}_{0,\ell}\|, & \alpha = 0, \\ \frac{5}{16}\left(\frac{3}{4}\right)^j \|\boldsymbol{e}_{0,k}\|, & \alpha = 1/2, \\ \frac{33}{64}\left(\frac{7}{8}\right)^j \max_{k-2\leq\ell\leq k+2}\|\boldsymbol{e}_{0,\ell}\|, & \alpha \in [1/2, 1]. \end{cases} \tag{4.38}$$

Clearly,

$$d_{\mathrm{H}}\left(\boldsymbol{g}([k, k+1]), [\boldsymbol{p}_{0,k}, \boldsymbol{p}_{0,k+1}]\right) \leq \sup_{k\leq x\leq k+1} \|\boldsymbol{g}(x) - \boldsymbol{g}_0(x)\| \leq \sum_{j=0}^{\infty} \sup_{k\leq x\leq k+1} \|\boldsymbol{h}_{2j}(x)\|.$$

Thus, the result follows by using (4.38) and the fact that

$$\frac{9}{64}\sum_{j=0}^{\infty}\left(\frac{5}{8}\right)^{2j} = \frac{3}{13}, \quad \frac{5}{16}\sum_{j=0}^{\infty}\left(\frac{3}{4}\right)^{2j} = \frac{5}{7}, \quad \frac{33}{64}\sum_{j=0}^{\infty}\left(\frac{7}{8}\right)^{2j} = \frac{11}{5}.$$

□

Theorem 4.4.1 suggests that the IG4-scheme with $\alpha = 1/2$ yields the limit curve that is in a sense the closest to the control polygon out of the choices of $\alpha \in [0, 1]$, as the distance is only bounded by the middle edge, which also supports the idea that the centripetal limit curve is free of artifacts. This phenomenon can also be seen in Figure 4.6. We further point out the known properties of the limit curve for $\alpha = 0$, that it tends to overshoot at short edges while being very close to the control polygon for long edges, which means that unwanted loops and cusps may occur. The loop artifact can be seen in Figure 1.3, and the cusp-like artifact is more visible in Figure 4.6. On the other hand, for $\alpha = 1$, the limit curve overshoots at long edges while being close to the control polygon at short edges, which may cause the limit curve to travel relatively far

away from the control polygon. This can be seen in Figure 4.6. Interestingly, as pointed out in [1], these findings comply with the theory for cubic splines, as shown by Floater in [15]. Very recently, in [25], new and slightly better Hausdorff bounds were shown for the IG4-scheme for the select cases $\alpha = 0, 1/2$. It was shown that the coefficient $3/13$ in (4.31) can be replaced with $2/9$, and the coefficient $5/7$ in (4.32) can be replaced with $2/3$.

4.5 Smoothness of the iterated geometric schemes

The smoothness of the limit curve is many respects the most important property of a subdivision scheme. For the iterated geometric schemes, the problem of showing their smoothness is difficult to resolve. A few years after the 2009 paper [1] on the IG4-scheme was published, Dyn and Hormann attempted in [2] to show that the IG4-scheme is G^1 continuous for planar control points by studying the summability of signed angles, but succeeded only for other geometric nonlinear schemes. G^1 continuity is different from C^1 continuity in the fact that the analysis is geometric and not parametric. A difficult obstacle to overcome in the parametric C^1 analysis of the IGm-schemes is that as a geometrically based reparameterization is carried out at each level, then it is not obvious as to which parameterization or grid we should study smoothness. Showing that the IG4-scheme is C^1 is still an unsolved problem. We will return to this topic in chapter 5 and show that the schemes fit into a newly presented framework by Ewald, Reif and Sabin for studying certain nonlinear schemes, and in chapter 6 where we do numerical experiments to support our theories.

Before moving on to the IG6-scheme, we briefly remark on the relation between the smoothness of the IGm-schemes and the m-point Dubuc-Deslauriers schemes mentioned in [1]. One may think that the IG4-scheme cannot be C^2 as the limit curve of the scheme applied to a regular polygon is independent of α and thus equal to the limit curve of the FPS, which is known to be at most $C^{2-\epsilon}$. However, for this fact to be true then the points in the polygon at level j would need to be equidistant for all $j \geq 0$. Starting with the control points $\boldsymbol{p}_{0,0} = (1, 0)$, $\boldsymbol{p}_{0,1} = (0, 1)$, $\boldsymbol{p}_{0,2} = (-1, 0)$, $\boldsymbol{p}_{0,3} = (0, -1)$, $\boldsymbol{p}_{0,4} = \boldsymbol{p}_{0,0}$, i.e. a square which is a regular 4-gon, we however get that $\|\boldsymbol{e}_{2,1}\|/\|\boldsymbol{e}_{2,0}\| = \sqrt{617}/\sqrt{505} \neq 1$, so the point $\boldsymbol{p}_{3,1}$ depends on α, and the limit curve is dependent on α. Since this difference happens at the third subdivision step, the limit curves for $\alpha \in (0, 1]$ will visually appear almost indistinguishable to the FPS limit curve, but strict equivalence does not hold in general. Nevertheless, the smoothness of the IGm-schemes are probably still bounded above by the smoothness of the corresponding Dubuc-Deslauriers schemes.

4.6 Convergence of the IG6-scheme

Although the IG6-scheme is similar in nature to the IG4-scheme, the technical details of proving its C^0 convergence are significantly more involved, due to the local quintic polynomial interpolation. Admittedly, we will not here be able to show the C^0 convergence of the IG6-scheme, but we will supply some preliminary analytical findings, and derive a bound for the $\boldsymbol{d}_{j,k}$ vector for this scheme with a centripetal parameterization.

Lemma 4.6.1. *For the IG6-scheme with simplified local notation,*

$$\begin{aligned}\|\boldsymbol{d}\| \leq\ & L_0(t_\star)l_0 + |L_0(t_\star) + L_1(t_\star)|l_1 + |L_0(t_\star) + L_1(t_\star) + L_2(t_\star) - 1/2|l_2 \\ & + |L_4(t_\star) + L_5(t_\star)|l_3 + L_5(t_\star)l_4,\end{aligned}$$

where $\boldsymbol{d}$ is the displacement vector.

Proof. The result follows by letting

$$\boldsymbol{d} = \sum_{i=0}^{5} L_i(t_\star)\boldsymbol{p}_i - \frac{\boldsymbol{p}_2 + \boldsymbol{p}_3}{2},$$

rewriting to differences of control points, taking norms, and using the fact that $L_0(t_\star)$ and $L_5(t_\star)$ are positive. Moreover, the partition of unity property of the Lagrange basis function is used to simplify the expression. □

Using Lemma 4.6.1, Monte Carlo numerical experiments suggest the following bound, for a select range of α, but a formal proof will not be given.

Conjecture 4.6.1. *For the IG6-scheme with $\alpha \in [0, 1/2]$,*

$$\|\boldsymbol{d}\| < \frac{1}{2}\max\{l_0, l_1, l_2, l_3, l_4\}.$$

For the IG4-scheme, we noticed that for $\alpha = 1$, the new point can get significantly far away from the middle edge. This phenomenon seems to be accentuated for the IG6-scheme, and even worse for higher m for the IGm-schemes in general.

For completeness, although it will not be used further, we will below derive an explicit expression for $\boldsymbol{d}_{j,k}$ for the IG6-scheme.

Quintic Lagrange interpolation

Let the parameter values $t_s = \{t_i\}_{i=0}^5$ be defined, as well as functional data $f_s = \{f_i\}_{i=0}^5$. We now define the auxiliary parameters $\tilde{t_s} = \tilde{\{}t_i\}_{i=0}^5$ and $\tilde{f_s} = \tilde{\{}f_i\}_{i=0}^5$, which are orderings of t_s and f_s respectively. Moreover, we let g be the quintic Lagrange interpolant to

the data $\tilde{f}_s$ at $\tilde{t_s}$, and h be the linear Lagrange interpolant to $\tilde{f}_0, \tilde{f}_1$ at $\tilde{t_0}, \tilde{t_1}$. By writing out the Newton forms, we have that

$$g(t) = \sum_{i=0}^{5} c_i \omega_i(t), \quad c_i = [\tilde{t_0}, \dots, \tilde{t_i}]f, \quad \omega_i = (t - \tilde{t_0}) \cdots (t - \tilde{t}_{i-1}), \quad \omega_0 = 1,$$
$$h(t) = f(\tilde{t_0}) + (t - \tilde{t_0})[\tilde{t_0}, \tilde{t_1}]f.$$

So,

$$\begin{aligned} g(t) = {} & f(\tilde{t_0}) + (t - \tilde{t_0})[\tilde{t_0}, \tilde{t_1}]f \\ & + (t - \tilde{t_0})(t - \tilde{t_1})[\tilde{t_0}, \tilde{t_1}, \tilde{t_2}]f \\ & + (t - \tilde{t_0})(t - \tilde{t_1})(t - \tilde{t_2})[\tilde{t_0}, \tilde{t_1}, \tilde{t_2}, \tilde{t_3}]f \\ & + (t - \tilde{t_0})(t - \tilde{t_1})(t - \tilde{t_2})(t - \tilde{t_3})[\tilde{t_0}, \tilde{t_1}, \tilde{t_2}, \tilde{t_3}, \tilde{t_4}]f \\ & + (t - \tilde{t_0})(t - \tilde{t_1})(t - \tilde{t_2})(t - \tilde{t_3})(t - \tilde{t_4})[\tilde{t_0}, \tilde{t_1}, \tilde{t_2}, \tilde{t_3}, \tilde{t_4}, \tilde{t_5}]f. \end{aligned}$$

And thus,

$$\begin{aligned} g(t) - h(t) = {} & (t - \tilde{t_0})(t - \tilde{t_1})[\tilde{t_0}, \tilde{t_1}, \tilde{t_2}]f \\ & + (t - \tilde{t_0})(t - \tilde{t_1})(t - \tilde{t_2})[\tilde{t_0}, \tilde{t_1}, \tilde{t_2}, \tilde{t_3}]f \\ & + (t - \tilde{t_0})(t - \tilde{t_1})(t - \tilde{t_2})(t - \tilde{t_3})[\tilde{t_0}, \tilde{t_1}, \tilde{t_2}, \tilde{t_3}, \tilde{t_4}]f \\ & + (t - \tilde{t_0})(t - \tilde{t_1})(t - \tilde{t_2})(t - \tilde{t_3})(t - \tilde{t_4})[\tilde{t_0}, \tilde{t_1}, \tilde{t_2}, \tilde{t_3}, \tilde{t_4}, \tilde{t_5}]f. \end{aligned}$$

With this formulation, we are in theory free to choose the ordering in $\tilde{t_s}$, although the case where $\tilde{t_0} = t_2$, $\tilde{t_1} = t_3$ is of interest in this case. If we choose the ordering $\tilde{t_s} = \{t_2, t_3, t_1, t_0, t_4, t_5\}$, then it follows that

$$\begin{aligned} d(t) := g(t) - h(t) = {} & (t - t_2)(t - t_3)[t_1, \dots, t_3]f + (t - t_1) \cdots (t - t_3)[t_0, \dots, t_3]f \\ & + (t - t_0) \cdots (t - t_3)[t_0, \dots, t_4]f + (t - t_0) \cdots (t - t_4)[t_0, \dots, t_5]f. \end{aligned}$$

Furthermore, in this setting we have that $t_\star = (t_2 + t_3)/2$, which implies that

$$\begin{aligned} d(t_\star) = {} & -\frac{1}{4}(t_3 - t_2)^2[t_1, \dots, t_3]f \\ & - \frac{1}{8}(t_2 + t_3 - 2t_1)(t_3 - t_2)^2[t_0, \dots, t_3]f \\ & - \frac{1}{16}(t_2 + t_3 - 2t_0)(t_2 + t_3 - 2t_1)(t_3 - t_2)^2[t_0, \dots, t_4]f \\ & - \frac{1}{32}(t_2 + t_3 - 2t_0)(t_2 + t_3 - 2t_1)(t_3 - t_2)^2(t_2 + t_3 - 2t_4)[t_0, \dots, t_5]f. \end{aligned}$$

So,

$$d(t_\star) = -\frac{1}{4}(t_3-t_2)^2\Big\{[t_1,\dots,t_3]f + \frac{1}{2}(t_2+t_3-2t_1)[t_0,\dots,t_3]f$$
$$+\frac{1}{4}(t_2+t_3-2t_0)(t_2+t_3-2t_1)[t_0,\dots,t_4]f$$
$$+\frac{1}{8}(t_2+t_3-2t_0)(t_2+t_3-2t_1)(t_2+t_3-2t_4)[t_0,\dots,t_5]f\Big\}.$$

By using

$$\boldsymbol{e}_{j,k} = \boldsymbol{p}_{j,k+1} - \boldsymbol{p}_{j,k}, \quad \boldsymbol{d}_{j,k} = \boldsymbol{p}_{j+1,2k+1} - \frac{\boldsymbol{p}_{j,k}+\boldsymbol{p}_{j,k+1}}{2},$$

it follows that

$$\boldsymbol{d}_{j,k} = -\frac{1}{4}(t_{j,k+1}-t_{j,k})^2\Big\{\boldsymbol{p}^{[2]}_{j,k-1} + \frac{1}{2}(t_{j,k}+t_{j,k+1}-2t_{j,k-1})\boldsymbol{p}^{[3]}_{j,k-2}+$$
$$\frac{1}{4}(t_{j,k}+t_{j,k+1}-2t_{j,k-2})(t_{j,k}+t_{j,k+1}-2t_{j,k-1})\boldsymbol{p}^{[4]}_{j,k-2}+$$
$$\frac{1}{8}(t_{j,k}+t_{j,k+1}-2t_{j,k-2})(t_{j,k}+t_{j,k+1}-2t_{j,k-1})(t_{j,k}+t_{j,k+1}-2t_{j,k+2})\boldsymbol{p}^{[5]}_{j,k-2}\Big\}.$$

Interestingly, as for $r=2$, we can bound the r-th divided differences also for $r=3$, with a certain choice of α.

Lemma 4.6.2. *Given an α-parameterization, where $\alpha = 1/3$, with corresponding consecutively distinct control points, then*

$$\|\boldsymbol{p}^{[3]}_{j,k}\| \le 2.$$

Proof. For a general α, we have that

$$\boldsymbol{p}^{[3]}_{j,k} = \frac{\frac{\boldsymbol{e}_{j,k+2}}{\|\boldsymbol{e}_{j,k+2}\|^\alpha} - \frac{\boldsymbol{e}_{j,k+1}}{\|\boldsymbol{e}_{j,k+1}\|^\alpha}}{(\|\boldsymbol{e}_{j,k+2}\|^\alpha + \|\boldsymbol{e}_{j,k+1}\|^\alpha)(\|\boldsymbol{e}_{j,k+2}\|^\alpha + \|\boldsymbol{e}_{j,k+1}\|^\alpha + \|\boldsymbol{e}_{j,k}\|^\alpha)}$$
$$- \frac{\frac{\boldsymbol{e}_{j,k+1}}{\|\boldsymbol{e}_{j,k+1}\|^\alpha} - \frac{\boldsymbol{e}_{j,k}}{\|\boldsymbol{e}_{j,k}\|^\alpha}}{(\|\boldsymbol{e}_{j,k+1}\|^\alpha + \|\boldsymbol{e}_{j,k}\|^\alpha)(\|\boldsymbol{e}_{j,k+2}\|^\alpha + \|\boldsymbol{e}_{j,k+1}\|^\alpha + \|\boldsymbol{e}_{j,k}\|^\alpha)}.$$

If we now let $l_i = \|\boldsymbol{e}_{j,i}\| \,\forall\, i$, to simplify notation, then it follows that

$$\|\boldsymbol{p}^{[3]}_{j,k}\| \le \frac{(l^{1-\alpha}_{k+2}+l^{1-\alpha}_{k+1})(l^\alpha_{k+1}+l^\alpha_k) + (l^{1-\alpha}_{k+1}+l^{1-\alpha}_k)(l^\alpha_{k+2}+l^\alpha_{k+1})}{(l^\alpha_{k+1}+l^\alpha_k)(l^\alpha_{k+2}+l^\alpha_{k+1})(l^\alpha_{k+2}+l^\alpha_{k+1}+l^\alpha_k)}.$$

Then by imposing $\alpha = 1/3$, we get

$$\begin{aligned}\|\boldsymbol{p}_{j,k}^{[3]}\| &\leq \frac{2l_{k+1} + l_{k+2}^{2/3}l_{k+1}^{1/3} + l_{k+2}^{2/3}l_k^{1/3} + l_{k+1}^{2/3}l_k^{1/3} + l_{k+1}^{2/3}l_{k+2}^{1/3} + l_k^{2/3}l_{k+2}^{1/3} + l_k^{2/3}l_{k+1}^{1/3}}{\zeta} \\ &= \frac{l_{k+1}}{\zeta} + \frac{\zeta - [l_k^{1/3}l_{k+1}^{2/3} + l_{k+1}^{2/3}l_{k+2}^{1/3} + 3l_k^{1/3}l_{k+1}^{1/3}l_{k+2}^{1/3}]}{\zeta} \leq 2, \\ \zeta :=\ & l_{k+1} + l_{k+2}^{2/3}l_{k+1}^{1/3} + l_{k+2}^{2/3}l_k^{1/3} + 2l_{k+1}^{2/3}l_k^{1/3} + 2l_{k+1}^{2/3}l_{k+2}^{1/3} + l_k^{2/3}l_{k+2}^{1/3} + l_k^{2/3}l_{k+1}^{1/3} \\ &\quad + 3l_k^{1/3}l_{k+1}^{1/3}l_{k+2}^{1/3},\end{aligned}$$

since $\zeta > l_k^{1/3}l_{k+1}^{2/3} + l_{k+1}^{2/3}l_{k+2}^{1/3} + 3l_k^{1/3}l_{k+1}^{1/3}l_{k+2}^{1/3}$. □

It is in fact possible to prove a general bound for $\|\boldsymbol{p}_{j,k}^{[r]}\|$ for $\alpha = 1/r$, but as this will lead to an unsafe IG6-scheme for $r > 2$, as we showed in Theorem 4.3.1, there will be no general IG6-scheme C^0 proof resulting from this idea.

We will now instead consider a different way of bounding $\boldsymbol{d}_{j,k}$ for the IG6-scheme, which as we shall see will allow as us prove C^0 of a new family of related nonlinear schemes.

Cubic subtraction

Instead of bounding the distance $\boldsymbol{d}_{j,k}$ between the center of the middle edge and the inserted point directly, we shall now aim to bound the distance $\boldsymbol{q}_{j,k}$ between the new point $\boldsymbol{\pi}_6^\star = \boldsymbol{\pi}_{j,k}^6(t_\star)$, residing on the quintic α-interpolant at $t_\star = (t_2 + t_3)/2$, and the point $\boldsymbol{\pi}_4^\star = \boldsymbol{\pi}_{j,k+1}^4(t_\star)$ which is the cubic α-interpolant to the inner four points evaluated at $t_\star = (t_2 + t_3)/2$. We may then, together with the already established bounds for $\boldsymbol{r}_{j,k}$, being defined as the $\boldsymbol{d}_{j,k}$ vector for the IG4-scheme, use the triangle inequality to obtain a bound for the IG6 $\boldsymbol{d}_{j,k}$ vector. This idea is illustrated in Figure 4.7, but note that the proportions are exaggerated for illustrative purposes.

Definition 4.6.1. *For an m-point subdivision scheme with $m \geq 4$, we define*

$$\boldsymbol{d}_{j,k} = \boldsymbol{p}_{j+1,2k+1} - \frac{\boldsymbol{p}_{j,k} + \boldsymbol{p}_{j,k+1}}{2}, \tag{4.39}$$

$$\boldsymbol{q}_{j,k} = \boldsymbol{\pi}_{j,k}^m(t_\star) - \boldsymbol{\pi}_{j,k+1}^{m-2}(t_\star), \tag{4.40}$$

$$\boldsymbol{r}_{j,k} = \boldsymbol{\pi}_{j,k+1}^{m-2}(t_\star) - \frac{\boldsymbol{p}_{j,k} + \boldsymbol{p}_{j,k+1}}{2}, \tag{4.41}$$

where $\boldsymbol{\pi}_{j,k}^m(t_\star)$ is the full degree $m-1$ α-interpolant to the data $\{\boldsymbol{p}_{j,i}\}_{i=k-m/2+1}^{k+m/2}$, and $\boldsymbol{\pi}_{j,k+1}^{m-2}(t_\star)$ is the degree $m-3$ α-interpolant to the inner $m-2$ points $\{\boldsymbol{p}_{j,i}\}_{i=k-m/2+2}^{k+m/2-1}$ using the inner $m-2$ parameters, both evaluated at $t_\star = (t_{j,k} + t_{j,k+1})/2$, and $\boldsymbol{p}_{j+1,2k+1}$ is the new point defined by the subdivision scheme refinement rules.

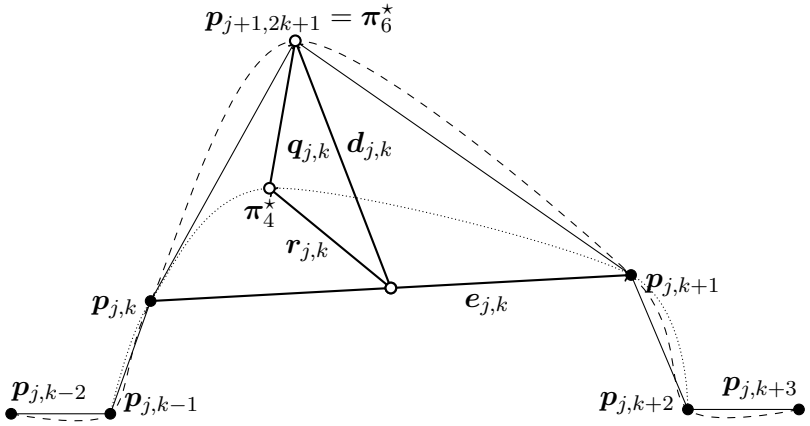

Figure 4.7: Alternative way of bounding $\boldsymbol{d}_{j,k}$ for the IG6-scheme.

Lemma 4.6.3. *For the IG6-scheme with a centripetal parameterization ($\alpha = 1/2$),*

$$\|\boldsymbol{q}_{j,k}\| < \frac{1}{2}\|\boldsymbol{e}_{j,k}\|. \tag{4.42}$$

Proof. For simplicity, we index $k-2, \ldots, k+3$ as $0, \ldots, 5$. Let $\pi_6(t)$ and $\pi_4(t)$ be the α-interpolants to $\{\boldsymbol{p}_i\}_{i=0}^5$ and $\{\boldsymbol{p}_i\}_{i=1}^4$, respectively, where we can use scalar quantities as they act independently on each coordinate after the α-parameterization. Let further $f : \mathbb{R} \to \mathbb{R}$ satisfy $f(t_i) = (\boldsymbol{p}_i)_v$, $i = 0, \ldots, 5$ for every $v \in \{0, 1, \ldots, d-1\}$. Using the Newton form of the interpolating polynomials, we find that

$$\begin{aligned} q(t_\star) :&= \pi_6(t_\star) - \pi_4(t_\star) \\ &= (t_\star - t_1)\cdots(t_\star - t_4)[t_0, \ldots, t_4]f + (t_\star - t_0)\cdots(t_\star - t_4)[t_0, \ldots, t_5]f \\ &= -\frac{(t_\star - t_1)\cdots(t_\star - t_4)}{t_5 - t_0}\left\{(t_0 - t_\star)[t_1, \ldots, t_5]f + (t_\star - t_5)[t_0, \ldots, t_4]f\right\}. \end{aligned}$$

By rewriting to vector form, it follows that

$$\begin{aligned} \boldsymbol{q}_{j,k} &= -\frac{u_2^2(2u_1+u_2)(u_2+2u_3)}{16u_{[0,4]}}\left\{(t_0 - t_\star)\boldsymbol{p}_1^{[4]} + (t_\star - t_5)\boldsymbol{p}_0^{[4]}\right\} \\ &= -\frac{u_2^2(2u_1+u_2)(u_2+2u_3)}{16u_{[0,4]}}\left\{\frac{t_0 - t_\star}{t_5 - t_1}\left(\boldsymbol{p}_2^{[3]} - \boldsymbol{p}_1^{[3]}\right) + \frac{t_\star - t_5}{t_4 - t_0}\left(\boldsymbol{p}_1^{[3]} - \boldsymbol{p}_0^{[3]}\right)\right\} \\ &= -\frac{u_2^2(2u_1+u_2)(u_2+2u_3)}{16u_{[0,4]}}\left\{\begin{array}{l} \dfrac{t_0 - t_\star}{t_5 - t_1}\left(\dfrac{\boldsymbol{p}_3^{[2]} - \boldsymbol{p}_2^{[2]}}{t_5 - t_2} - \dfrac{\boldsymbol{p}_2^{[2]} - \boldsymbol{p}_1^{[2]}}{t_4 - t_1}\right) + \\ \dfrac{t_\star - t_5}{t_4 - t_0}\left(\dfrac{\boldsymbol{p}_2^{[2]} - \boldsymbol{p}_1^{[2]}}{t_4 - t_1} - \dfrac{\boldsymbol{p}_1^{[2]} - \boldsymbol{p}_0^{[2]}}{t_3 - t_0}\right) \end{array}\right\}, \end{aligned}$$

where we used the local indexation $\boldsymbol{p}_i^{[r]}$ also for the r-th divided difference starting at $\boldsymbol{p}_i$. For a centripetal parameterization, i.e. $\alpha = 1/2$, then $u_2^2/l_2 = l_2^{2\alpha-1} = 1$, so

$$\begin{aligned}\frac{\|\boldsymbol{q}_{j,k}\|}{l_2} &\leq \frac{(2u_1+u_2)(u_2+2u_3)}{32u_{[0,4]}}\left\{\begin{array}{l}\dfrac{2u_0+2u_1+u_2}{u_{[1,4]}}\left(\dfrac{\|\boldsymbol{p}_3^{[2]}\|+\|\boldsymbol{p}_2^{[2]}\|}{u_{[2,4]}}+\dfrac{\|\boldsymbol{p}_2^{[2]}\|+\|\boldsymbol{p}_1^{[2]}\|}{u_{[1,3]}}\right)+\\ \dfrac{u_2+2u_3+2u_4}{u_{[0,3]}}\left(\dfrac{\|\boldsymbol{p}_2^{[2]}\|+\|\boldsymbol{p}_1^{[2]}\|}{u_{[1,3]}}+\dfrac{\|\boldsymbol{p}_1^{[2]}\|+\|\boldsymbol{p}_0^{[2]}\|}{u_{[0,2]}}\right)\end{array}\right\}\\ &\leq \frac{(2u_1+u_2)(u_2+2u_3)}{16u_{[0,4]}}\left\{\begin{array}{l}\dfrac{2u_0+2u_1+u_2}{u_{[1,4]}}\left(\dfrac{1}{u_{[2,4]}}+\dfrac{1}{u_{[1,3]}}\right)+\\ \dfrac{u_2+2u_3+2u_4}{u_{[0,3]}}\left(\dfrac{1}{u_{[1,3]}}+\dfrac{1}{u_{[0,2]}}\right)\end{array}\right\},\end{aligned}$$

since $\|\boldsymbol{p}_i^{[2]}\| \leq 1 \,\forall\, i \,|\, \alpha = 1/2$, as shown before. Furthermore, by rewriting to a common denominator, we get

$$\begin{aligned}\frac{\|\boldsymbol{q}_{j,k}\|}{l_2} &\leq \frac{(2u_1+u_2)(u_2+2u_3)}{16u_{[0,4]}}\left\{\begin{array}{l}\dfrac{2u_0+2u_1+u_2}{u_{[1,4]}}\left(\dfrac{u_{[1,3]}+u_{[2,4]}}{u_{[2,4]}u_{[1,3]}}\right)+\\ \dfrac{u_2+2u_3+2u_4}{u_{[0,3]}}\left(\dfrac{u_{[0,2]}+u_{[1,3]}}{u_{[1,3]}u_{[0,2]}}\right)\end{array}\right\}\\ &= \frac{(2u_1+u_2)(u_2+2u_3)}{16u_{[0,4]}u_{[1,4]}u_{[2,4]}u_{[1,3]}u_{[0,2]}u_{[0,3]}}\left\{\begin{array}{l}u_{[0,3]}u_{[0,2]}(2u_{[0,1]}+u_2)(u_{[1,3]}+u_{[2,4]})+\\ u_{[1,4]}u_{[2,4]}(u_2+2u_{[3,4]})(u_{[0,2]}+u_{[1,3]})\end{array}\right\}\\ &= \frac{\nu(u_0,\ldots,u_4)}{\zeta(u_0,\ldots,u_4)} = \frac{\nu}{2\nu+C(u_0,\ldots,u_4)} < \frac{1}{2},\end{aligned}$$

where

$$\begin{aligned}\nu &:= (2u_1+u_2)(u_2+2u_3)\left\{\begin{array}{l}u_{[0,3]}u_{[0,2]}(2u_{[0,1]}+u_2)(u_{[1,3]}+u_{[2,4]})+\\ u_{[1,4]}u_{[2,4]}(u_2+2u_{[3,4]})(u_{[0,2]}+u_{[1,3]})\end{array}\right\},\\ \zeta &:= 16u_{[0,4]}u_{[1,4]}u_{[2,4]}u_{[1,3]}u_{[0,2]}u_{[0,3]},\\ C &:= \zeta - 2\nu,\end{aligned}$$

and we used that $C > 0$, since ζ contains terms which are not found in ν. Defining the full numerator as the function ν and the full common denominator as the function ζ, as above, and using a computer algebra system, namely Matlab's Symbolic Math Toolbox, to compute the coefficients of the unique expanded terms in the numerator and denominator, we find that all the terms of ν occur in ζ with at least double the coefficient. In fact only ten of the common terms in ζ have a coefficient twice as high as the corresponding coefficient in ν. The rest have even higher coefficients in ζ. The complete list of the coefficient in ζ divided by the corresponding coefficient in ν can be

found below.

Listing 4.1: Complete list of sorted coefficient ratios

```
2 2 2 2 2 2 2 2 2 2 16/7 16/7 16/7 16/7 5/2 5/2 68/27 68/27
8/3 8/3 8/3 8/3 36/13 36/13 44/15 44/15 3 55/18 59/19 59/19
16/5 16/5 114/35 114/35 64/19 64/19 24/7 100/29 100/29 168/47
168/47 18/5 18/5 80/21 80/21 80/21 80/21 96/25 96/25 144/37
144/37 160/41 160/41 4 4 4 4 4 4 4 4 4 4 4 4 4 4 4 4 4 4 56/13
56/13 192/43 192/43 24/5 24/5 24/5 24/5 216/43 216/43 88/17
88/17 16/3 16/3 52/9 52/9 6 6 6 6 7 7 120/17 120/17 352/47
352/47 15/2 15/2 8 8 10 10 57/5 57/5 12 12 12 12 12 12 12 12
124/9 124/9 432/29 432/29 16 16 16 16 16 33/2 33/2 17 17 52/3
52/3 18 18 112/5 112/5 68/3 68/3 76/3 76/3 28 28 28 28 68 68
```

This is the same type of coefficient comparison process as in the proof of Theorem 4.3.2, just on a grander scale. Therefore, we conclude that we at least have the bound

$$\|\boldsymbol{q}_{j,k}\| < \frac{1}{2} l_2 = \frac{1}{2}\|\boldsymbol{e}_{j,k}\|.$$

□

Corollary 4.6.1. *For the IG6-scheme with $\alpha = 1/2$,*

$$\|\boldsymbol{d}_{j,k}\| < \frac{3}{4}\|\boldsymbol{e}_{j,k}\|.$$

Proof. By using the centripetal bound (4.12) on $\boldsymbol{r}_{j,k}$, since this is the $\boldsymbol{d}_{j,k}$ vector for the IG4-scheme, we get $\|\boldsymbol{r}_{j,k}\| \leq \|\boldsymbol{e}_{j,k}\|/4$, and thus

$$\|\boldsymbol{d}_{j,k}\| \leq \|\boldsymbol{q}_{j,k}\| + \|\boldsymbol{r}_{j,k}\| < \frac{3}{4}\|\boldsymbol{e}_{j,k}\|.$$

□

This is admittedly not sufficient for C^0 convergence of the IG6-scheme, as we need $\|\boldsymbol{d}_{j,k}\| < \|\boldsymbol{e}_{j,k}\|/2$, but it is a step in the right direction.

The proof of Lemma 4.6.3 is perhaps not the most elegant, but as we exhaustively go through every relevant coefficient in the coefficient comparison process, it is valid. Alternatively, to show that $\|\boldsymbol{q}_{j,k}\|/l_2 < 1/2$, one could use that we can assume without loss of generality that $u_4 \geq u_0$. By symmetry, it is perhaps enough to show that

$$\phi := \frac{(2u_1 + u_2)(u_2 + 2u_3)u_{[0,3]}u_{[0,2]}(2u_{[0,1]} + u_2)(u_{[1,3]} + u_{[2,4]})}{16u_{[0,4]}u_{[1,4]}u_{[2,4]}u_{[1,3]}u_{[0,2]}u_{[0,3]}} < \frac{1}{4}.$$

Then, by letting $\phi = (a+b)/(c+d)$, where

$$
\begin{aligned}
a &:= (2u_1+u_2)(u_2+2u_3)u_{[0,3]}u_{[0,2]}(2u_{[0,1]}+u_2)u_{[1,3]},\\
b &:= (2u_1+u_2)(u_2+2u_3)u_{[0,3]}u_{[0,2]}(2u_{[0,1]}+u_2)u_{[2,4]},\\
c &:= 16u_{[0,4]}u_{[1,4]}u_{[2,4]}u_{[1,3]}u_{[0,2]}u_{[0,1]}, \quad d := 16u_{[0,4]}u_{[1,4]}u_{[2,4]}u_{[1,3]}u_{[0,2]}u_{[2,3]},
\end{aligned}
$$

we can use that in general $(a+b)/(c+d) \leq \max\{a/c, b/d\}$ for positive real numbers a, b, c, d. For the case a/c, we for example find that

$$
\frac{a}{c} \leq \frac{8u_{[1,2]}u_{[2,3]}u_{[0,3]}(u_{[0,2]})^2u_{[1,3]}}{16u_{[0,4]}u_{[1,4]}u_{[2,4]}u_{[1,3]}u_{[0,2]}u_{[0,1]}} = \frac{u_{[1,2]}u_{[2,3]}u_{[0,3]}u_{[0,2]}}{2u_{[0,4]}u_{[1,4]}u_{[2,4]}u_{[0,1]}}.
$$

By letting $u_0 \geq u_2$, $u_1 \geq u_3$, we find that

$$
\frac{a}{c} \leq \frac{u_{[0,1]}u_{[2,3]}u_{[1,4]}u_{[2,4]}}{2u_{[0,4]}u_{[1,4]}u_{[2,4]}u_{[0,1]}} = \frac{u_{[2,3]}}{2u_{[0,4]}} \leq \frac{u_{[2,3]}}{4u_{[2,3]}+u_4} < \frac{1}{4}.
$$

This is only an outline of an alternative strategy since we only considered one configuration of edge lengths and only a/c, but it is evident that the same general principle also goes for the other cases. Showing this for every possible case would however require a lot of writing without yielding any significant additional insights.

Numerical Monte Carlo experiments, where the l_i are randomized, indicate that the sharpest possible bound on $\|\boldsymbol{q}_{j,k}\|$, using this cubic subtraction strategy, is very close to the bound in Lemma 4.6.3. Thus, we cannot hope to show that the IG6-scheme is C^0 for $\alpha = 1/2$ using this approach. Based on the idea of bounding $\boldsymbol{q}_{j,k}$, we can however introduce a new family of nonlinear schemes and prove C^0 for a subset of these schemes.

4.7 The iterated geometric blending schemes

Using an α-parameterization[5], and given an even number $m \geq 4$, we define the subdivision refinement rules for the iterated geometric blending m-point schemes (IGBm-schemes) as follows

$$
\boldsymbol{p}_{j+1,2k} = \boldsymbol{p}_{j,k}, \tag{4.43}
$$

$$
\boldsymbol{p}_{j+1,2k+1} = (1-\lambda)\boldsymbol{\pi}^{m-2}_{j,k+1}(t_\star) + \lambda\boldsymbol{\pi}^{m}_{j,k}(t_\star), \tag{4.44}
$$

$$
t_\star = \frac{t_{j,k}+t_{j,k+1}}{2}, \tag{4.45}
$$

where $\lambda \in \mathbb{R}$ is a blending parameter, and $\boldsymbol{\pi}^{m}_{j,k}(t_\star)$ and $\boldsymbol{\pi}^{m-2}_{j,k+1}(t_\star)$ are defined in Definition 4.6.1. Thus the scheme is a binary nonlinear m-point scheme, where in a sense the

[5]Which is recomputed at each level, as for the IGm-schemes.

influence of the outer two points at each insertion is determined by λ. Note that for an IGBm-scheme with an even number $m \geq 4$, and $\lambda \in \mathbb{R}$, we have

$$\begin{aligned}
\boldsymbol{r}_{j,k} &= \boldsymbol{\pi}_{j,k+1}^{m-2}(t_\star) - (\boldsymbol{p}_{j,k} + \boldsymbol{p}_{j,k+1})/2, \\
\boldsymbol{p}_{j+1,2k+1} &= (1-\lambda)\boldsymbol{\pi}_{j,k+1}^{m-2}(t_\star) + \lambda \boldsymbol{\pi}_{j,k}^{m}(t_\star) \\
&= \boldsymbol{\pi}_{j,k+1}^{m-2}(t_\star) + \lambda \left(\boldsymbol{\pi}_{j,k}^{m}(t_\star) - \boldsymbol{\pi}_{j,k+1}^{m-2}(t_\star) \right) \\
&= \boldsymbol{\pi}_{j,k+1}^{m-2}(t_\star) + \lambda \boldsymbol{q}_{j,k}, \\
\boldsymbol{d}_{j,k} &= \boldsymbol{p}_{j+1,2k+1} - (\boldsymbol{p}_{j,k} + \boldsymbol{p}_{j,k+1})/2 \\
&= \boldsymbol{r}_{j,k} + \lambda \boldsymbol{q}_{j,k}.
\end{aligned}$$

It is natural to think that there may be some kind of correlation between the IGB4-scheme for $\alpha = 0$ and the FPTS.

Lemma 4.7.1. *The IGB4-scheme for $\alpha = 0$ is equivalent to the FPTS with $w = \lambda/16$.*

Proof. For $m = 4$, we have $\boldsymbol{\pi}_1^{m-2}(t_\star) = (\boldsymbol{p}_1 + \boldsymbol{p}_2)/2$. Furthermore, for $\alpha = 0$, the cubic Lagrange basis function values become

$$L_0^\star = -\frac{1}{16}, \quad L_1^\star = \frac{9}{16}, \quad L_2^\star = \frac{9}{16}, \quad L_3^\star = -\frac{1}{16}.$$

Therefore, $\boldsymbol{p}^\star$ in (4.44) for the IGB4 scheme becomes

$$\begin{aligned}
\boldsymbol{p}^\star &= \lambda \sum_{i=0}^{3} L_i^\star \boldsymbol{p}_i + (1-\lambda)\frac{\boldsymbol{p}_1 + \boldsymbol{p}_2}{2} \\
&= -\frac{\lambda}{16}\boldsymbol{p}_0 + \left(\frac{9\lambda}{16} + \frac{1-\lambda}{2} \right) \boldsymbol{p}_1 + \left(\frac{9\lambda}{16} + \frac{1-\lambda}{2} \right) \boldsymbol{p}_2 - \frac{\lambda}{16}\boldsymbol{p}_3 \\
&= -\frac{\lambda}{16}\boldsymbol{p}_0 + \left(\frac{\lambda}{16} + \frac{1}{2} \right) \boldsymbol{p}_1 + \left(\frac{\lambda}{16} + \frac{1}{2} \right) \boldsymbol{p}_2 - \frac{\lambda}{16}\boldsymbol{p}_3,
\end{aligned}$$

which is exactly (1.7) of the FPTS with $w = \lambda/16$. □

Hence, the IGB4-scheme is one possible generalization of the FPTS. For $\lambda \in [0, 1]$, the odd insertion rule (4.44) is a convex combination of the insertion points $\boldsymbol{\pi}_{j,k+1}^{m-2}(t_\star)$ and $\boldsymbol{\pi}_{j,k}^{m}(t_\star)$ for the corresponding iterated geometric schemes, and for a general $\lambda \in \mathbb{R}$, the insertion point resides on the line prescribed by these two points. For $\lambda = 0$ and $\lambda = 1$, the scheme is respectively equivalent to the corresponding iterated geometric schemes of orders $m - 2$ and m. It is worth noting that for most practical purposes, λ outside a sensible range will produce limit curves of little use. We will first address the case IGB6 for $\alpha = 0$, which is a linear scheme, and hence the Laurent analysis of chapter 2 is applicable.

Theorem 4.7.1. *The IGB6-scheme with $\alpha = 0$ is*

$$C^0 \quad \textit{for} \quad \lambda \in \left(-\frac{2(5\sqrt{201}-9)}{9},\ \frac{8(\sqrt{5889}-27)}{45} \right) \approx (-13.75,\ 8.84), \tag{4.46}$$

$$C^1 \quad \textit{for} \quad \lambda \in \left(-\frac{8(\sqrt{273}-15)}{9},\ \frac{8(3\sqrt{37}-5)}{21} \right) \approx (-1.35,\ 5.04), \tag{4.47}$$

$$C^2 \quad \textit{for} \quad \lambda \in \left(0,\ \frac{64}{27} \right) = (0,\ 2.\overline{370})\,. \tag{4.48}$$

Proof. The odd insertion rule for the IGB6-scheme with $\alpha = 0$ becomes

$$p_{j+1,2k+1} = \frac{3\lambda}{256}\left(p_{j,k-2} + p_{j,k+3}\right) - \frac{9\lambda+16}{256}\left(p_{j,k-1} + p_{j,k+2}\right) + \frac{3(\lambda+24)}{128}\left(p_{j,k} + p_{j,k+1}\right).$$

Thus its symbol is

$$\begin{aligned} m(z) &= \frac{3\lambda}{256}\left(z^{-5}+z^{5}\right) - \frac{9\lambda+16}{256}\left(z^{-3}+z^{3}\right) + \frac{3(\lambda+24)}{128}\left(z^{-1}+z\right) + 1 \\ &= \frac{(z+1)^4\left\{3\lambda(z-1)^4(z^2+1) - 16z^2(z^2-4z+1)\right\}}{256z^5}. \end{aligned}$$

Starting with $n = 0$ (C^0 analysis) and $\ell = 1$, we get

$$2\left|\frac{3\,\lambda}{128} + \frac{1}{16}\right| + \frac{3\,|\lambda|}{128} + \frac{1}{2} < 1,$$

which holds for $\lambda \in (-80/9, 16/3)$. However, for $\ell = 2$ we obtain

$$\begin{aligned} \max\Bigg(&\frac{9\,|\lambda|^2}{65536} + \frac{3\,|\lambda|}{512} + \left|\frac{9\,\lambda^2}{8192} + \frac{21\,\lambda}{2048} + \frac{1}{256}\right| + \left|\frac{9\,\lambda^2}{8192} - \frac{15\,\lambda}{2048} + \frac{57}{256}\right| + \\ &\left|\frac{27\,\lambda^2}{65536} + \frac{21\,\lambda}{1024} + \frac{17}{256}\right| + \left|\frac{27\,\lambda^2}{65536} + \frac{3\,\lambda}{4096}\right| + \left|\frac{63\,\lambda^2}{65536} + \frac{39\,\lambda}{4096} + \frac{9}{256}\right|, \\ &\frac{9\,|\lambda|^2}{65536} + \frac{3\,|\lambda|}{512} + \left|\frac{9\,\lambda^2}{8192} - \frac{3\,\lambda}{2048} + \frac{1}{256}\right| + \left|-\frac{9\,\lambda^2}{8192} + \frac{15\,\lambda}{2048} + \frac{71}{256}\right| + \\ &\left|\frac{27\,\lambda^2}{65536} - \frac{3\,\lambda}{1024} + \frac{1}{256}\right| + \left|\frac{27\,\lambda^2}{65536} + \frac{3\,\lambda}{4096}\right| + \left|-\frac{63\,\lambda^2}{65536} + \frac{57\,\lambda}{4096} + \frac{7}{256}\right| \Bigg) < 1, \end{aligned}$$

which yields the improved interval of convergence in (4.46).

For $n = 1$ (C^1 analysis) and $\ell = 2$, we get the inequality

$$\max\Bigg(\frac{9\,|\lambda|^2}{8192}+\left|\frac{9\,\lambda^2}{4096}-\frac{45\,\lambda}{512}+\frac{1}{2}\right|+2\left|\frac{9\,\lambda^2}{8192}-\frac{21\,\lambda}{1024}\right|+2\left|\frac{9\,\lambda^2}{16384}-\frac{3\,\lambda}{128}+\frac{1}{8}\right|,$$
$$\frac{9\,|\lambda|^2}{4096}+\left|-\frac{9\,\lambda^2}{4096}+\frac{21\,\lambda}{512}+\frac{1}{4}\right|+\left|\frac{27\,\lambda^2}{4096}-\frac{9\,\lambda}{512}+\frac{1}{32}\right|+$$
$$\left|\frac{27\,\lambda^2}{8192}+\frac{3\,\lambda}{512}\right|+\left|\frac{45\,\lambda^2}{8192}+\frac{15\,\lambda}{512}+\frac{1}{32}\right|,$$
$$2\left|-\frac{9\,\lambda^2}{4096}+\frac{9\,\lambda}{256}+\frac{7}{64}\right|+2\left|\frac{9\,\lambda^2}{8192}+\frac{3\,\lambda}{1024}\right|+2\left|\frac{27\,\lambda^2}{8192}-\frac{33\,\lambda}{1024}+\frac{1}{64}\right|\Bigg)<1,$$

which results in (4.47).
We now turn to $n = 2$ (C^2 analysis). Again the case for $\ell = 1$ is inconclusive, i.e. $\|S^1_{\boldsymbol{b}}\|_\infty \geq 1$, so we look at $\|S^2_{\boldsymbol{b}}\|_\infty$, and get the inequality

$$\max\Bigg(\Big|9\lambda^2/2048+69\lambda/256-3/8\Big|+\Big|45\lambda^2/2048-63\lambda/256+5/8\Big|+$$
$$\Big|27\lambda^2/4096+21\lambda/256\Big|+\Big|63\lambda^2/4096-15\lambda/256\Big|+9\lambda^2/1024,$$
$$\Big|9\lambda^2/512-9\lambda/64+1/16\Big|-3\lambda/64+\Big|9\lambda/128-9\lambda^2/512+3/8\Big|$$
$$+\Big|9\lambda^2/512+9\lambda/256\Big|+3|\lambda|/256+9\lambda^2/512+3/16\Bigg)<1.$$

This is the same as

$$0<\lambda<\frac{4(\sqrt{193}-7)}{9},\quad \frac{4(1-\sqrt{7})}{3}<\lambda<\frac{64}{27},$$

which holds for $\lambda \in (0, 64/27)$, so we get (4.48). □

We remark that it seems that a nonzero contribution from the outer two points is needed to produce a C^2 limit curve, which is expected as the FPS is not C^2 and no C^2 binary interpolatory four-point scheme has been found. The bounds on λ for C^n, $n = 0, 1, 2$ are almost certainly not the best possible, but are sufficient to cover some applications in CAGD. Note also that the IGB6 scheme with $\alpha = 0$ is the same as the six-point scheme with tension parameter θ in [10] with $3\lambda/256 = \theta$, which is shown to be C^2 for $0 < \theta < 0.042$ in [20] by considering $\ell = 10$, and translates to $0 < \lambda < 3.584$. Detailed Laurent polynomial analysis corresponding to the proof of Theorem 4.7.1 can be found in [21]. More interesting and relevant is perhaps the potentially unexplored nonlinear case for $\alpha \neq 0$, which we will consider now.

Theorem 4.7.2. *The IGB4-scheme is C^0 and safe for all $\lambda \in (-2, 2)$ with $\alpha = 1/2$, and $\lambda \in [-1, 1]$ for all $\alpha \in (1/2, 1]$. The IGB6-scheme is C^0 and safe for all $\lambda \in [-1/2, 1/2]$ with $\alpha = 1/2$.*

Proof. We begin by proving that the IGB6-scheme is displacement-safe for the indicated range of λ. Fix $\alpha = 1/2$. Using Lemma 4.6.3, we have that

$$\|\lambda \boldsymbol{q}_{j,k}\| = |\lambda| \|\boldsymbol{q}_{j,k}\| < \frac{1}{2}\left(\frac{\|\boldsymbol{e}_{j,k}\|}{2}\right) = \frac{\|\boldsymbol{e}_{j,k}\|}{4} \quad \forall \quad \lambda \in [-1/2, 1/2].$$

Thus, by (4.12),

$$\|\boldsymbol{d}_{j,k}\| \leq \|\boldsymbol{r}_{j,k}\| + |\lambda| \|\boldsymbol{q}_{j,k}\| < \frac{\|\boldsymbol{e}_{j,k}\|}{4} + \frac{\|\boldsymbol{e}_{j,k}\|}{4} = \frac{\|\boldsymbol{e}_{j,k}\|}{2}.$$

For the IGB4-scheme, $\boldsymbol{r}_{j,k} = \boldsymbol{0}$, since $\boldsymbol{\pi}^2_{j,k+1}(t_\star)$ is simply the midpoint of the central edge $\boldsymbol{e}_{j,k}$ for any $\alpha \in [0, 1]$. Therefore,

$$\|\boldsymbol{d}_{j,k}\| \leq |\lambda| \|\boldsymbol{q}_{j,k}\| < \begin{cases} \frac{\|\boldsymbol{e}_{j,k}\|}{2} & \forall \quad \lambda \in (-2, 2), \quad \alpha = 1/2, \\ \frac{\|\boldsymbol{e}_{j,k}\|}{2} & \forall \quad \lambda \in [-1, 1], \quad \alpha \in (1/2, 1]. \end{cases}$$

These follow by the bound (4.12) on $\|\boldsymbol{d}_{j,k}\|$ and Theorem 4.3.2 for the IG4-scheme, respectively.
For both the IGB4 and IGB6 schemes, with the intervals of λ, we get

$$\max\left(\|\boldsymbol{e}_{j+1,2k}\|, \|\boldsymbol{e}_{j+1,2k+1}\|\right) \leq \|\boldsymbol{e}_{j,k}\|/2 + \|\boldsymbol{d}_{j,k}\| \leq \eta \|\boldsymbol{e}_{j,k}\|,$$

where $\eta < 1$ is a positive real number. Let again $\boldsymbol{g}_j$ be the piecewise linear interpolant to the data $(2^{-j}k, \boldsymbol{p}_{j,k})$. We get

$$\begin{aligned} \|\boldsymbol{g}_{j+1} - \boldsymbol{g}_j\|_\infty = \sup_{k\in\mathbb{Z}} \|\boldsymbol{d}_{j,k}\| &\leq \frac{1}{2} \sup_{k\in\mathbb{Z}} \|\boldsymbol{e}_{j,k}\| \\ &\leq \frac{\eta}{2} \sup_{k\in\mathbb{Z}} \|\boldsymbol{e}_{j-1,k}\| \leq \cdots \leq \frac{\eta^j}{2} \sup_{k\in\mathbb{Z}} \|\boldsymbol{e}_{0,k}\|. \end{aligned}$$

Since $\eta < 1$, then $\{\boldsymbol{g}_j\}_{j=0,1,\ldots}$ is a Cauchy sequence in the sup-norm, and consequently the limit curve is C^0. The safety of both schemes follows immediately as they are displacement safe by construction. □

We remark that in the proof of Theorem 4.7.2 there is also no actual requirement on λ to be a constant, and thus the scheme can be adapted to a nonuniform or nonstationary scheme where λ is dependent on j and k, and as long as the absolute value of each $\lambda_{j,k}$ is sufficiently small, then the limit curve is still C^0.

In figure Figure 4.8, we observe that the largest deviation between the limit curves for ranges of λ seems to occur when the outer two distances between control points are significantly different from the inner lengths. We have shown that the curves in Figure 4.8 for $\lambda = 0, 1/2, -1/2$ are C^0, and we observe that they are fairly close to the

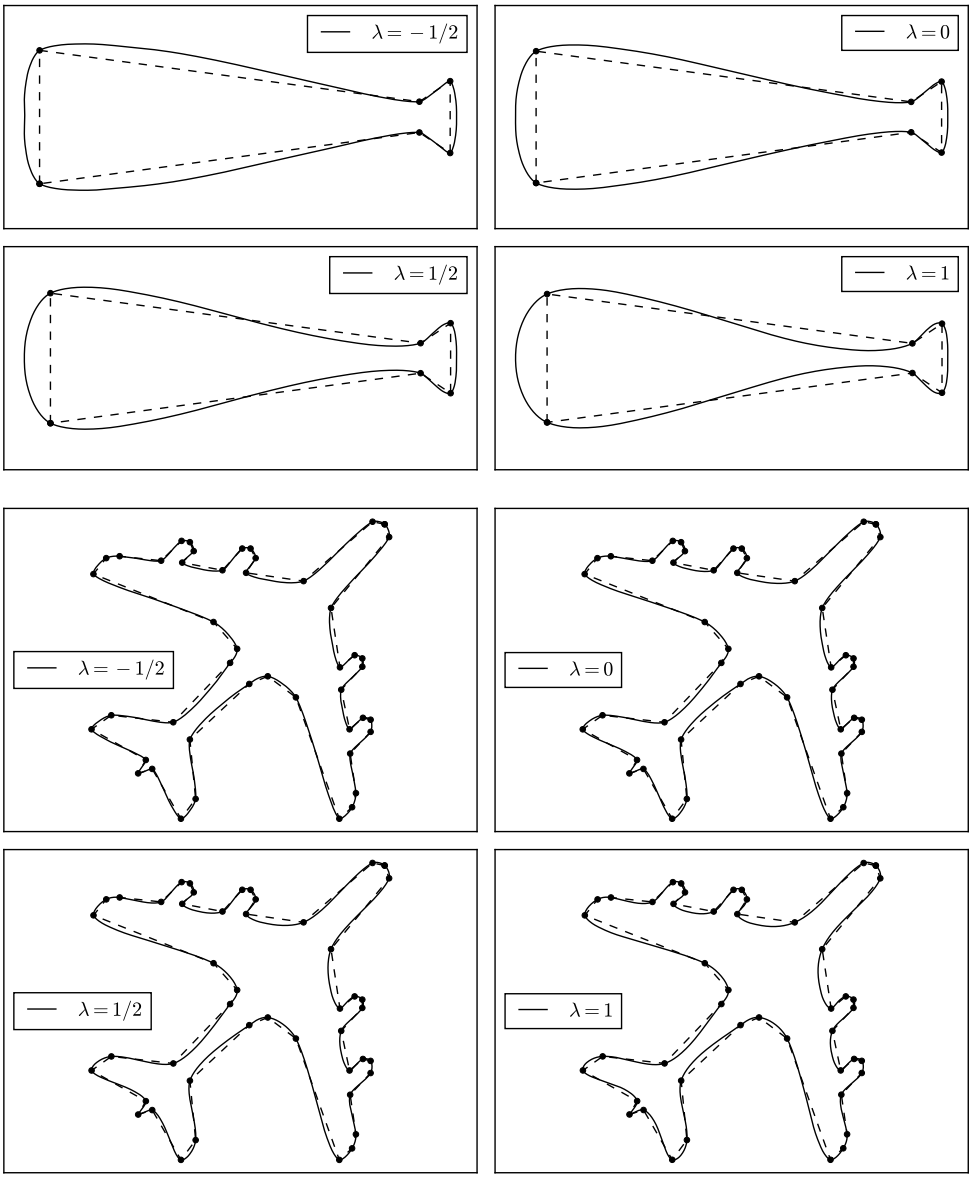

Figure 4.8: IGB6 limit curves for $\alpha = 1/2$ and various choices of blending parameter λ.

limit curve for $\lambda = 0$, i.e. the centripetal IG4 limit curve. Although it is very likely that the IG4-scheme is not C^2, the same is not necessarily the case for the IGB6-scheme with $\lambda \neq 0$ close to 0, as for the linear scheme in Theorem 4.7.1. Thus, it appears that we can get limit curves close to the tight limit curve for the centripetal IG4-scheme, with possibly elevated smoothness. Further numerical tests on the smoothness of these schemes will be done in chapter 6.

Chapter Five

Analysis of geometric subdivision

Although the nonlinear four-point scheme of the previous chapter has better shape preserving properties than the classical four-point scheme in terms of achieving better results when it comes to certain artifacts, the nonlinear scheme does not preserve curvature when the control polygon is sampled from a function with a simple curvature profile, e.g. a circle. In this chapter, we look at the circle preserving scheme (CPS) in [12] by Sabin and Dodgson in relation to a recent article by Ewald et al. [13], where a powerful framework for studying a certain type of nonlinear subdivision schemes is presented. We further prove that the schemes of chapter 4 fit into this framework, and propose a modification to the iterated geometric schemes to better control the local spacing of the points as j increases.

5.1 Circle preserving subdivision

The circle preserving scheme (CPS), of [12], is defined as follows,

$$\begin{aligned} \boldsymbol{p}_{j+1,2k} &= \boldsymbol{p}_{j,k}, \\ \boldsymbol{p}_{j+1,2k+1} &= \boldsymbol{C}(\dot{t}), \end{aligned}$$

where $\boldsymbol{C}(\dot{t})$ is a point on the circle $\boldsymbol{C}$, passing through $\boldsymbol{p}_{j,k}$ and $\boldsymbol{p}_{j,k+1}$, with curvature $\kappa_\star$ that is the arithmetic mean of the curvature κ_1 of the circle $\boldsymbol{C}_1$ prescribed by the points $\boldsymbol{p}_{j,k-1}, \boldsymbol{p}_{j,k}, \boldsymbol{p}_{j,k+1}$ and κ_2 of the circle $\boldsymbol{C}_2$ prescribed by $\boldsymbol{p}_{j,k}, \boldsymbol{p}_{j,k+1}, \boldsymbol{p}_{j,k+2}$. Moreover, the specific point $\boldsymbol{p}_{j+1,2k+1} = \boldsymbol{C}(\dot{t})$ on this circle $\boldsymbol{C}$ is chosen such that

$$\frac{\|\boldsymbol{p}_{j+1,2k+1} - \boldsymbol{p}_{j,k}\|}{\|\boldsymbol{p}_{j+1,2k+1} - \boldsymbol{p}_{j,k+1}\|} = \sqrt{\frac{\|\boldsymbol{p}_{j,k+1} - \boldsymbol{p}_{j,k-1}\|}{\|\boldsymbol{p}_{j,k+2} - \boldsymbol{p}_{j,k}\|}} \tag{5.1}$$

is satisfied. The purpose of this is to make the points asymptotically locally uniformly spaced in the limit. The notion of curvature κ chosen is the *curvature axis vector*, defined

as

$$\kappa_i = \frac{(\boldsymbol{p}_{i+1} - \boldsymbol{p}_i) \times (\boldsymbol{p}_i - \boldsymbol{p}_{i-1})}{\|\boldsymbol{p}_{i+1} - \boldsymbol{p}_i\| \|\boldsymbol{p}_i - \boldsymbol{p}_{i-1}\| \|\boldsymbol{p}_{i-1} - \boldsymbol{p}_{i+1}\|}, \quad i = 1, 2,$$

at the points $\boldsymbol{p}_{j,i}$, where we used local indexation. Thus, $\kappa_\star = (\kappa_1 + \kappa_2)/2$. This curvature definition uses a vector that is perpendicular to the osculating plane spanned by the respective points, and thus allows control points in both $\mathbb{R}^2$ and $\mathbb{R}^3$.

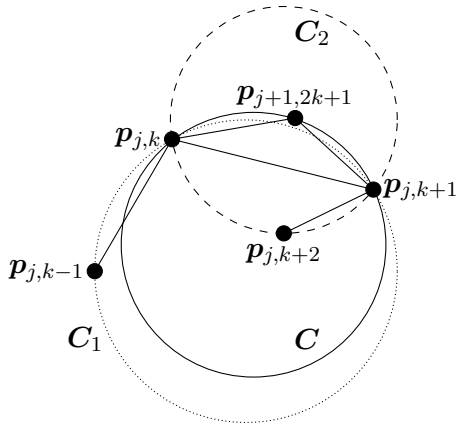

Figure 5.1: CPS construction in $\mathbb{R}^2$.

To analyze this scheme, the authors in [12] considered the case after many iterations, where consecutive points are locally almost equidistant. In this case, it can be shown that the new point at each refinement is sufficiently close to the corresponding new point of the FPS to also result in a C^0 limit curve, i.e. that the schemes are asymptotically equivalent.

Recently, in [13], a new method was established for analyzing the smoothness of a selection of geometric nonlinear subdivision schemes, including the CPS. We will here touch upon some aspects of the paper in question.

5.2 Convergence analysis of GLUE-schemes

In this section we shall review the fundamentals of [13] in order to place and adapt the schemes of chapter 4 to fit into the framework of this paper. There will be no attempt to go through all the technicalities of the paper, but rather to get a basic understanding of some of the key concepts. In order to more closely follow the discussion of [13], we use a slightly different notation in this section to avoid complications. Let $\mathbb{E} := \mathbb{R}^d$, and let a sequence of control points be called a *chain*. A chain of at least n control points is written as $\mathbb{E}^{\geq n}$, and a chain of N points in denoted $\mathbb{E}^N$, for $n, N \in \mathbb{N}$. In this

section we allow a point of a chain, i.e. a vector, to be written as lowercase nonbold letters, write chains as uppercase bold letters, and reserve the uppercase bold letter $\boldsymbol{G}$ for a subdivision scheme acting on chains. We let $\boldsymbol{G}(\boldsymbol{P})$ denote the chain resulting from letting the subdivision scheme $\boldsymbol{G}$ act on the chain $\boldsymbol{P}$, and let $(\boldsymbol{P})_i$ denote the i-th point of a chain $\boldsymbol{P}$. Furthermore, we let $\#\boldsymbol{P}$ denote the number of points of a chain $\boldsymbol{P}$.

A similarity $S = (\varrho, Q, s) : \mathbb{E} \to \mathbb{E}$ is comprised of the positive scalar scaling factor $\varrho \in \mathbb{R}$, an orthogonal transformation matrix $Q \in \mathbb{R}^{d\times d}$, and a shift vector $s \in \mathbb{E}$. S applied to a point $p \in \mathbb{E}$ is defined as $S(p) = \varrho Qp + s$. Moreover, the norm of S is given as $\|S\| = \varrho$, and the group of similarities in $\mathbb{E}$ is denoted by $\mathcal{S}(\mathbb{E})$. Application of S to a chain $\boldsymbol{P} \in \mathbb{E}^N$ is understood as $S(\boldsymbol{P}) = [S(p_0), \ldots, S(p_{N-1})]$. We let e be the first unit vector in $\mathbb{E}$, and

$$\boldsymbol{E}_N := [e, 2e, \ldots, Ne], \quad \boldsymbol{e} := \boldsymbol{E}_n = [e, 2e, \ldots, ne].$$

We are now ready to properly define a *GLUE-scheme*, using the definition from [13]. Note that the number m in the following definition is not the same m as we are used to[1], and the definition uses a somewhat different indexation of the points.

Definition 5.2.1. *[13] Given $m \in \mathbb{N}$, let $n := 2m + 1$. The function $\boldsymbol{G} : \mathbb{E}^{\geq n} \to \mathbb{E}^{\geq n}$ defines a geometric, local, uniform, equilinear subdivision scheme (or briefly GLUE-scheme) in $\mathbb{E}$ with spread n if $\#\boldsymbol{G}(\boldsymbol{P}) = 2\#\boldsymbol{P} - n + 1$ and if it satisfies the following properties:*

(G) $\boldsymbol{G}$ commutes with similarities; i.e.,

$$\boldsymbol{G} \circ S = S \circ \boldsymbol{G}, \quad S \in \mathcal{S}(\mathbb{E}).$$

(L) The points p'_{2i} and p'_{2i+1} of the chain $\boldsymbol{P}' := \boldsymbol{G}(\boldsymbol{P})$ depend only on $p_i, \ldots, p_{i+m}$.

(U) There exist functions g_0, $g_1 : \mathbb{E}^{m+1} \to \mathbb{E}$ independent of i such that

$$p'_{2i+\lambda} = g_\lambda(p_i, \ldots, p_{i+m}), \quad \lambda \in \{0, 1\}, \quad 0 \leq i < \#\boldsymbol{P} - m.$$

These functions are $C^{1,\nu}$ in a neighborhood of $\boldsymbol{E}_{m+1}$ for some $\nu > 0$, called the regularity parameter of $\boldsymbol{G}$.

(E) The standard linear chain $\boldsymbol{e}$ is scaled down and translated by $\boldsymbol{G}$ according to

$$\begin{aligned}\boldsymbol{G}(\boldsymbol{e}) &= [e/2 + (m+\tau)e/2, \ldots, (n+1)e/2 + (m+\tau)e/2] \\ &= (\boldsymbol{E}_{n+1} + (m+\tau)e)/2,\end{aligned}$$

for some $\tau \in [0, 1)$, called the shift of $\boldsymbol{G}$. In particular, the scheme is called primal if $\tau = 0$, and dual if $\tau = 1/2$.

[1] It is 1 lower, corresponding to the index of the rightmost control point used at each insertion.

The number $n = 2m + 1$ in Definition 5.2.1 comes from the minimal length of a chain such that the subdivision scheme can be applied an infinite number of times, when no boundary data are given. If $\#\boldsymbol{P} < n$ then we will run out of points and the limit curve will not be well defined.

Lemma 5.2.1. *The iterated geometric M-point schemes are GLUE-schemes for all $\alpha \in [0, 1]$.*

Proof. Geometric property (G):
Clearly, since the schemes are binary and interpolatory, we have that

$$(\boldsymbol{G}(S(\boldsymbol{P})))_{2k} = (S(\boldsymbol{G}(\boldsymbol{P})))_{2k} \quad \forall k.$$

Let $\hat{p}_i := S(p_i)$ for all k be the points resulting from the similarity transform S. Furthermore, let $\hat{d}_i := \hat{p}_{i+1} - \hat{p}_i$. Then,

$$\begin{aligned}\hat{p}_i &= \varrho Q p_i + s,\\ \hat{d}_i &= (\varrho Q p_{i+1} + s) - (\varrho Q p_i + s) = \varrho Q d_i.\end{aligned}$$

We define the transformed parameters as follows,

$$\hat{t}_{i+1} = \hat{t}_i + \|\hat{d}_i\|^\alpha, \quad \hat{t}_0 = 0.$$

Thus,

$$\hat{t}_{i+1} = \hat{t}_i + \|\varrho Q d_i\|^\alpha = \hat{t}_i + \varrho \|d_i\|^\alpha, \quad \hat{t}_0 = 0,$$

since Q is orthogonal, i.e. it preserves lengths and angles, and we can write

$$\|Q d_i\|_2^2 = (Q d_i)^T (Q d_i) = d_i^T Q^T Q d_i = d_i^T I_d d_i = d_i^T d_i = \|d_i\|_2^2.$$

This implies that S just stretches the parameters uniformly, i.e., $\hat{t}_i = \varrho t_i \, \forall \, i$. Therefore, the transformed evaluation point simply becomes $\hat{t}_\star = \varrho t_\star$. For simplicity we number the indices $\{k - M/2 + 1, \ldots, k + M/2\}$ as $\{0, \ldots, M - 1\}$. Combining these facts yields

$$\begin{aligned}(\boldsymbol{G}(S(\boldsymbol{P})))_{2k+1} &= \sum_{i=0}^{M-1} \prod_{\substack{r=0\\ r\neq i}}^{M-1} \frac{\hat{t}_\star - \hat{t}_r}{\hat{t}_i - \hat{t}_r} \hat{p}_i = \sum_{i=0}^{M-1} \prod_{\substack{r=0\\ r\neq i}}^{M-1} \frac{\varrho(t_\star - t_r)}{\varrho(t_i - t_r)} (\varrho Q p_i + s)\\ &= \varrho Q \sum_{i=0}^{M-1} \prod_{\substack{r=0\\ r\neq i}}^{M-1} \frac{t_\star - t_r}{t_i - t_r} p_i + s \sum_{i=0}^{M-1} \prod_{\substack{r=0\\ r\neq i}}^{M-1} \frac{t_\star - t_r}{t_i - t_r}\\ &= \varrho Q \sum_{i=0}^{M-1} L_i(t_\star) p_i + s \sum_{i=0}^{M-1} L_i(t_\star) = \varrho Q \sum_{i=0}^{M-1} L_i(t_\star) p_i + s\\ &= (S(\boldsymbol{G}(\boldsymbol{P})))_{2k+1} \quad \forall k,\end{aligned}$$

where we used that $\{L_i(t_\star)\}_{i=0}^{M-1}$ form a partition of unity. Thus $\boldsymbol{G}\circ S = S\circ\boldsymbol{G}\ \forall S \in \mathcal{S}(\mathbb{E})$, and we have shown the geometric property of the schemes.

Local property (L):
For the iterated geometric M-point schemes, $m = M-1$, so since $p'_{2i} = p_{(m-1)/2}$, and p'_{2i+1} is a point on the α-interpolant to the points $p_i, \ldots, p_{i+m}$, then the local property holds.

Uniform property (U):
We have that g_0 is just the identity in the sense that $g_0(p_i, \ldots, p_{i+m}) = p_{(m-1)/2}$. Moreover, g_1 is a degree m polynomial. Therefore, g_0 and g_1 are C^∞ in a neighborhood of $\boldsymbol{E}_{m+1}$. So in context of the definition, the regularity parameter of $\boldsymbol{G}$ is $\nu = 1$.

Equilinear property (E):
Clearly, for $\boldsymbol{G}$ applied to $\boldsymbol{e}$, we get

$$\begin{aligned} t_{i+1} - t_i = \|(\boldsymbol{e})_{i+1} - (\boldsymbol{e})_i\|^\alpha = \|[1,0,\ldots,0]\|^\alpha = 1, \quad i = 0,1,\ldots,n-1 \quad \forall \alpha \in \mathbb{R} \\ \implies t_i = i, \quad i = 0,1,\ldots,n \quad \forall \alpha \in \mathbb{R}, \end{aligned}$$

i.e. equidistant parameters with unity spacing. This will also hold for $\boldsymbol{G}$ applied to any linear shift of $\boldsymbol{e}$. Letting $\hat{\boldsymbol{e}} := [0, e, \ldots, me]$, we need to show that

$$p^\star := (\boldsymbol{G}(\hat{\boldsymbol{e}}))_{2k+1} = [m/2, 0, \ldots, 0] \quad \forall \text{ odd } m \in \mathbb{Z}_{\geq 1}. \tag{5.2}$$

This is sufficient since $\hat{\boldsymbol{e}}$ is $\boldsymbol{e}$ shifted to start at the origin and truncated to $m < n$, and we can thus apply the shift commutativity property of (G) to show (E) [2]. Furthermore, it suffices to look at the first element $(p^\star)_0$ of $p^\star$, since its other elements evidently amount to the zero vector. We have that $t_\star = [(m+1)/2 - 1 + (m+1)/2]/2 = m/2$. Furthermore, we have that

$$\begin{aligned} (p^\star)_0 =& f(t_0) + (t_\star - t_0)[t_0,t_1]f + (t_\star - t_0)(t_\star - t_1)[t_0,t_1,t_2]f + \cdots \\ &+ (t_\star - t_0)\cdots(t_\star - t_{m-1})[t_0,\ldots,t_m]f, \end{aligned} \tag{5.3}$$

where $f(t_i) := ((\hat{\boldsymbol{e}})_i)_0 = i$, $i = 0,\ldots,m$. Moreover,

$$\begin{aligned} [t_0,t_1]f = [t_1,t_2]f = \cdots = [t_{m-1},t_m]f = 1 \\ \implies [t_0,t_1,t_2]f = [t_1,t_2,t_3]f = \cdots = [t_{m-2},t_{m-1},t_m]f = 0, \end{aligned}$$

which further implies that every divided difference in (5.3) of order higher than one vanishes, since the numerators become zero. This is also evident from the formula for

[2] Meaning that it suffices to show this for a single insertion point

divided differences for equidistant points, $[t_0, t_1, \ldots, t_n]f = (\Delta^n f(t_0))/(h^n n!)$, where in this case $h = 1$. Thus,

$$(p^\star)_0 = f(t_0) + (t_\star - t_0)[t_0, t_1]f = 0 + (m/2 - 0)\frac{1-0}{1-0} = m/2. \tag{5.4}$$

It remains to find τ for these schemes. By defining $\hat{m} := (m+1)/2$, we get

$$\begin{aligned}\boldsymbol{G}(\boldsymbol{e}) &= [\hat{m}e, (\hat{m}+1/2)e, (\hat{m}+1)e, \ldots, (\hat{m}+n-(m+1))e, (\hat{m}+n-(m+1/2))e] \\ &= (\boldsymbol{E}_{n+1} + me)/2,\end{aligned}$$

where we used a shifted variant of (5.4) at each insertion. Hence $\tau = 0$, and consequently the schemes are primal. It is worth noting that the shift by $me/2$ comes from the somewhat nonstandard choice of indexation used. □

Corollary 5.2.1. *The iterated geometric blending M-point schemes are GLUE-schemes.*

We note, as was done for the IG4-scheme in [1], that $\mathcal{S}(\mathbb{E})$ only contains solid body- and isotropic transformations, since scaling one component differently using a general affine transformation, will cause problems. The convergence analysis of GLUE-schemes in [13] relies on studying the decay of a quantity known as *relative distortion*, which is invariant under the similarity transformations of $\mathcal{S}(\mathbb{E})$. The relative distortion measures how far a subchain $\boldsymbol{p}$ of a chain $\boldsymbol{P}$ is from its *linear component*, meaning in a sense how straight $\boldsymbol{p}$ is.

An important distinction to make about the framework in [13], is that it is not purely analytical, but instead show the mathematical details behind an algorithm to produce certain constants for numerical tests. The constant γ that we are interested in here, is a bound for the *straightening*, or maximum local deviation from a straight line, measured by the relative distortion, that the points at level j can be in order for the limit curve to be smooth. These constants only need to be computed once for a given GLUE-scheme, and are mathematically rigorous through interval arithmetic, but can be improved.

Then, whenever the GLUE scheme is applied to given control points, one can test numerically whether the points at level j satisfy requirements generated by these constants, and thus if a certain smoothness of the limit curve is guaranteed for these control points. This implies that the method is data dependent, and there may be control points for which the method takes many iterations, or never, falls under the requirement set by γ. If we were to find the constant γ, we could then implement this condition in the software for generating the subdivision curves, and display whether this condition is satisfied to the end user in a CAGD setting.

A possible drawback of the framework in question is that it relies on the fact that the subdivided points are in a sense asymptotically locally uniformly spaced as $j \to \infty$.

This is a built-in feature of the CPS due to (5.1), but we show that this is never the case for any IGm-scheme with chordal parameterization ($\alpha = 1$), when the points are placed in order on a straight line and unevenly spaced.

Lemma 5.2.2. *For an IGm-scheme and control points $\{\boldsymbol{p}_{0,k}\}_{k\in\mathbb{Z}}$ in order by the index k on a straight line in the v-th coordinate, $v \in \{0, 1, \ldots, d-1\}$, then*

$$\boldsymbol{p}_{j+1,2k+1} = (\boldsymbol{p}_{j,k} + \boldsymbol{p}_{j,k+1})/2, \quad j = 0, 1, 2, ...,$$

is always the case for $\alpha = 1$ (chordal parameterization).

Proof. It suffices to show that all divided differences of order 2 vanish. We find that

$$\boldsymbol{p}_k^{[2]} = \frac{\frac{\boldsymbol{p}_{k+2}-\boldsymbol{p}_{k+1}}{t_{k+2}-t_{k+1}} - \frac{\boldsymbol{p}_{k+1}-\boldsymbol{p}_k}{t_{k+1}-t_k}}{t_{k+2}-t_k} = \frac{l_k(\boldsymbol{p}_{k+2}-\boldsymbol{p}_{k+1}) - (\boldsymbol{p}_{k+1}-\boldsymbol{p}_k)l_{k+1}}{l_{k+1}(l_k+l_{k+1})l_{k+1}},$$

where we dropped the level j for convenience. Thus, by looking at the v-th coordinate component only,

$$\left(\boldsymbol{p}_k^{[2]}\right)_v = \frac{l_k l_{k+1} - l_k l_{k+1}}{l_{k+1}(l_k+l_{k+1})l_{k+1}} = 0,$$

since the points are ordered by index on a line in this coordinate. Clearly $\left(\boldsymbol{p}_k^{[2]}\right)_i = 0 \,\forall\, i \neq v$, so $\boldsymbol{p}_k^{[2]} = \boldsymbol{0}$ and all higher order divided differences also vanish, and the result follows directly from the Newton form of the α-interpolant. □

A consequence of Lemma 5.2.2 is that around a control point connecting two edges of very different lengths, there will always be a relatively large difference in the lengths of the edges connected by the control point in question at every level of subdivision. The analogue also seems to hold for points not on a straight line, i.e. just unequally spaced. This phenomenon can be observed in the lower left plot of Figure 5.2, even though the points are not on a straight line.

One possible way to alleviate this problem for the IG4-scheme is to instead use the rule (5.1) by Sabin and Dodgson to select $t_\star$ at each refinement, such that

$$t_\star = \frac{t_{j,k} + \sigma t_{j,k+1}}{1+\sigma}, \quad \sigma := \sqrt{\frac{t_{j,k+1} - t_{j,k-1}}{t_{j,k+2} - t_{j,k}}} = \sqrt{\frac{\|\boldsymbol{e}_{j,k-1}\|^\alpha + \|\boldsymbol{e}_{j,k}\|^\alpha}{\|\boldsymbol{e}_{j,k}\|^\alpha + \|\boldsymbol{e}_{j,k+1}\|^\alpha}}. \tag{5.5}$$

The general idea of choosing parameters based on a monotonicity preserving scheme was also discussed in [23], and it was in fact shown there that the scheme (5.5) for choosing the evaluation point is C^1, which is certainly not true for (4.4), which is just a two-point scheme. For equidistant $\{t_{j,i}\}_{i=k-1}^{k+2}$, and therefore for $\alpha = 0$, the new choice (5.5) is just

the midpoint between the middle two parameters, but otherwise there appears to be an edge unevenness compensation such that $\boldsymbol{p}_{j+1,2k+1}$ is chosen closer to the neighboring point $\boldsymbol{p}_{j,k}$ or $\boldsymbol{p}_{j,k+1}$ of the shortest of the edges $\boldsymbol{e}_{j,k-1}$ and $\boldsymbol{e}_{j,k+1}$. To avoid confusion, we from now on let SD-$t_\star$ be the choice (5.5), and let MP-$t_\star$ be the usual choice (4.4). Moreover, we only use the SD-$t_\star$ when mentioned, and one can assume that the MP-$t_\star$ is used otherwise.

This modification to the scheme, using SD-$t_\star$, seems to result in limit curves similar to the limit curves of the IG4-scheme with MP-$t_\star$, but with the apparent added property that the points at level j become locally asymptotically equidistant as $j \to \infty$ for all $\alpha \in [0, 1]$. This can clearly be seen in Figure 5.2. Of course, altering $t_\star$ will require new C^0 proofs, and moreover it is possible that there will be different requirements on α for the IG4-scheme to be safe. Preliminary results indicate that the same results with respect to safety and C^0 convergence seem to hold also for this new choice of $t_\star$. A curious thought is whether it is possible to choose a $t_\star$ such that the scheme is safe for a wider interval of α. The more involved choice of $t_\star$ in (5.5) could complicate the convergence analysis, but if we can show the ratio property as done by Sabin and Dodgson, we could potentially use a similar proof for C^0 as for the CPS, i.e. by asymptotic equivalence to the FPS. It is not difficult to see that the IG4-scheme with this new choice of $t_\star$ is also a GLUE-scheme.

Although for $\alpha \in [0, 1)$, the edges at level j seem to shrink slowly to be locally equidistant for the midpoint $t_\star$, the new choice for $t_\star$ (SD-$t_\star$) seems to make this happen significantly faster, which means that it is conceivable that the proximity conditions of [26] could be used for some choice of $t_\star$. This could in turn also reduce the number of iterations before the straightening requirement of [13] is fulfilled, and even yield curves that visually look smoother for lower j as there are fewer abrupt changes in edge lengths.

In [13], it is shown that the CPS is $C^{2-\epsilon}$ for chains in $\mathbb{E}^{\geq 7}$ whenever the relative distortion falls below the value of $\gamma = 0.08$. It is therefore likely that similar results may be shown for a selection of the IGm-schemes by using what we have established above.

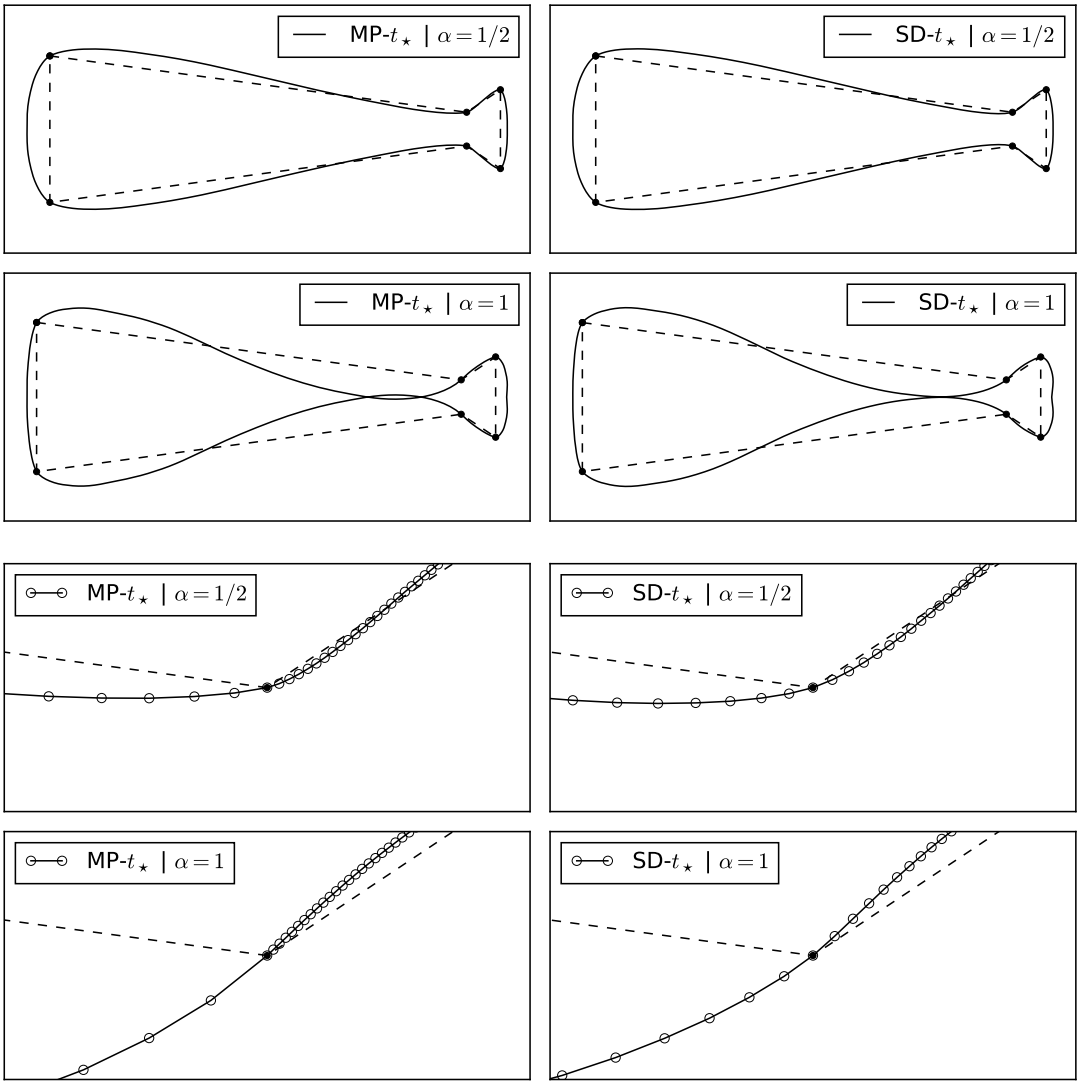

Figure 5.2: The uppermost two pairs of plots depict the limit curves generated by the IG4-scheme for the different choices of $t_\star$ with $\alpha = 1/2$ and $\alpha = 1$, respectively. The lower two pairs of plots are corresponding zoomed-in views at level $j = 6$ for these choices of $t_\star$ and the same control points, at a segment of highly varying initial edge lengths. The hollow circles illustrate the points, or vertices, P_6 of the polygon $\boldsymbol{g}_6$.

Chapter Six

Numerical results and conclusion

In this chapter we will review some ideas for starting smoothness analysis on the iterated geometric schemes, and also provide numerical results to supplement this.

6.1 Numerical results for the iterated geometric schemes

For the IG4-scheme, we proved that the limit curve is continuous for the whole of $\alpha \in [1/2, 1]$. However, as strong of a result does not seem to be the case for the IGm-schemes in general for higher m. There are two main aspects that need attention when studying the C^0 convergence of the IGm-schemes, namely that the edges get smaller with j and that the scheme is safe and thus well defined. For even $m \geq 8$ and $\alpha = 1$, we can construct controls point such that, at least numerically, the edges diverge locally. Furthermore, these schemes do not seem to be safe for $\alpha = 1/2$ with $m \geq 8$. We therefore instead concentrate on the smoothness of the IG4- and IG6-schemes.

All the numerical experiments of this chapter will use the control points of the upper plot of Figure 4.8, as we require the control points to be significantly unevenly spaced locally, in order for α to have an effect.

Smoothness

To numerically measure the C^r smoothness of the schemes, the authors in [1] used

$$\psi_{r,j} := \max_k \|\Delta \boldsymbol{p}_{j,k}^{[r]}\| = \max_k \|\boldsymbol{p}_{j,k+1}^{[r]} - \boldsymbol{p}_{j,k}^{[r]}\|,$$

and numerically studied the decay and rate of convergence of this quantity as j grows. A problem with this approach is, as discussed, with respect to which parameters, or grid points, $\{x_{j,k}\}_{k\in\mathbb{Z}}$ one should calculate the $\psi_{r,j}$ for $r \geq 1$. In [1], they argued that

as $\boldsymbol{p}_{j,k}^{[1]}$ for uniform grid points $\{\breve{x}_{j,k}\}$ do not seem to result in a continuous curve for points based on centripetal and chordal parameterizations for certain initial data, which can be observed in the left hand plots of Figure 6.3, then a better choice is to use chordal parameters $\{\tilde{x}_{j,k}\}_{k\in\mathbb{Z}}$ for the $\psi_{r,j}$. The left hand plots of Figure 6.3 are very similar to Figure 4 of [1], due to the control points being similar to the ones used in [1]. A problem with the chordal grid approach is that the resulting grid will not be a traditional multilevel grid satisfying $\tilde{x}_{j+1,2k} = \tilde{x}_{j,k}$ in general, so here we instead consider some other ideas.

An interesting idea is to instead introduce the concept of a *geometric grid* based on the iterated geometric subdivision scheme itself. In this method, we let the grid points $\{x_{j,k}\} = \{\tau_{j,k}\}$, where the $\{\tau_{j,k}\}$ are generated by the points P_{j-1} for $j \geq 1$. We concentrate here on the case for the IG4-scheme, but the idea extends naturally to higher orders. Let

$$\begin{aligned} \boldsymbol{p}_{j+1,2k} &= \boldsymbol{p}_{j,k}, & \tau_{j+1,2k} &= \tau_{j,k}, \\ \boldsymbol{p}_{j+1,2k+1} &= \boldsymbol{\pi}_{j,k}^{4}(t_\star) = \sum_{i=k-1}^{k+2} c_{j,i}\boldsymbol{p}_{j,i}, & \tau_{j+1,2k+1} &= \sum_{i=k-1}^{k+2} c_{j,i}\tau_{j,i}, \end{aligned}$$

where $\{c_{j,i}\}$ are the Lagrangian coefficients based locally on the points at level j, as usual, and $\{\tau_{0,k}\}$ is some initial parameterization. Consequently, we have that $\sum_{i=k-1}^{k+2} c_i = 1$. Although other alternatives may be possible, we focus here on the case where the initial grid points $\{\tau_{0,k}\}$ are generated by an α-parameterization based on the same α as the subdivision scheme.

An important distinction is that the refinement of the $\{\tau_{0,k}\}$ is not the same as treating the grid points as data points and directly applying the subdivision scheme to this data, but rather using the Lagrange coefficients originating from the actual points. This means that we have a much more direct relation between the coefficients in the numerator and denominator of the first divided differences than we would have if we directly used an α-parameterized grid for analysis. Using

$$\tilde{\boldsymbol{p}}_{j,k}^{[r]} := \frac{\tilde{\boldsymbol{p}}_{j,k+1}^{[r-1]} - \tilde{\boldsymbol{p}}_{j,k}^{[r-1]}}{\tau_{j,k+r} - \tau_{j,k}} \quad \forall\, r \geq 1, \quad \tilde{\boldsymbol{p}}_{j,k}^{[0]} := \boldsymbol{p}_{j,k},$$

we find that

$$\begin{aligned} \tilde{\boldsymbol{p}}_{j+1,2k}^{[1]} &= \frac{\boldsymbol{p}_{j+1,2k+1} - \boldsymbol{p}_{j+1,2k}}{\tau_{j+1,2k+1} - \tau_{j+1,2k}} = \frac{\sum_{i=k-1}^{k+2} c_{j,i}\boldsymbol{p}_{j,i} - \boldsymbol{p}_{j,k}}{\sum_{i=k-1}^{k+2} c_{j,i}\tau_{j,i} - \tau_{j,k}} \\ &= \frac{a_{j,k-1}(\boldsymbol{p}_{j,k} - \boldsymbol{p}_{j,k-1}) + a_{j,k}(\boldsymbol{p}_{j,k+1} - \boldsymbol{p}_{j,k}) + a_{j,k+1}(\boldsymbol{p}_{j,k+2} - \boldsymbol{p}_{j,k+1})}{a_{j,k-1}(\tau_{j,k} - \tau_{j,k-1}) + a_{j,k}(\tau_{j,k+1} - \tau_{j,k}) + a_{j,k+1}(\tau_{j,k+2} - \tau_{j,k+1})} \\ &= \frac{a_{j,k-1}(\tau_{j,k} - \tau_{j,k-1})\tilde{\boldsymbol{p}}_{j,k-1}^{[1]} + a_{j,k}(\tau_{j,k+1} - \tau_{j,k})\tilde{\boldsymbol{p}}_{j,k}^{[1]} + a_{j,k+1}(\tau_{j,k+2} - \tau_{j,k+1})\tilde{\boldsymbol{p}}_{j,k+1}^{[1]}}{a_{j,k-1}(\tau_{j,k} - \tau_{j,k-1}) + a_{j,k}(\tau_{j,k+1} - \tau_{j,k}) + a_{j,k+1}(\tau_{j,k+2} - \tau_{j,k+1})}, \end{aligned}$$

where $a_{j,k-1} = -c_{j,k-1}$, $a_{j,k} = c_{j,k+1}+c_{j,k+2}$, $a_{j,k+1} = c_{j,k+2}$, $\sum_{i=k-1}^{k+1} a_{j,i} = 0$. Therefore,

$$\tilde{\boldsymbol{p}}^{[1]}_{j+1,2k} = \sum_{i=k-1}^{k+1} b_{j,i}\tilde{\boldsymbol{p}}^{[1]}_{j,i}, \quad b_{j,i} := \frac{a_{j,i}(\tau_{j,i+1}-\tau_{j,i})}{\sum_{w=k-1}^{k+1} a_{j,w}(\tau_{j,w+1}-\tau_{j,w})},$$

where $\sum_{i=k-1}^{k+1} b_{j,i} = 1$. Similarly,

$$\begin{aligned}\tilde{\boldsymbol{p}}^{[1]}_{j+1,2k+1} &= \frac{\boldsymbol{p}_{j+1,2k+2}-\boldsymbol{p}_{j+1,2k+1}}{\tau_{j+1,2k+2}-\tau_{j+1,2k+1}} = \frac{\boldsymbol{p}_{j,k+1}-\sum_{i=k-1}^{k+2} c_{j,i}\boldsymbol{p}_{j,i}}{\tau_{j,k+1}-\sum_{i=k-1}^{k+2} c_{j,i}\tau_{j,i}} \\ &= \frac{\tilde{a}_{j,k-1}(\tau_{j,k}-\tau_{j,k-1})\tilde{\boldsymbol{p}}^{[1]}_{j,k-1} + \tilde{a}_{j,k}(\tau_{j,k+1}-\tau_{j,k})\tilde{\boldsymbol{p}}^{[1]}_{j,k} + \tilde{a}_{j,k+1}(\tau_{j,k+2}-\tau_{j,k+1})\tilde{\boldsymbol{p}}^{[1]}_{j,k+1}}{\tilde{a}_{j,k-1}(\tau_{j,k}-\tau_{j,k-1}) + \tilde{a}_{j,k}(\tau_{j,k+1}-\tau_{j,k}) + \tilde{a}_{j,k+1}(\tau_{j,k+2}-\tau_{j,k+1})},\end{aligned}$$

where $\tilde{a}_{j,k-1} = c_{j,k-1}$, $\tilde{a}_{j,k} = c_{j,k-1}+c_{j,k}$, $\tilde{a}_{j,k+1} = -c_{j,k+2}$, $\sum_{i=k-1}^{k+1}\tilde{a}_{j,i} = 0$. And hence,

$$\tilde{\boldsymbol{p}}^{[1]}_{j+1,2k+1} = \sum_{i=k-1}^{k+1} \tilde{b}_{j,i}\tilde{\boldsymbol{p}}^{[1]}_{j,i}, \quad \tilde{b}_{j,i} := \frac{\tilde{a}_{j,i}(\tau_{j,i+1}-\tau_{j,i})}{\sum_{w=k-1}^{k+1}\tilde{a}_{j,w}(\tau_{j,w+1}-\tau_{j,w})},$$

with $\sum_{i=k-1}^{k+1}\tilde{b}_{j,i} = 1$. Thus,

$$\begin{aligned}\Delta\tilde{\boldsymbol{p}}^{[1]}_{j+1,2k} &= \tilde{\boldsymbol{p}}^{[1]}_{j+1,2k+1} - \tilde{\boldsymbol{p}}^{[1]}_{j+1,2k} = \sum_{i=k-1}^{k+1}(\tilde{b}_{j,i}-b_{j,i})\tilde{\boldsymbol{p}}^{[1]}_{j,i} \\ &= \delta_{j,k-1,k}\Delta\tilde{\boldsymbol{p}}^{[1]}_{j,k-1} + \delta_{j,k,k+1}\Delta\tilde{\boldsymbol{p}}^{[1]}_{j,k},\end{aligned}$$

where $\delta_{j,k-1,k} = b_{j,k-1}-\tilde{b}_{j,k-1}$, and $\delta_{j,k,k+1} = \tilde{b}_{j,k+1}-b_{j,k+1}$, since $\sum_{i=k-1}^{k+1}(\tilde{b}_{j,i}-b_{j,i}) = 0$. Likewise,

$$\begin{aligned}\tilde{\boldsymbol{p}}^{[1]}_{j+1,2(k+1)} &= \frac{\sum_{i=k}^{k+3}\hat{c}_{j,i}\boldsymbol{p}_{j,i}-\boldsymbol{p}_{j,k+1}}{\sum_{i=k}^{k+3}\hat{c}_{j,i}\tau_{j,i}-\tau_{j,k+1}} = \frac{\sum_{i=k}^{k+2}\hat{a}_{j,i}(\boldsymbol{p}_{j,i+1}-\boldsymbol{p}_{j,i})}{\sum_{i=k}^{k+2}\hat{a}_{j,i}(\tau_{j,i+1}-\tau_{j,i})} \\ &= \sum_{i=k}^{k+2}\hat{b}_{j,i}\tilde{\boldsymbol{p}}^{[1]}_{j,i}, \quad \hat{b}_{j,i} := \frac{\hat{a}_{j,i}(\tau_{j,i+1}-\tau_{j,i})}{\sum_{w=k}^{k+2}\hat{a}_{j,w}(\tau_{j,w+1}-\tau_{j,w})},\end{aligned}$$

with $\hat{a}_{j,k} = -\hat{c}_{j,k}$, $\hat{a}_{j,k+1} = \hat{c}_{j,k+2}+\hat{c}_{j,k+3}$, $\hat{a}_{j,k+2} = \hat{c}_{j,k+3}$. Therefore,

$$\begin{aligned}\Delta\tilde{\boldsymbol{p}}^{[1]}_{j+1,2k+1} &= \tilde{\boldsymbol{p}}^{[1]}_{j+1,2(k+1)} - \tilde{\boldsymbol{p}}^{[1]}_{j+1,2k+1} = \sum_{i=k}^{k+2}\hat{b}_{j,i}\tilde{\boldsymbol{p}}^{[1]}_{j,i} - \sum_{i=k-1}^{k+1}\tilde{b}_{j,i}\tilde{\boldsymbol{p}}^{[1]}_{j,i} \\ &= \hat{\delta}_{j,k-1,k}\Delta\tilde{\boldsymbol{p}}^{[1]}_{j,k-1} + \hat{\delta}_{j,k,k+1}\Delta\tilde{\boldsymbol{p}}^{[1]}_{j,k} + \hat{\delta}_{j,k+1,k+2}\Delta\tilde{\boldsymbol{p}}^{[1]}_{j,k+1},\end{aligned}$$

where $\hat{\delta}_{j,k-1,k} = \tilde{b}_{j,k-1}$, $\hat{\delta}_{j,k,k+1} = \hat{b}_{j,k+1}-\tilde{b}_{j,k+1}+\hat{b}_{j,k+2}$, $\hat{\delta}_{j,k+1,k+2} = \hat{b}_{j,k+2}$. We thus have schemes for $\Delta\tilde{\boldsymbol{p}}^{[1]}_{j+1,2k}$ and $\Delta\tilde{\boldsymbol{p}}^{[1]}_{j+1,2k+1}$, as we have for the standard FPS over a regular grid.

By moving on to second divided differences, we find that

$$\tilde{\boldsymbol{p}}^{[2]}_{j+1,2k} = s_{j,k-1}\tilde{\boldsymbol{p}}^{[2]}_{j,k-1} + s_{j,k}\tilde{\boldsymbol{p}}^{[2]}_{j,k}, \quad s_{j,i} := \frac{\delta_{j,i,i+1}(\tau_{j,i+2} - \tau_{j,i})}{\tau_{j,i+1} - \tau_{j,i}},$$

and that

$$\tilde{\boldsymbol{p}}^{[2]}_{j+1,2k+1} = \tilde{s}_{j,k-1}\tilde{\boldsymbol{p}}^{[2]}_{j,k-1} + \tilde{s}_{j,k}\tilde{\boldsymbol{p}}^{[2]}_{j,k} + \tilde{s}_{j,k+1}\tilde{\boldsymbol{p}}^{[2]}_{j,k+1},$$
$$\tilde{s}_{j,i} := \frac{\hat{\delta}_{j,i,i+1}(\tau_{j,i+2} - \tau_{j,i})}{\sum_{w=k}^{k+3} \hat{c}_{j,w}\tau_{j,w} - \sum_{w=k-1}^{k+2} c_{j,w}\tau_{j,w}}.$$

A difficulty in continuing, and finding explicit schemes for $\Delta\tilde{\boldsymbol{p}}^{[2]}_{j+1,2k}$ and $\Delta\tilde{\boldsymbol{p}}^{[2]}_{j+1,2k+1}$, as can be done for the FPS, is that the $\{s_{j,i}\}$ and $\{\tilde{s}_{j,i}\}$ do not necessarily sum to simple constants locally, which means that using similar techniques as for $r = 1$ will be harder.

j	$\delta_{j,k-1,k}$	$\delta_{j,k,k+1}$	$\hat{\delta}_{j,k-1,k}$	$\hat{\delta}_{j,k,k+1}$	$\hat{\delta}_{j,k+1,k+2}$
1	0.0770229	0.2820809	-0.0439309	0.8060199	-0.1211928
	0.2910886	0.2910886	-0.1455443	0.7089114	-0.1455443
	0.2820809	0.0770229	-0.1211928	0.8060199	-0.0439309
	0.4471966	0.2602610	-0.2128083	0.6417607	-0.1364102
5	0.2715896	0.2405514	-0.1345902	0.7437918	-0.1213427
	0.2601699	0.2337790	-0.1283528	0.7528498	-0.1184460
	0.2696158	0.2282926	-0.1329171	0.7507560	-0.1157473
	0.2740313	0.2266210	-0.1350349	0.7493312	-0.1149486
8	0.2504237	0.2496713	-0.1252591	0.7499527	-0.1247885
	0.2503197	0.2497974	-0.1251962	0.7499415	-0.1248624
	0.2502042	0.2497643	-0.1251328	0.7500158	-0.1248515
	0.2502465	0.2497573	-0.1251531	0.7499982	-0.1248488
12	0.2500146	0.2499843	-0.1249938	0.7500005	-0.1250057
	0.2500158	0.2499846	-0.1249944	0.7499998	-0.1250058
	0.2500159	0.2499727	-0.1249950	0.7500057	-0.1249993
	0.2500280	0.2499665	-0.1250019	0.7500027	-0.1249953

Figure 6.1: Randomized excerpt of consecutive values of the coefficients for the scheme for the first divided differences with $\alpha = 1/2$, for different levels j. These are deliberately sampled around the interior points due to the difficulties at the boundaries.

By looking at Figure 6.2, it seems like the IG4-scheme is C^1 with respect to the geometric grid, and the $\{\psi_{1,j}\}$ appear to decay linearly for large j. We have similar findings for the chordal grid choice.

Behavior as j grows

Since we have found schemes for the forward differences of the first divided differences for a geometric grid, it would be interesting to see how the coefficients of this scheme, which are now dependent on the $\{\tau_{j,k}\}$ for $\alpha \neq 0$, behave in relation to the corresponding coefficients for Dubuc's four-point scheme with a regular grid. For $\alpha = 0$, a geometric grid with a regular initial grid, is the same as a regular grid. Thus, we know from the proof of Theorem 2.1.1 that for $\alpha = 0$, $\delta_{j,k-1,k} = \delta_{j,k,k+1} = 1/4$, and $\hat{\delta}_{j,k-1,k} = \hat{\delta}_{j,k+1,k+2} = -1/8$, $\hat{\delta}_{j,k,k+1} = 3/4$. In Figure 6.1, we see that although the coefficients for $\alpha = 1/2$ start out by being relatively far away from the uniform coefficients, it appears that the limits are the uniform coefficients. This seems to indicate that the scheme for the forward differences of the first divided differences of the IG4-scheme behaves like the corresponding scheme for the FPS, over a geometric grid in the limit. However, there seems to be an anomaly in the $\hat{\delta}_{j,i,i+1}$ near the boundaries of the $\{\tau_{j,k}\}$, which may be related to the choice of boundary conditions of the $\{\tau_{j,k}\}$. Notably, this issue seems to be much less severe when using the other proposed $t_\star$ in (5.5), which is logical as the local edge lengths approach uniformity and thus renders the boundary error less influential for low j and approaching zero for $j \to \infty$.

Another interesting idea is to consider the divided differences for the alternative choice of $t_\star$ in (5.5), and use a regular grid since the local edge lengths seem to be locally equal asymptotically. Plots of the divided differences for this choice can be viewed in the right hand plots of Figure 6.3, and it appears that the discontinuities have disappeared with the change of $t_\star$, which looks promising. We have found examples for the IG4-scheme with $\alpha = 1$ for both the chordal grid and the geometric grid with MP-$t_\star$, where the $\{\psi_{1,j}\}$ increase for the first three iterations before starting to be strictly decreasing. This is two more iterations than for the FPS, which could make analysis difficult at least for $\alpha = 1$. However, by using SD-$t_\star$, the $\{\psi_{1,j}\}$ do not seem to have this problem, and behave similarly like for the FPS, but has the drawback of being more analytically complicated.

In the case of C^2 smoothness for the six-point schemes using $\psi_{2,j}$, it seems to be harder to get conclusive results. For the IG6-scheme, the geometric grid only appears to be well defined for $\alpha \in [0, 1/2]$, while it seems to be well defined for all of $\alpha \in [0, 1]$ for the IG4-scheme. This is of course assuming that the points at every level are consecutively distinct, which we only have shown for the IG4-scheme for $\alpha \in [1/2, 1]$. We will thus restrict the analysis to $\alpha = 1/2$, and only show some preliminary findings in the form of the figure Figure 6.4. Again, it looks like SD-$t_\star$ yields better smoothness results, and it seems like the IG6-scheme is C^2 for $\alpha = 1/2$. Furthermore, although less convincing, the plots indicate that it is possible that the IGB6-scheme is C^2 with SD-$t_\star$ for $\alpha = 1/2, \lambda = 1/2$, as we showed for the linear case in Theorem 4.7.1.

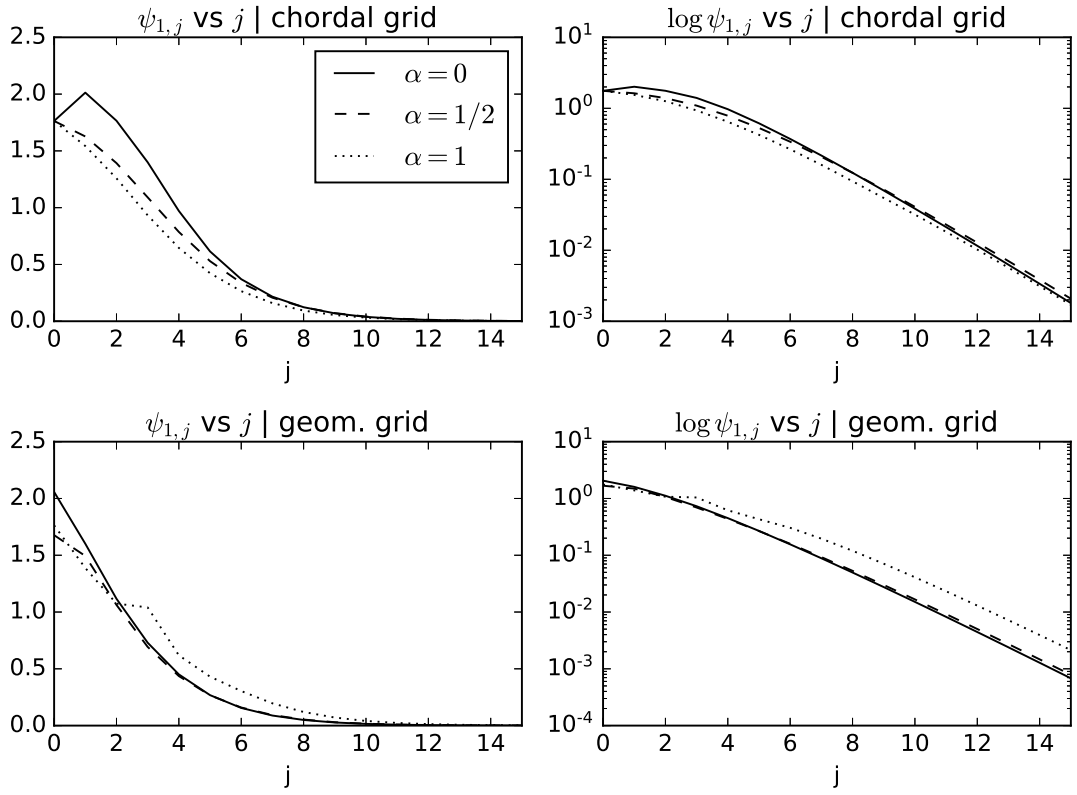

Figure 6.2: Numerical results on the first divided differences using different strategies for generating the grid. The upper two plots are $\psi_{1,j}$ with respect to chordal grid parameters, and the lower two plots are $\psi_{1,j}$ based on a geometric grid with the same α for the initial parameterization as in the curves. The solid, dashed, and dotted lines correspond to curves with $\alpha = 0, 1/2, 1$, respectively. Note that the rightmost plots are semi-log plots.

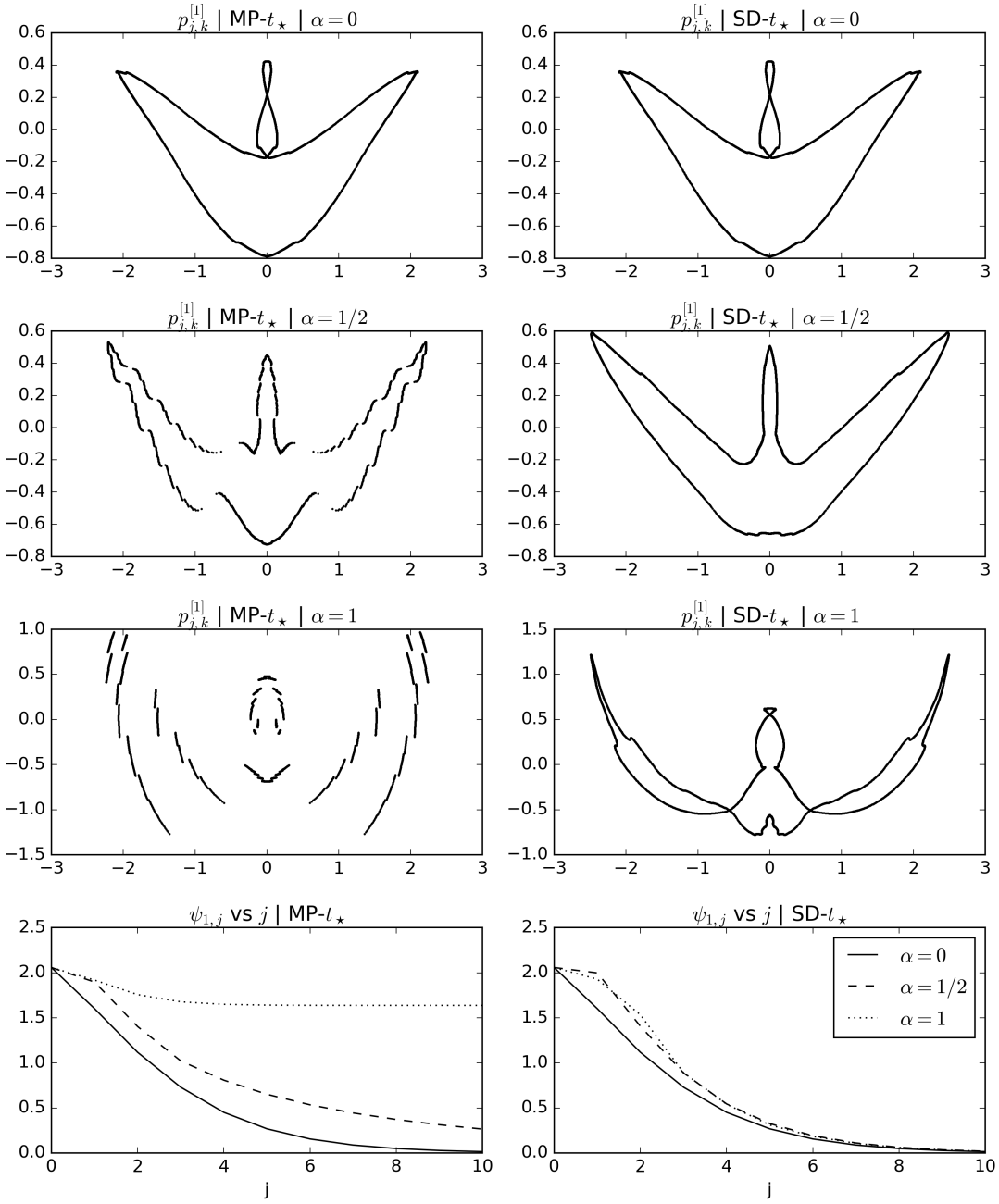

Figure 6.3: The upper six plots are point cloud plots of the $\{\boldsymbol{p}^{[1]}_{j,k}\}$ for the IG4-scheme, after $j = 10$ iterations using a regular grid, for curves based on different α and with different choices of $t_\star$. The lower two plots are of the $\{\psi_{1,j}\}$, for the different choices of $t_\star$, with respect to a regular grid.

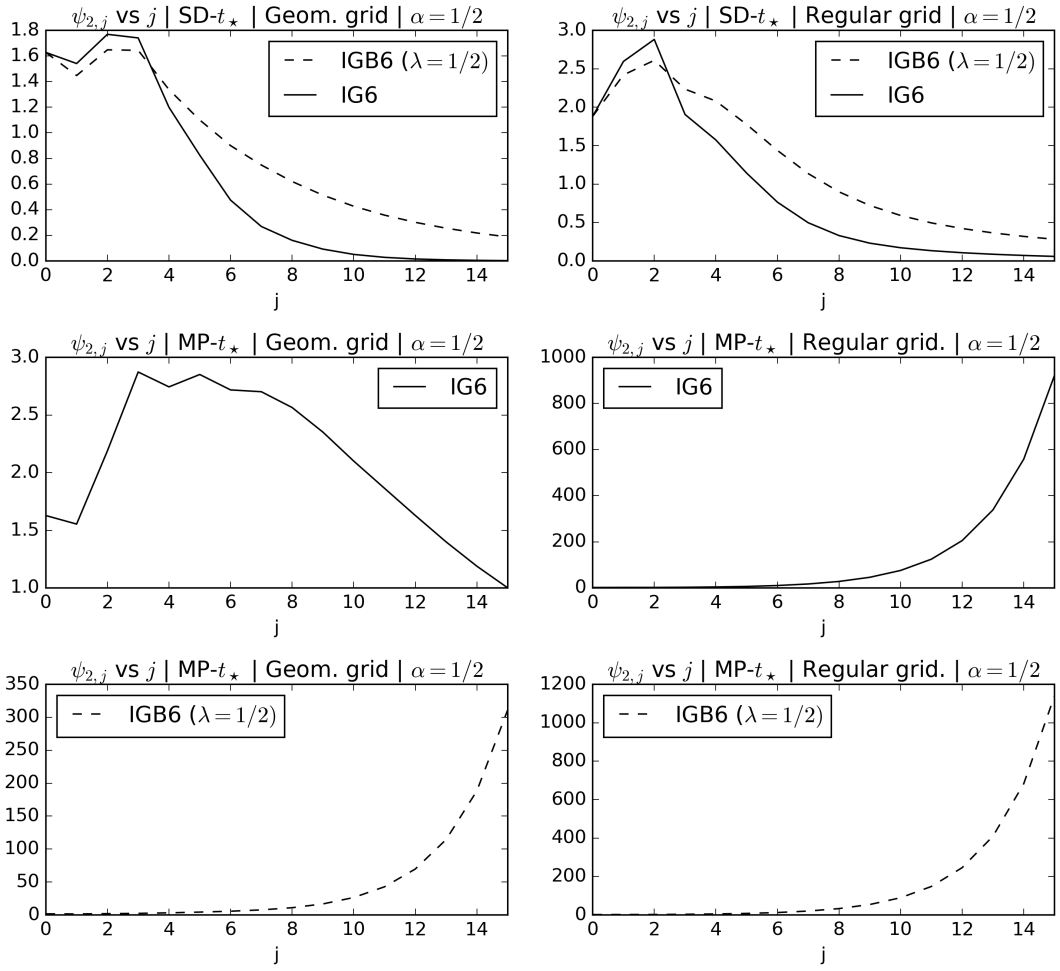

Figure 6.4: Numerical results for the second divided differences, using $\psi_{2,j}$, for the IG6-scheme and the IGB6-scheme with $\lambda = 1/2$, both using $\alpha = 1/2$. The plots show the four different combinations of using SD-$t_\star$ or MP-$t_\star$ and a geometric grid or a regular grid.

6.2 Conclusion

We have in this thesis in particular looked at a class of nonlinear interpolatory curve subdivision schemes, namely the iterated geometric schemes, and the related iterated geometric blending schemes. We proved that the IG4-scheme is safe and C^0 for $\alpha \in [1/2, 1]$, and that the IG4- and IG6-schemes are unsafe for $\alpha \in [0, 1/2)$. This means that the question about when the IG4-scheme is C^0 for $\alpha \in [0, 1]$, now is fully answered.

Using a new approach for bounding the IG6 displacement vector, we managed to show that nonlinear versions of the four-point- and six-point tension parameter schemes are C^0 for select values of a blending (or tension) parameter λ. The case for the IGB6-scheme with $\alpha = 1/2$ and λ close to zero is especially interesting as this could potentially yield a limit curve close to the tight IG4 limit curve with possible C^2 smoothness.

Later on, we showed that the these schemes fit into a new framework by Ewald et al. for analyzing geometric nonlinear schemes, which may lead to a condition for the limit curve to be $C^{1,\beta}$ that can be applied in practice. In regards to smoothness we also discussed a new way of generating the multilevel grid, the geometric grid, which appears to yield interesting preliminary analytic and numerical results. We also discussed an alternative way to choose the evaluation point $t_\star$, which appears to grant the curve better numerical convergence and smoothness results.

This study of nonlinear interpolatory curve subdivision schemes has been an interesting one, and there are still many details about these schemes waiting to be discovered.

6.3 Future work

Future work could include doing more research on the IG6-scheme, and to extend the iterated geometric schemes to surfaces, although the problem of consecutive distinctness is not obvious how to resolve in general for surfaces, and may require further modifications of the subdivision refinement rules. And of course is proving that the IG4-scheme is C^1 still an unresolved problem and highly topical. For this reason, further work on the geometric grid idea could be done to possibly progress in proving this. To derive numerical bounds for smoothness, as in [13], one could continue from where we left chapter 5 and actually find the constant γ.

Furthermore are the invalidity problems of chapter 4 still not resolved in general outside the cases $m = 4, 6$, so proving Conjecture 4.3.1, and perhaps even generalizing this to self-intersections, could be a possible topic. Since this in fact is a problem in parametric polynomial interpolation, it may also be relevant in other contexts outside subdivision.

Bibliography

[1] Dyn, Floater, Hormann, *Four-point curve subdivision based on iterated chordal and centripetal parameterizations*, Computer Aided Geometric Design, Vol. 26, Issue 3, 2009, p. 279–286.

[2] Dyn, Hormann, *Geometric conditions for tangent continuity of interpolatory planar subdivision curves*, Computer Aided Geometric Design, Vol. 29, Issue 6, 2012, p. 332–347.

[3] Dubuc, *Interpolation through an Iterative Scheme*, Journal of Mathematical Analysis and Applications, Vol. 114, Issue 1, 1986, p. 185–204.

[4] Deslauriers, Dubuc, *Symmetric Iterative Interpolation Processes*, Constructive Approximation, Vol. 5, Issue 1, 1989, p. 49–68.

[5] Dyn, Gregory, Levin, *A 4-point interpolatory subdivision scheme for curve design*, Computer Aided Geometric Design, Vol. 4, Issue 4, 1987, p. 257–268.

[6] Dahlquist, Björck, *Numerical Methods in Scientific Computing*, SIAM, Vol. 1, 2008.

[7] Floater, *Interpolation by subdivision* (Lecture notes in the course MAT-INF4160), http://www.uio.no/studier/emner/matnat/math/MAT-INF4160/h16/undervisningsmateriale/fourpt.pdf, visited 16.05.17.

[8] Floater, *A piecewise polynomial approach to analyzing interpolatory subdivision*, Journal of Approximation Theory, Vol. 163, Issue 11, 2011, p. 1547–1563.

[9] Hechler, Mößner, Reif, *C^1-Continuity of the generalized four-point scheme*, Linear Algebra and its Applications, Vol. 430, Issues 11–12, 2009, p. 3019–3029.

[10] Dyn, *Subdivision schemes in computer-aided geometric design*, Advances in Numerical Analysis, 1992, p. 36–104.

[11] Daubechies, Guskov, Sweldens, *Regularity of irregular subdivision*, Constructive Approximation, Vol. 15, Issue 3, 1999, p. 381–426.

[12] Sabin, Dodgson, *A circle-preserving variant of the four-point subdivision scheme*, Mathematical Methods for Curves and Surfaces: Tromsø 2004, Modern Methods in Mathematics, 2005, p. 275–286.

[13] Ewald, Reif, Sabin, *Hölder Regularity of Geometric Subdivision Schemes*, Constr. Approx. Vol. 42, 2015, p. 425–458.

[14] Dyn, Levin, *Subdivision schemes in geometric modeling*, Acta Numerica, Vol. 11, 2002, p. 73–144.

[15] Floater, *On the deviation of a parametric cubic spline interpolant from its data polygon*, Computer Aided Geometric Design, Vol. 25, Issue 3, 2008, p 148–156.

[16] von Koch, *On a continuous curve without tangents, constructible from elementary geometry*, 1904.

[17] Marinov, Dyn, Levin, *Geometrically Controlled 4-Point Interpolatory Schemes*, Advances in Multiresolution for Geometric Modelling, 2005, p. 301–315.

[18] Levin, *Using Laurent polynomial representation for the analysis of the nonuniform binary subdivision schemes*, Advances in Computational Mathematics, Vol. 11, Issue 1, 1999, p. 41–54.

[19] Zheng, Li, Peng, Tang, *A Multicontrol p-ary Subdivision Scheme to Generate Fractal Curves*, Applied Mechanics and Materials, Vols. 263-266, 2013, p 1830–1833.

[20] Lee, Lee, Yoon, *Stationary binary subdivision schemes using radial basis function interpolation*, Advances in Computational Mathematics, Vol. 25, Issue 1, 2006, p. 57–72.

[21] Mustafa, Khan, Hashmi, *A Generalized Proof of the Smoothness of 6-Point Interpolatory Scheme*, Journal of Information and Computing Science, Vol. 5, 2010, p. 299–304.

[22] Lyche, Mørken, *Spline Methods Draft* (Lecture notes in the course MAT-INF4170), http://www.uio.no/studier/emner/matnat/ifi/ INF-MAT5340/v13/undervisningsmateriale/book.pdf, visited 16.05.17.

[23] Floater, Beccari, Cashman, Romani, *A smoothness criterion for monotonicity-preserving subdivision*, Advances in Computational Mathematics, Vol. 39, Issue 1, 2013, p. 193–204.

[24] Dyn, Floater, Hormann, *A C2 Four-Point Subdivision Scheme with Fourth Order Accuracy and its Extensions*, Mathematical Methods for Curves and Surfaces: Tromsø 2004, 2005, p. 145–156.

[25] Deng, Jin, Li, Xu, *A formula for estimating the deviation of a binary interpolatory subdivision curve from its data polygon*, Applied Mathematics and Computation, Vol. 304, 2017, p. 10–19.

[26] Wallner, Dyn, *Convergence and C1 analysis of subdivision schemes on manifolds by proximity*, Computer Aided Geometric Design, Vol. 22, Issue 7, 2005, p. 593–622.